CHALMERS
UNIVERSITY OF TECHNOLOGY

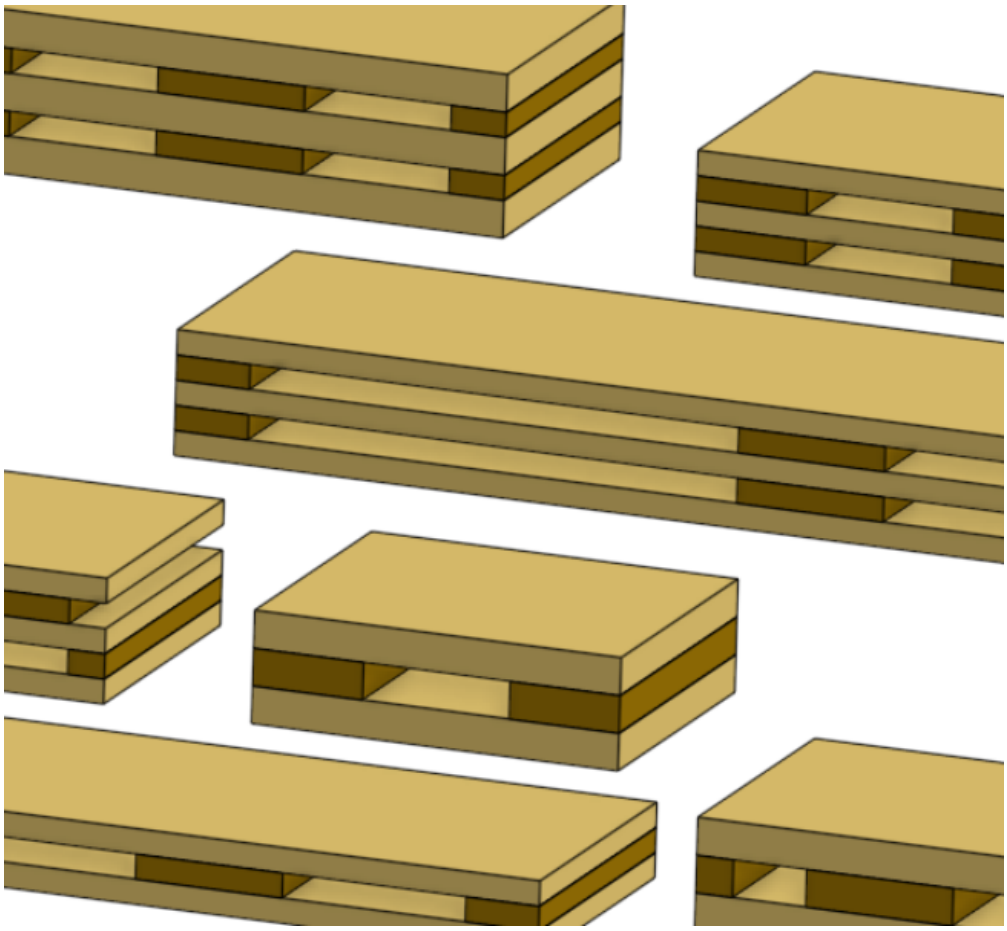

Analytical investigation for application of Hollow CLT elements

Master's thesis in Structural Engineering and Building Technology

Elliot Sterneling
Mohannad Ellhajj

DEPARTMENT OF ARCHITECTURE AND CIVIL ENGINEERING
CHALMERS UNIVERSITY OF TECHNOLOGY
Gothenburg, Sweden 2025
www.chalmers.se

Master's thesis 2025

Analytical investigation for application of Hollow CLT elements

Master's thesis in Structural Engineering and Building Technology

Elliot Sterneling
Mohannad Ellhajj

CHALMERS
UNIVERSITY OF TECHNOLOGY

Department of Architecture and Civil Engineering
Division of Structural Engineering
Chalmers University of Technology
Gothenburg, Sweden 2025

Analytical investigation for application of Hollow CLT elements
Master's thesis in Structural Engineering and Building Technology
ELLIOT STERNELING
MOHANNAD ELHAJJ

Supervisor: Yutaka Goto , Building Technology, Architecture and Civil Engineering
Examiner: Robert Jockwer , Structural Engineering, Architecture and Civil Engineering

Master's Thesis 2025
Department of Architecture and Civil Engineering
Division of Structural Engineering
Chalmers University of Technology
SE-412 96 Gothenburg
Telephone +46 31 772 1000

Cover: Selection of different CLT elements with air gaps.

Typeset in LaTeX
Printed by Chalmers Reproservice
Gothenburg, Sweden 2025

Analytical investigation for application of Hollow CLT elements

Master's thesis in Structural Engineering and Building Technology

ELLIOT STERNELING

MOHANNAD ELLHAJJ

Department of Structural Engineering
Chalmers University of Technology

Abstract

The construction sector today are responsible for a large portion of the global carbon emissions, which leads to a higher demand for making the industry more sustainable. With these increasing demands put a higher pressure on reducing the raw material used in construction. Timber is in comparison with others a more sustainable material because it is relatively eco-friendly.

This thesis aims to investigate the application and extent of where and when it is appropriate to implement air gaps into the cross layers of CLT elements in relation to structural and hygrothermal performance, as well as how the evaluation should be structured to acquire the most volume efficient layout. The optimal arrangement for enhancing both structural and environmental performance was determined by methodically evaluating important elements like heat transmission, moisture transport, and material interactions.

The investigation of structural performance showed that air gaps could be applied to a meaningful extent in most situations and still satisfy structural requirements saving approximately 20% of the material usage, where even with constrained widths of the air gaps, a significant reduction of the volume in relation to its solid counterpart. For the Hygrothermal performance no major impact could be observed from the air gaps other than the thermal and moisture storage capacity decreased.

Keywords: Cross-laminated timber, CLT, air gaps

Acknowledgements

We would like to express our humble appreciations to our supervision Yutaka Goto and examiner Robert Jockwer for providing us with the opportunity to work on this thesis and all of the help and insight they provided.

Elliot Sterneling, Mohannad Elhajj, Gothenburg, June 2024

List of Acronyms

Below is the list of acronyms that have been used throughout this thesis listed in alphabetical order:

CLT	Cross Laminated Timber
SAM	Shear Analogy Method

Nomenclature

Below is the nomenclature of indices, sets, parameters, and variables that have been used throughout this thesis.

Greek Letters

γ_i	Gamma factor
$\sigma_{c,d}$	Compression perpendicular to grain
γ_M	partial factor for material properties
ψ_i	Reduction factor
ξ	Damping ratio
λ_{void}	Void ratio
ρ	Density
δ	Vapour permeability
δ_{eq}	Equivalent vapour permeability
μ	Vapour diffusion resistance factor
λ	Thermal conductivity
λ_{eq}	Equivalent thermal conductivity

Roman upper case Letters

$\boldsymbol{A}$	Area
B_i	Width of each configuration
B_{tot}	Total width of the panel
$\boldsymbol{D}$	Thickness of CLT panels
$\boldsymbol{E}$	Young's modulus
$\boldsymbol{EI}$	Bending stiffness
$\boldsymbol{G}$	Shear modulus

G_k	Dead load
$\boldsymbol{I}$	Moment of inertia
I_{eff}	Effective moment of inertia
$\boldsymbol{L}$	Length
$\boldsymbol{M}$	Moment
N_{ED}	Acting load per meter
$\boldsymbol{P}$	Compressive capacity
$\boldsymbol{Q}$	Variable load
$\boldsymbol{R}$	Thermal resistance
R_{eq}	Equivalent thermal resistance
$\boldsymbol{S}$	Stress
$\boldsymbol{T}$	Temperature
$\boldsymbol{V}$	Volume
$\boldsymbol{V}$	shear
$\boldsymbol{W}$	Moment of resistance
$\boldsymbol{Z}$	Vapour transmission

Roman lower case Letters

$\boldsymbol{a}$	Distance
$\boldsymbol{b}$	Width
f_1	Fundamental frequency
f_d	Design strength
f_k	Characteristic strength value
f_{md}	Bending design strength value
f_{vd}	Design value for the rolling shear strength
$\boldsymbol{h}$	Height
h_a	Convection/Conduction coefficient
h_r	Radiative coefficient
k_{crit}	Lateral buckling factor
k_{def}	Deformation factor
k_{mod}	Modification factor
k_{sys}	System strength factor
$\boldsymbol{m}$	Weight

n_{40}	Number of frequencies below 40 Hz
p_{atm}	Atmosphere pressure
$\boldsymbol{q}$	Distributed load
$\boldsymbol{t}$	Thickness
v	Velocity
$\boldsymbol{w}$	Deflection

Contents

List of Figures

List of Tables

1
Introduction

1.1 Background

It is apparent that to face climate change, there is a demand to moderate carbon emissions from all industries. Data show that the construction industry is responsible for a major part of Sweden's emissions, accounting for approximately 21.7% of the 2021 emissions according to Boverket [Boverket, 2024]. Where approximately 60% of the emissions are from domestic production. This leads to higher demands on the construction industry, which is to be more environmentally sustainable in addition to being structurally adequate. This gives an opportunity to optimise timber as a building material, which has characteristics such as being renewable.

Cross-laminated timber (CLT) is a engineered wood product consisting of layers with glued lumber where grain direction of each consecutive layer are rotated 90°. The CLT can be used for walls, floors, and roofs, whether the building is made of pure wood or combined with other materials, such as concrete. Introducing the air gaps in the cross layers of the panel can reduces the amount of applied wood while maintaining sufficient structural performance, providing lighter structures with better sustainability.

In recent years, the usage of CLT has become more popular in the Swedish market. To reduce the ecological footprint by using more ecologically friendly and sustainable materials, such as CLT. By providing environmentally friendly solutions, CLT presents an attractive alternative to traditional building materials. CLT panels contribute to less carbon dioxide emissions and another advantage is that CLT can be recycled for use in other industries. Timber constructions give an aesthetic character that is more modern and attractive compared to other materials.

In a previous study conducted by Kurzawinska H and Tahmasebi M, they performed shear testings of CLT panels with air gaps and concluded that with overlapping air gaps gave the element higher net rolling shear and net shear modulus compared to symmetrically aligned air gaps. [Kurzawinska and Tahmasebi, 2023] They also identified the width of overlap between layers to contribute to the net shear. In another study conducted by Nilsson R and Nilsson T [Nilsson and Nilsson, 2022] about the moisture analysis of CLT, they monitored a minor increase of the vapour-permeability by the introduction of air-gaps into the solid cross-sections. Furthermore, they could not see any impairing effects on moisture safety.

1.2 Aim

The aim of this thesis is to develop a parametric model to evaluate the optimal layout and dimensions of air gaps introduced into a CLT element, based on the input of geometry and loading. The model shall fulfil the structural and hygrothermal conditions subjected to the boundaries of the element. The goal is to optimise material usage while still maintaining sufficient capabilities, which in return relieves the environmental impact.

The first objective of this thesis was to determine the structural and hygrothermal requirements of CLT elements applied in a general building. With the requirements identified, it is possible to establish the requiered structural capacity and what moisture status that needs to be avoided

The latter objective of the thesis was to develop a parametric model to determine the structural design that demands the least amount of volume under different requirements. Where the model evaluates in the iterations, the first as solid CLT elements and the second with air gaps implemented. The resulting design is taken as the basis for the investigationon the hygrothermal performance of CLT elements with air gaps in relation to solid CLT.

1.3 Methodology

This project was carried out by constructing a parametric model to obtain a wide range of different scenarios for CLT elements where the implications of adding air gaps were investigated. To be able to produce the analytical model it was needed to first identify the requirements for ordinary application of CLT, this laid the foundation for the parameters that are of interest. An evaluation was then performed on the results to see which operations resulted in the greatest volume reductions and if the ai gap widths were reasonable, if not, then the model was adapted and extended to obtain more enhanced results.

1.3.1 Analytical investigation of CLT requirements

A case study was conducted on a multistory reference CLT building to collect design requirements, demand for wall and floor design for structural capacity, and hygroscopic performance. But also, more practical requirements were also investigated. This was achieved by following Eurocode and Boverkets directives to design the elements. Designing the building with hand calculations gave a deeper understanding of where and what the introduction of air gaps would affect the performance of the building.

1.3.2 Analytical model and parametrisation

When the requirements for the general application of CLT elements were determined, an analytical model was set up for the reference building. The analytical model was first designed for traditional CLT and then based on the solid CLT it was evaluated again with air gaps introduced.

The evaluation with air gaps were conducted with different logical operations based on parameters. With the different logical operations it was posible to propose range a suitable configuration of CLT elements that fulfilled the design demands. The parameters depicted the circumstances and alternatively any predetermined dimensions, such as location, overall dimension of the structure, predetermined element dimensions, and what attribute was of most interest. The script was constructed in MATLAB.

The resulting exterior walls were then taken as input for the hygrothermal model to obtain their equivalent traits to be plugged into a numerical model (WUFI), to evaluate the performance of the hollow walls in Swedish condition in relation to its solid counter part.

1.3.3 Evaluation of optimised configurations

With the finalised parametric model, an evaluation of what is defined as an optimal design depends on what the aim is and who the stakeholder is will be conducted. The process to achieve this will be to determine a selection of stakeholders and quantify their needs in a way that defines what is considered optimised.

1.4 Limitations

In this project, Swedish conditions will be taken into consideration, and the limited focus will revolve around the building's ability to bear loads and the hygrothermal performance. No experiments will be conducted because this thesis will be based on previous studies. The reason for this is due to the limited time and capabilities. The project's aim is environmental, meaning the focus will be on reducing raw materials in wood panels and the impact of this reduction on the building, about how these panels are transported or the manufacturing process, nor the economic cost of reducing the raw materials in the CLT panels will not be mentioned. In addition to that, the connection methods between the CLT panels will not be calculated or discussed.

2

Structural Theory

CLT as a wood product has beneficial properties that have many applications in construction because the structure of the wood panels is malleable. The properties of the wood panels are malleable according to the size and shape to which it is intended to be adapted when the panels are reshaped and glued during manufacturing. Compared to traditional materials, CLT is a better choice from an environmental perspective, as wood is a fully recyclable material, and cross-laminated timber is stiff and has good strength. Large structures can withstand large loads, since wooden boards made of cross-laminated timber have good load-bearing capacity. This provides good opportunities for wood to be used in new ways, as the cross section is moldable in the plane and the geometry can be changed and even sharply curved.[Anders Gustafsson, 2019]

2.1 Material properties

CLT has orthotropic properties, which means that its mechanical qualities change depending on which way the load is applied in relation to the wood grain. Because it does not behave in a uniform way, CLT can easily spread loads along different directions, giving structures the strength and stability they need. It is also less likely to vary naturally because CLT is made up of layers. This makes the material more regular and reliable. The material qualities of CLT include a high strength-to-weight ratio, good resistance to earthquakes, and good heat protection. It can be used in a lot of different building situations because it is stable in size and does not catch fire. CLT is also recyclable, stores carbon and helps build in a way that is good for the environment.

In particular, class C24 is important when looking at the grade of wood used to make CLT, according to Brandner[Brandner et al., 2016] C24 is one of the most common strength classes used in CLT elements. The number 24 in the strength class name for softwood wood means that the wood has a minimum typical bending strength of 24 MPa. This classification ensures that the wood meets strict quality standards for its mechanical features. This means that it can be used in building uses where strength and stability are very important.

2.2 CLT design

There are three main ways in which the load can be distributed: along the x-axis, along the y-axis, and perpendicular to the plane (z-axis). Specific names for these directions are used in the CLT standard, SS-EN 16351, which is often used in structural analysis. The maximum load-bearing capacity is not always perpendicular to the x-axis, which runs parallel to the grain of the outermost layer of boards (also called the global axis in the x-direction). As a universal y-axis, the y-axis runs perpendicular to the grain of the topmost layer of the boards. The z-axis, which follows the thickness of the panel and is perpendicular to the x-y plane, stands for the global axis in the z-direction.

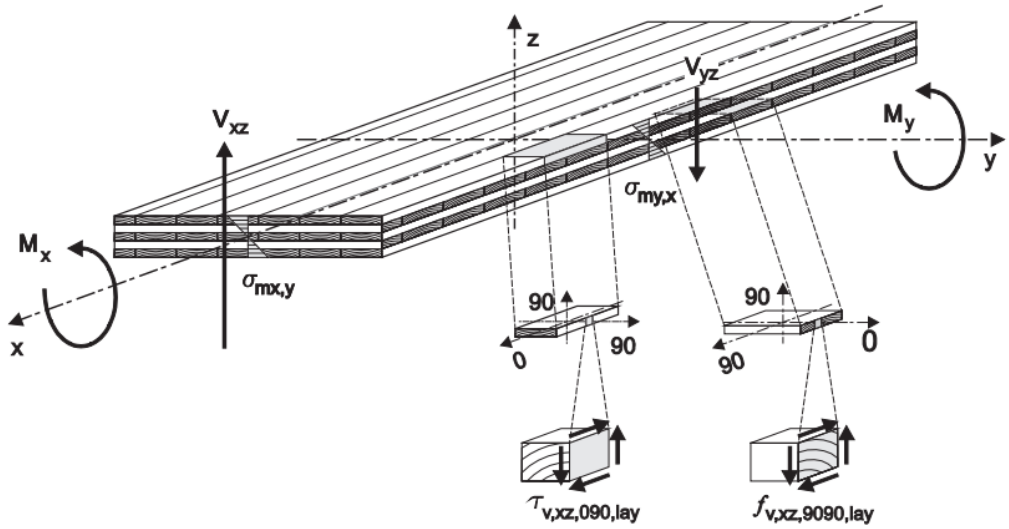

Figure 2.1: Cross laminated wood with loads perpendicular to the plane, indicators for forces, moments, resistances, and strengths [SSI 16351:2015,]

When the local axes of a board or layer are perpendicular to the grain, they are represented as 90 degrees, and when they are parallel to the grain, they are represented as 0. Shear in a plane parallel and perpendicular to the grain is indicated by the term 090, which denotes a local plane with directions of 0 and 90. To further illustrate shear on a plane perpendicular to the grain in both directions, 9090 is used to indicate a local plane with directions of 90 and 90.

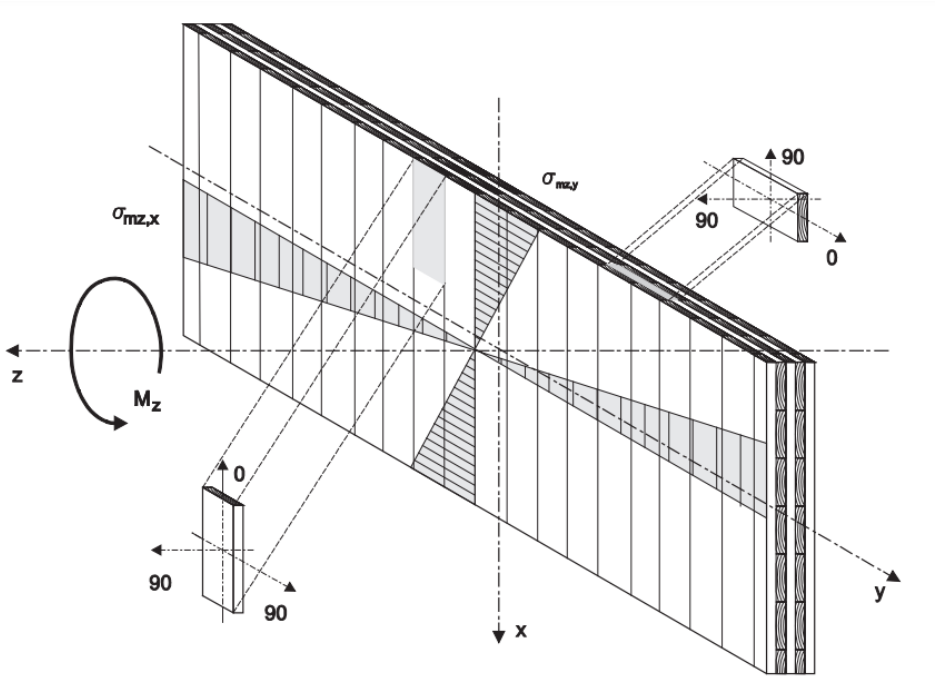

Figure 2.2: Forces,resistances, moments, , and strengths indicators in cross laminated wood with loads in the plane [SSI 16351:2015,]

For symmetrical cross-sections where the modulus of elasticity perpendicular to the grain is negligible ($E_{mm90} = 0$), it is assumed that the modulus of elasticity parallel to the grain is consistent across all boards and is represented as E_0. However, for CLT with non symmetrical or heterogeneous cross sections, additional considerations are necessary for mechanical property analysis. These designations and assumptions play a crucial role in structural assessments and design considerations for CLT components and assemblies.

2.3 Gamma method

In the CLT panels the Gamma method, a calculation method can be used as alleged in Eurocode 5 to define the deflection of a beam. The Gamma method is used to cross-sections contents of 3- and 5-layer panels, and in this way, the theory behind this method can be used to describe shear deformations, and also the cross-section bending stiffness can be calculated with the Gamma method. The method introduces even an effective moment of inertia (I_{ef}) to report the shear forces and is usable for the cross-sections with 3- and 5-layers to calculate its pure bending stiffness.

The gamma methods for 3 layers can be calculated by using these equations when the thicknesses ($t_1 = t_3$) if the cross-sections are symmetric.

$$\gamma_1 = 1 \tag{2.1}$$

$$\gamma_3 = \frac{1}{1 + \frac{\pi^2 E_{x,3} t_3}{l_{ref}^2} \frac{t_2}{G_{9090,2}}} \tag{2.2}$$

$$I_{x,ef} = \frac{b_x t_1^3}{12} + \gamma_1 b_x t_1 a_1^2 + \frac{b_x t_3^3}{12} + \gamma_3 b_x t_3 a_3^2 \tag{2.3}$$

$$a_3 = \frac{t_2}{2} + \frac{t_3}{2} \tag{2.4}$$

To use the following equations to calculate the Gamma methods for 5 layers the requirement must be met that the cross-section be symmetric so the thicknesses will be the same for the longitudinal layers ($t_1 = t_3 = t_5$) and the strength is the same ($\gamma_1 = \gamma_5$).

$$\gamma_1 = \frac{1}{1 + \frac{\pi^2 E_{x,1} t_1}{l_{ref}^2} \frac{t_2}{G_{9090,2}}} \tag{2.5}$$

$$I_{x,ef} = \frac{b_x t_1^3}{12} + \gamma_1 b_x t_1 a_1^2 + \frac{b_x t_3^3}{12} + \frac{b_x t_5^3}{12} + \gamma_5 b_x t_5 a_5^2 \tag{2.6}$$

$$a_1 = \frac{t_1}{2} + t_2 + \frac{t_3}{2} - a_3 \tag{2.7}$$

When the $a_3 = 0$.

The Gamma method is yet not applicable to cross-sections with more than 5-layer panels, to calculate cross-sections that have more than 5-layer panels the advanced method should be used, called the Extended Gamma method.[pro Holz, 2018]

2.4 Timoshenko

The beam is represented in the Timoshenko beam theory as a collection of linked components that are subject to shearing and bending deformations.[Anders Gustafsson, 2019] This method makes it possible to depict how beams perform under different loading scenarios more realistically. To account for shear deformations, the theory adds new terms to the governing equations, which improves the prediction of beam deflections and stresses.

Timoshenko beam theory relies on the shear correction factor, k, which is an essential component. The effect of shear deformation on the overall behavior of the beam is explained by this component. The characteristics of the material, the loading circumstances, and the beam's shape determine the value of k. For beams subjected to concentrated stresses or having large aspect ratios, the Timoshenko beam theory can produce more accurate findings by including the shear correction factor in the calculations.

$$k = \frac{\sum G_i A_i}{(EI_{net})^2} \int_{-\frac{h}{2}}^{\frac{h}{2}} \frac{[E(z)S(z)]^2}{G(z)b} dz \tag{2.8}$$

Layers of CLT are related to the Timoshenko technique because shear deformation in thick composite beams, such as CLT, can be accounted for using the Timoshenko beam theory. The shear in the radial-tangential plane called the rolling shear acts on the cross-layers of CLT, which is made up of orthogonal layers of structurally graded wood.[Rahman et al., 2020]

$$w = \frac{5qL^4}{384EI_{net}} + \frac{qL^2}{8S_x} \tag{2.9}$$

$$w = \frac{qL^4}{185EI_{net}} + \frac{9qL^2}{128S_x} \tag{2.10}$$

$$S_x = k_x \sum G_{xi} b_{xi} t_x i \tag{2.11}$$

Expanding on the classic Bernoulli-Euler beam theory, the Timoshenko beam theory takes shear deformation in thick beams into account. In CLT, the Timoshenko approach considers shear deformation in the cross-layers of the panels. Importantly, compared to other engineered wood products, CLT experiences more shear deformation under out-of-plane pressure because of the lower shear modulus of the cross-layers in certain orientations.[Rahman et al., 2020]

2.5 Shear Analogy Method

To anticipate the mechanical behavior of CLT panels, especially with regard to their bending and shear stiffness, the Shear Analogy Method is a popular design approach. The idea behind this approach is that by taking into account bending and shear deformation, one may get a good idea of how a CLT panel would behave.

An essential equation employed in the Shear Analogy Method is the calculation of the apparent bending stiffness (EI_{SAM}) of the composite beam. This value takes into account the combined effects of shear and bending deformation. The expression for the equation is:

$$(EI)_{SAM} = \frac{(EI)_{eff}}{\left(1 + \frac{K_s (EI)_{eff}}{(GA)_{eff} L^2}\right)} \tag{2.12}$$

$$(EI)_{eff} = \sum_{i=\parallel}^{n} E_i \cdot b \left(\frac{t_i^3}{12} + t_i \cdot a_i^2\right) + \sum_{i=\perp}^{n} E_{i,\perp} \cdot b \left(\frac{t_i^3}{12} + t_i \cdot a_i^2\right) \tag{2.13}$$

$$GA_{eff} = \frac{a^2}{\left(\frac{t_1}{2 \cdot G_1 \cdot b}\right) + \left(\sum_{i=2}^{(n-1)} \frac{t_i}{G_i \cdot b}\right) + \left(\frac{t_n}{2 \cdot G_n \cdot b}\right)} \tag{2.14}$$

$$K_s = \gamma \cdot \left(\frac{k_s}{k_b}\right) \tag{2.15}$$

Where $(EI)_{SAM}$ denotes the evident rigidity under compression. The effective bending stiffness of the composite beam is denoted by $(EI)_{eff}$. Tabel 2.1 shows the k factors for simply supported and continuous span. K_s represents a factor that is calculated as the ratio of deflection caused by bending and shear presented in Table 2.1. The effective shear rigidity of the composite beam is denoted by GA_{eff}, while the length of the beam is denoted by L.

Table 2.1: k_b and k_s factor

	Simply supported	Continuous span
k_b	$\frac{5}{384}$	$\frac{1}{185}$
k_s	$\frac{1}{8}$	$\frac{9}{128}$

The equation 2.12 facilitates the assessment of the CLT panel's overall bending stiffness through the integration of bending and shear deformation. By employing the Shear Analogy Method and analogous equations, it is possible to predict the structural behaviour of CLT panels and improving their design to suit a wide range of applications.

3

Structural Investigation

The structural investigation is divided into 5 parts, the first part was to define and design a reference building to which the study can be applied. With the reference building, the following part is addressed in which we define the requirements that the CLT elements had to fulfil to be of appropriate design. With the requirements defined, an evaluation was performed to investigate which of the stiffness models was more accurate in relation to solid CLT and hollow CLT. Then the parameterised model was created on the basis of the defined requirements and the more appropriate stiffness model.

3.1 Reference Object

To make the analytical investigation more applicable, a reference building is determined to be studied concerning the effect that hollow CLT elements bring in relation with if the building would be designed with traditional CLT. Thus, certain demands need to be setup so that any effects can be of relevance. The relevant demand is that the building is; mainly consisting of shear walls, multistory so a varying magnitude of loads can be evaluated for the walls, have a selection of different geometric for the walls and flooring to give a wider range of resulting effects.

In this case, the reference building was chosen from WoodSolutions which features a mid-rise residential building presented in Figure 3.1 [WoodSolutions, 2019]. The reference building in question was a good candidate for this project, as it consisted of multiple storeys and a variation of floor spans. It measures 34 metres wide by 22.5 metres deep and 24.8 meters high, spanning eight stories and a ground floor. In terms of use, the selected building has six apartments on every level with two cores at the centre. The mid-rise residential building taken from WoodSolutions serves as an excellent point of reference due to its consistence of shear walls and the wide selection of geometries for the walls and flooring. Primarily made up of shear walls; these elements are critical components in providing lateral support against horizontally acting wind forces.

Figure 3.1: Visualisation of building [WoodSolutions, 2019]

Picking a reference building with a larger selection of floor spans will produce a wider range of results to evaluate. It can be seen in Figure 3.2 that a varying selection of span lengths can be applied for the reference building. The floor plan of the reference building also allows the application of different spans such as simply supported or continuous span, which is described in more detail later.

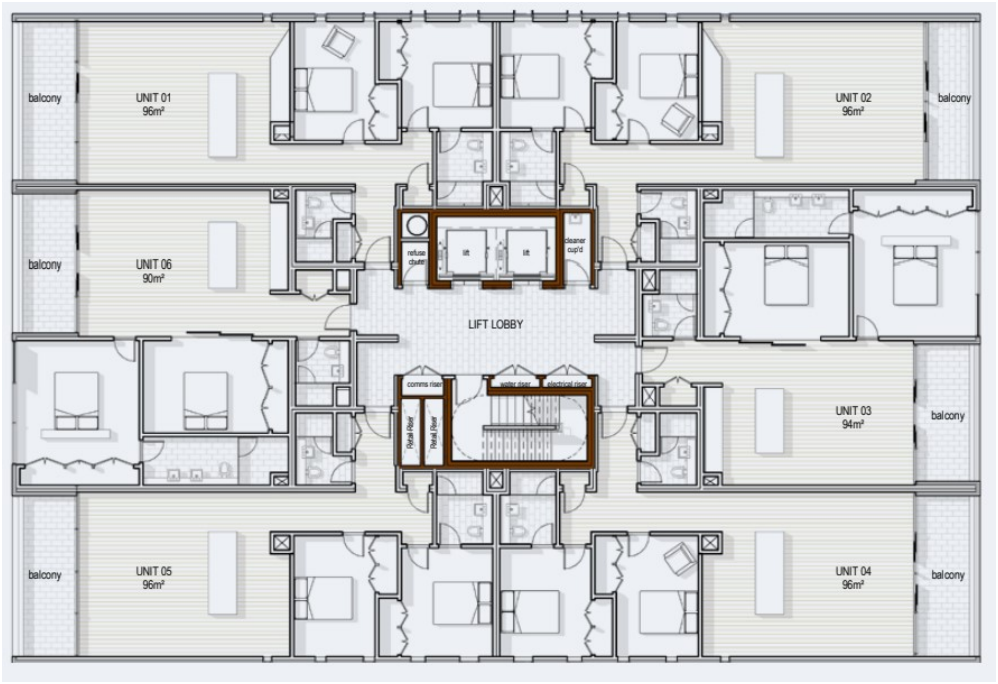

Figure 3.2: Floor plan reference building [WoodSolutions, 2019]

3.2 Modified reference Building

The determined reference building was modified in some areas to fit the objectives more closely. The major modifications were to replace any columns and beams with walls to keep the emphasis on CLT elements. The general dimensions were kept, while the placement of walls and flooring was assumed more freely and an eight-storey was added. All modifications and specifics on dimensions were produced by modelling the building in CAD software (Onshape); by doing this gives a more realistic understanding of the structural design of the building and proved to be useful as all of the wall and floor elements could be categorised and attached with relevant dimensions to be supplied as inputs for the analytical investigation. The 3D model was also parameterised so any revisions on the object could be executed with ease.

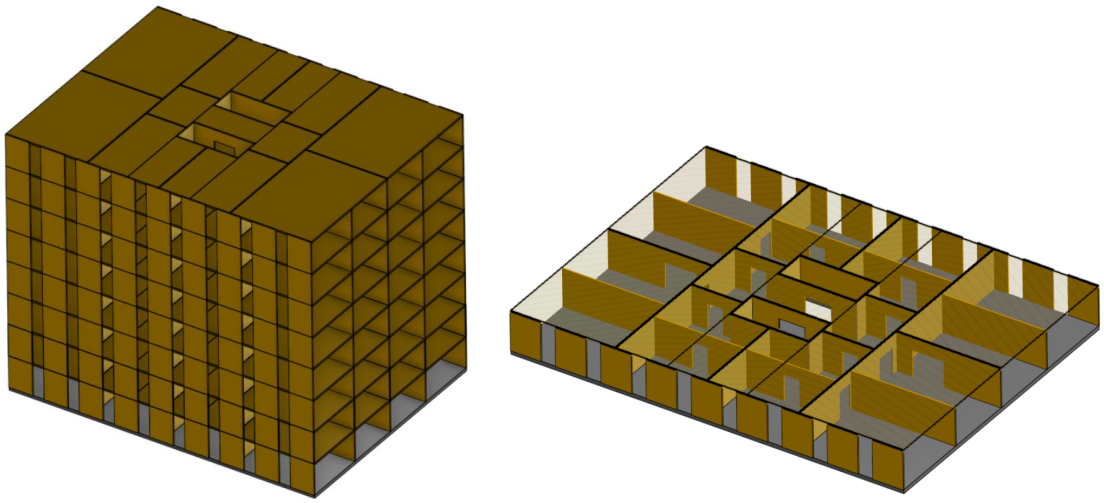

Figure 3.3: 3D model of reference building and structural floor plan.

3.2.1 Flooring Geometric

Since the structure of the building is symmetric in both directions, it was determined that there were five unique selections of floor spans presented in Figure 3.4. The floor spans labelled as *F1, F2* and *F3* where designed as continuous spans and *F4* and *F5* where designed as simply supported spans. All of the floor spans have the same direction going between the long sides. Presented in Table 3.1 are all relevant dimensions required to perform the structural investigation of the flooring.

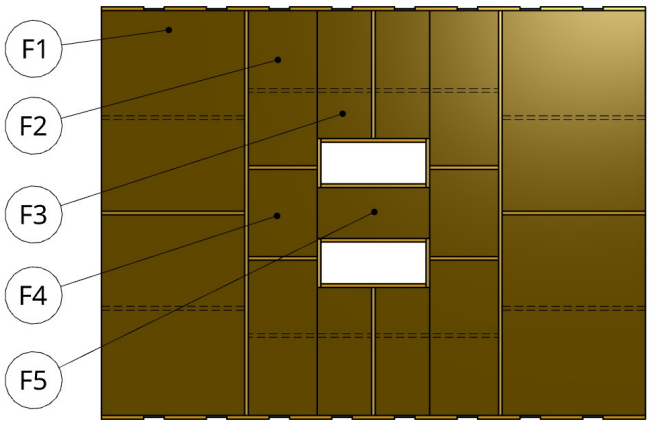

Figure 3.4: Selection of floor spans

The presented parameters in Table 3.1 are as follows; the total span length (L_{tot}), the individual span lengths if it is a coninius span (L_1, L_2) and also the width of the floor spans (B_{width}). Where all the parameters are presented for the five unique spans.

Table 3.1: Parameters of the floors from the 3D model.

L_{tot}	[m]	**F1**	11.15	**F2**	8.65	**F3**	7.15	**F4**	4.9	**F5**	2.9
L_1	[m]	**F11**	5.9	**F21**	4.4	**F31**	4.4	**F41**	4.9	**F51**	2.9
L_2	[m]	**F12**	5.15	**F22**	4.15	**F32**	2.65	**F42**	0	**F52**	0
B_{width}	[m]	**F1b**	7.95	**F2b**	3.9	**F3b**	3	**F4b**	3.9	**F5b**	6.1

3.2.2 Wall Geometric

From the reference building, it was determined that there are 10 unique walls, of which 7 were of greater interest because they obtained the highest vertical loading due to them supporting the flooring. The selection of walls for investigation is presented in Figure 3.5.

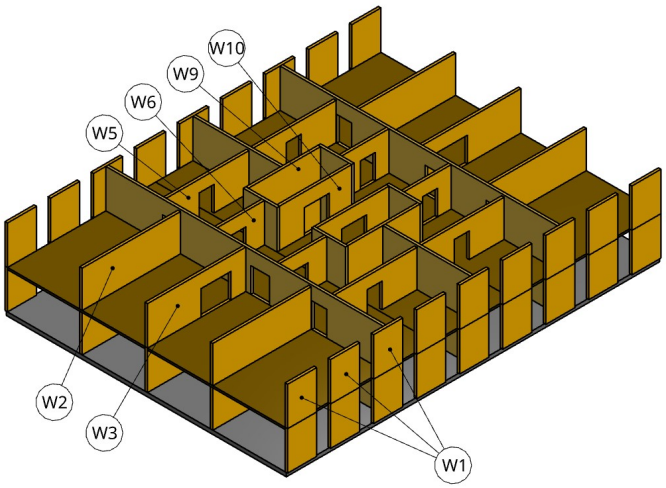

Figure 3.5: Selection unique walls

Presented in Table 3.2 is the relevant dimension needed in the investigation of walls, except for what floor span that is neighbouring. This is relevant since, depending on the span configuration, it will take a different portion of the load. The relating floor spans are as follows:

- W1 takes the load from F1 end-support.
- W2 takes the load from F1 mid-support.
- W3 takes the load from F1 end-support.
- W5 takes the load from F2 mid-support.
- W6 takes the load from F4 and F2 end-supports.
- W9 takes the load from F3 end-support.
- W10 takes the load from F5 end-support.

The parameters presented in Table 3.2 are defined as following; The total width of the wall (B_0), the width of the wall without any cutouts for doors and windows ($B_{ef,1},\ B_{ef,2}$) and the distance to neighbouring walls to estimate to evaluate the portion of the floor load going to the wall ($D_1,\ D_2$).

Table 3.2: Wall selections geometric

B_0	[m]	**W1b**	30	**W2b**	7.95	**W3b**	7.95	**W5b**	6.9
$B_{ef,1}$	[m]	**W11b**	20.997	**W21b**	7.95	**W31b**	4.35	**W51b**	2.85
$B_{ef,2}$	[m]	**W12b**	0	**W22b**	0	**W32b**	1.2	**W52b**	2.85
D_1	[m]	**W1d1**	0	**W2d1**	5.9	**W3d1**	5.15	**W5d1**	4.4
D_2	[m]	**W1d2**	5.9	**W2d2**	5.15	**W3d2**	5.15	**W5d2**	4.15

B_0	[m]	**W6b**	3.9	**W9b**	5.9	**W10b**	5.9
$B_{ef,1}$	[m]	**W61b**	1.2	**W91b**	5.9	**W101b**	2
$B_{ef,2}$	[m]	**W62b**	1.5	**W92b**	0	**W102b**	1.9
D_1	[m]	**W6d1**	4.15	**W9d1**	2.655	**W10d1**	2.9
D_2	[m]	**W6d2**	4.9	**W9d2**	0	**W10d2**	0

3.3 Analytical investigation

This section presents the necessary design requirements that are needed to evaluate the structural applicability of the CLT element.

3.3.1 Acting loads

The loads applied to the structure is wind, live and dead load. All acting loads are presented in Table 3.3 except for the self-weight of the element which depends on the dimensions of the element, where the volumetric load is taken as 5 kN/m^3.

Table 3.3: Acting loads

Imposed load	Q_k	2	kPa
Wind load	Q_w	1.7	kPa
Applied dead load	G_k	1.1	kPa

The load combinations are designed on the basis of SS-EN 1990 with the ψ-factor taken as 0.7 for residential buildings. and applied in the load combinations

$$q_{SLS} = G_k + Q_k \tag{3.1}$$

$$q_{ULS} = 1.35 \cdot G_k + 1.5 \cdot Q_k \tag{3.2}$$

$$q_{ULS,wind} = 1.5 \cdot \psi_{0,i} \cdot Q_w \tag{3.3}$$

3.3.2 Floor design criteria

The floor design is governed by three aspects; the deflection of the floor, the moment capacity, and also the eigenfrequency.

3.3.2.1 Deflection

The assessment of appropriate floor measurements in the context of CLT panels and European standards depends mainly on deflection criteria. The deflection of the floor span becomes a dictating element in floor design according to the analytical investigation described in the article. The allowed deflection limitations for a floor span are defined according to SS-EN 1995-1-1:2024 and further enhanced with other restrictions from Swedish Wood, presented in table 3.4. [Anders Gustafsson, 2019]

Table 3.4: Limitation of deflection according to SS-EN 19951-1:2024 and Swedish Wood [Anders Gustafsson, 2019].

	w_{inst}	w_{fin}
According to Eurocode 5	L/300-L/500	L/150-L/300
Based on field experience	L/400-L/600	L/200-L/250

Table 3.4 lists the permitted deflection values obtained from Eurocode 5 and actual experience together with the deflection restrictions according to SS-EN 1995-1-1:2024 and Swedish Wood. w_{inst} and w_{fin} are the two stages of deflection that are distinguished in the table. Here, instantaneous deflection is denoted by w_{inst}, and the final amount of deflection after the creep factor k_{def} is taken into account by w_{fin}.

$$w_{fin} = w_{inst}(1 + k_{def}) \quad : k_{def} = 0.8(creep\ factor) \tag{3.4}$$

Equation (3.4) denotes the acting final deflection and defines w_{fin} as a function of creep factor k_{def} and w_{inst}. The parameters including load, floor span length and stiffness $(EI)_{SAM}$, are included into the deflection formula Equation (3.5) and (3.6). The deflection values are appropriately adjusted by computing the creep factor k_{def} as 0.8 times the creep factor.

$$w_{inst} = \frac{q_{SLS} \cdot 5 \cdot L^4}{384 \cdot (EI)_{SAM}} \tag{3.5}$$

$$w_{inst} = \frac{q_{SLS} \cdot L^4}{185 \cdot (EI)_{SAM}} \tag{3.6}$$

3.3.2.2 Moment Capacity

The proper determination of the moment capacity of the floors is important for satisfying the ultimate limit state (ULS). The structure can be single-span supported or continuous-span throughout. Consequently, the maximum acting moment of both types of spans will be determined. Equation 3.8 is the determining equation for finding the moment capacity of both cases. For variable stress state, it is necessary to rigorously account for stress conditions. This analysis is crucial for the serviceability of the floor and is of great importance for safety. The given moment divided by the W_{SAM} gives the stress on the section, which is derived from the $(EI)_{SAM}$. In the next step, the design stress limit (f_{md}) will be compared to a carefully evaluated safety factor ($k_{sys} = 1{,}15$).

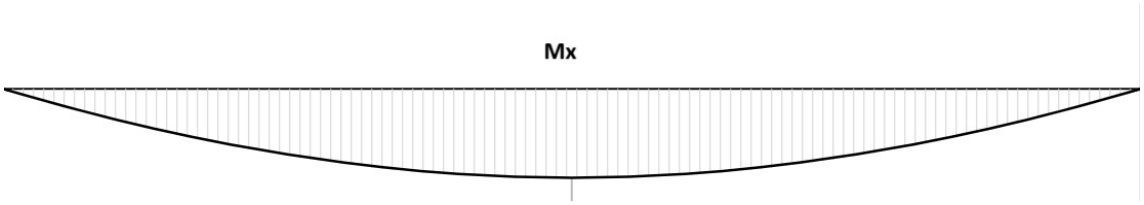

Figure 3.6: Moment diagram for one span

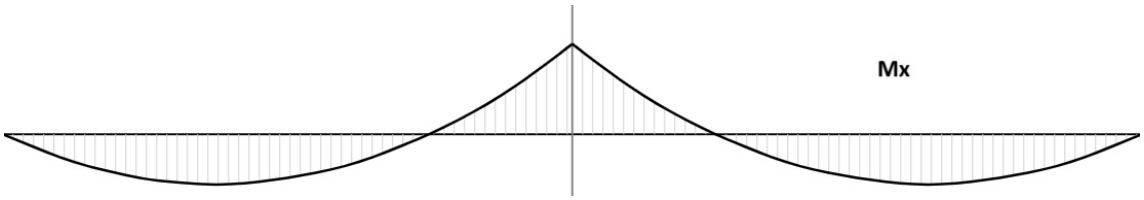

Figure 3.7: Moment diagram for continue span

The moment diagrams are important in structural analysis because the figures show how bending moments distributes across different types of spans. Figures 3.6 and 3.7 show the moment diagram for a single span and the moment diagram for a continuous span, respectively. The parabola shape in Figure 3.6 represents the highest value of a binding moment in the middle, but in Figure 3.7 because the structure is continuous, the moment distribution is different, and it shows both positive and negative moments. Equation 3.7 represents the moment at the mid-span for a simply supported beam and a continuous span. To make sure the section can hold the weight, the ultimate limit state (ULS) condition must be met by the section modulus, as shown in Equation 3.8 Thus, it can be rigorously analysed whether the section withstands the loads well enough and whether the ULS will be satisfied or not.

$$M_{max,d} = \begin{cases} \frac{q_{ULS} \cdot L^2}{8}, & ; Simply\ Supported \\ \\ MAX\left(\frac{9 \cdot q_{ULS} \cdot L^2_{max}}{128}; \frac{q_{ULS} \cdot (L_1^2 + L_2^2)}{8}\right) & ; Continius\ Span \end{cases} \tag{3.7}$$

$$\sigma_{m,d} = \frac{M_{max,d}}{W_{SAM}} \leq f_{m,d} \cdot k_{sys} \tag{3.8}$$

3.3.2.3 Compression perpendicular to grain

A alternative check is performed for the continuous floor spans to verify that the perpendicular compression of the mid support does not exceed the capacity of the floor. Since the force conducted from the walls is transferred through the continuous spans. In the sections loaded perpendicular to the grain the elements are assumed to be solid to avoid any complications of the local strength. The compressive stress is controlled against the compressive strength of the element and adjusted by the factor $k_{c,90}$ with a value of 1.9 for the CLT elements.

$$\sigma_{c,d} = \frac{N_{c,d,n}}{A_{ef}} \leq f_{c,90,d} \cdot k_{c,90} \tag{3.9}$$

A_{ef} represents the effective contact area with a compression force perpendicular to the grain, which is equal to the neighbouring wall's contact area by adding 30 mm on each side. This most likely refers to the actual area of the compressed wood rather than the whole wooden component's area.

$k_{c,90}$ is a factor that considers the degree of compression as well as how the load functions. CLT guidance values of $k_{c,90}$ depend on load location. The $k_{c,90}$ value of 1.9 is applied at the central load with a direction parallel to the grain.

3.3.2.4 Vibration (Eigen Frequencies)

The final requirement for the floor elements to fulfil is the vibration check, since the reference object is a residential building, gives a specific set of requirements according to EN-SS 1995-1-1:2004. Among the things that cause vibrations, include walking, which can give a ill perception of the structure for residents.

The lowest fundamental frequency,(f_1) is an important metric in floor vibration analysis; it is the inherent frequency of vibration for the entire floor system. Equation 3.10 follows to determine this frequency.

$$f_1 = \frac{\pi}{2L^2}\sqrt{\frac{(EI)_{SAM,L}}{m}} \tag{3.10}$$

Where it is the longitudinal stiffness that is utilised $(EI)_{SAM,L}$ and m is the mass of the floor per metre. The equation shows that the fundamental frequency will be higher with a lighter or stiffer floor. For the fundamental frequency, a comfortable range is determined to be equal to or above 8 Hz. [Anders Gustafsson, 2019].

With the lowest eigenfrequency greater than 8 Hz comes a requirement to check that the velocity response is not too high either, since higher frequencies also can be unpleasant for occupants. Whereas velocity response can indicate such a frequency if it exceeds the limit of equation 3.11 .

$$v \leq b^{(f_1\xi-1)} \tag{3.11}$$

Where b is a preset factor set to 100; ξ is the unit less damping ratio of the floor. The energy lost on the floor by friction and other internal processes is represented by the damping ratio ξ. Higher damping ratios indicate that floor vibrations fade more quickly after activation.

$$v = \frac{4 \cdot (0.4 + 0.6 \cdot n_{40})}{m \cdot B \cdot L + 200} \tag{3.12}$$

$$n_{40} = \left[\left(\left(\frac{40}{f_1}\right)^2 - 1\right) \cdot \left(\frac{B}{L}\right)^4 \cdot \left(\frac{(EI)_{SAM,L}}{(EI)_{SAM,B}}\right)\right]^{0.25} \tag{3.13}$$

3.3.3 Wall design criteria

The wall design is dictated by the combination of bending and compression load for the exterior walls and pure compression for the interior walls. The moment of inertia is derived from the shear analogy stiffness. Here, it can be noted that any modifications to the cross layers will be apparent in the k_{crit} and W_{SAM}.

$$\frac{N_{Ed} \cdot f_b}{k_{crit} \cdot A_{net} \cdot f_{c,0,d}} + \frac{M_{Ed}}{W_{SAM} \cdot f_{m,d}} \leq 1 \tag{3.14}$$

The structural design issues for CLT components must take into account the different loading scenarios, which include pure compression and compression with wind stress. It is necessary to carefully assess whether the wall can bear different weights in such circumstances. The load correction factor f_b controls how successfully loads are transmitted between wall sections and structural stability. The factor is applied to amplify the acting load, which is more apparent for walls with openings, therefore concentrating the load on solid spans of the wall.Figure 3.8 shows wall 6 which has an opening. To calculate the f_b factor by dividing b_0 over b_{ef} where b_{ef} is the summations of effective spans.

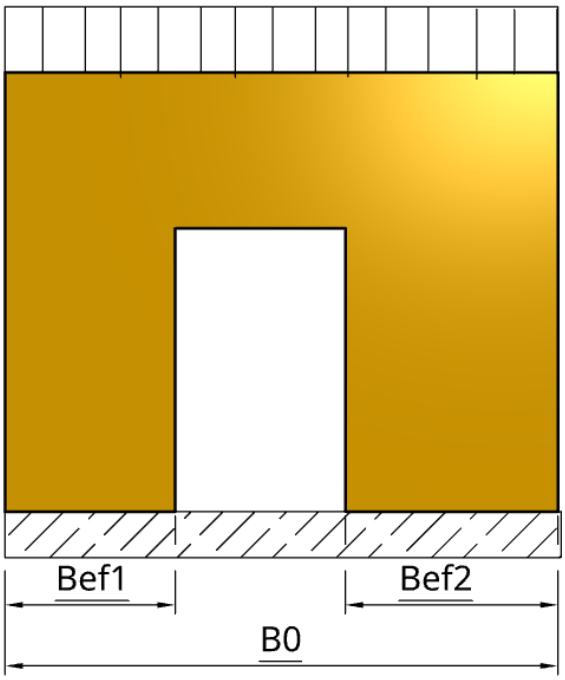

Figure 3.8: Wall panel with opening W6.

With CLT stiffness, the structural response can be understood in different loading scenarios by knowing that the critical buckling factor k_{crit} is a factor that depends on the stiffness characteristics of the wall. It is used to calculate the critical buckling load factor. The critical buckling factor is necessary to calculate the stability of the wall under compressive loads. In other words, the value of k_{crit} will help to determine the capacity of the wall to withstand buckling under compressive loads.

A_{net} is the area of the longitudinal layers within a wall. The A_{net} value is very important for the distribution and transfer of loads in the structural system. It has an immediate impact on the structural behavior and load-carrying capacity of the wall assembly. It is necessary to show via precise computation that the structure can support the vertical loads (N_{Ed}).

The bending capacity of the floor system, which is presented by the section modulus (W_{SAM}), in order to ensure structural integrity and performance. Basic to the design and study of CLT structures, these elements improve the overall effectiveness and security of the building.

3.3.4 Material properties

CLT panels with strength classes C24 display material characteristics that are necessary for applications in the structural environment. According to SS-EN 338:2016, and as shown in the table 3.5 the C24 strength class has strength and stiffness properties with bending of 24 MPa, shear strength of 4 MPa, and compression parallel and perpendicular to the grain 21 and 2,5 MPa, respectively. The C24 CLT panels provide strong resilience to different loading situations. The stiffness properties of C24 have a mean modulus of elasticity parallel bending of 11 GPa, a 5% percentile modulus of elasticity parallel bending of 7,4 GPa, mean modulus of elasticity perpendicular of 0,37 GPa, and a mean shear modulus of 0,69 GPa, ensuring the integrity and efficiency of the structure. The C24 strength class has a high degree of strength and stiffness properties that make these properties effective for load-bearing structures.

The Modification Factor k_{mod} is 0.8, according to [SSI 16351:2015,], the load duration class is medium-term and the climate class is 1 so to get design values that guarantee adequate safety, characteristic values of strength attributes are multiplied by 0.8.
The robustness of material characteristics is enabled, for example, by adding safety factors to account for volatility in material properties and increases in material flaws, by the partial factor for material, γ_M, which in this case is 1.25.

The bending design strength f_{md} is 15.36 MPa. Shows the highest stress that the wood can bear before breaking. The typical compression strength parallel to the grain f_{c0d} is 13.44 MPa important structural design criterion is the maximum stress the wood can withstand when compressed perpendicular to the grain. When stresses are applied perpendicular to the grain, its equivalent strength f_{c90d} is 1.6 MPa. This measure is necessary to evaluate the compressive resistance of grain orientation in the timber.

Table 3.5: Material data C24, MPa

	f_{mk}	$f_{c,0,k}$	$f_{c,90,k}$	$E_{m,0,mean}$	$E_{m,0,k}$	$E_{m,90,mean}$	$G_{m,0,mean}$
C24	24	21	2.50	11000	7400	370	690

3.3.5 CLT configurations

The range of configurations that is evaluated is based on 3 and 5 layer CLT elements with total heights ranging from 60 mm to 200 mm, and the layer thickness t_i being 20, 30 or 40 mm independently and 120 mm wide as a standard dimension for lumbar. The catalogue presented in Table 3.6 contains 36 different configurations, where the first 9 are 3 layered and the remaining 27 are 5 layered.

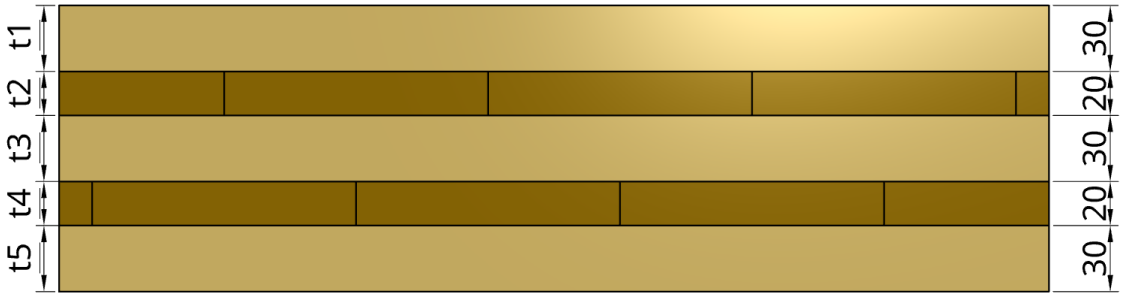

Figure 3.9: CLT arangement example, configuration number 22.

All of these configurations also include subcategories for introduced air gaps, where the air gaps are described with a formula constructed by Hanna Kurzawinska and Mohammad Tahmasebi [Kurzawinska and Tahmasebi, 2023], where the parameters are presented in Figure 3.10.

$$\lambda_{void} = \frac{a}{a+b} \tag{3.15}$$

This formula describes the volume reduction in the cross layers and can be applied in the stiffness equations to describe the effects of the air gaps, by reducing the perpendicular shear G_{90} and elasticity E_{90} with the void ratio.

$$G_{\perp} = \lambda_{void} \cdot G_{90} \qquad E_{\perp} = \lambda_{void} \cdot E_{90} \tag{3.16}$$

The void ration is also used to describe the volume reduction per square meter of the CLT element, by formulating the compact height (h_c) of the element.

$$h_c = \sum(t_{i,\parallel}) + \lambda_{void} \cdot \sum(t_{i,\perp}) \qquad V_r = 1 - \frac{h_c}{h_{tot}} \tag{3.17}$$

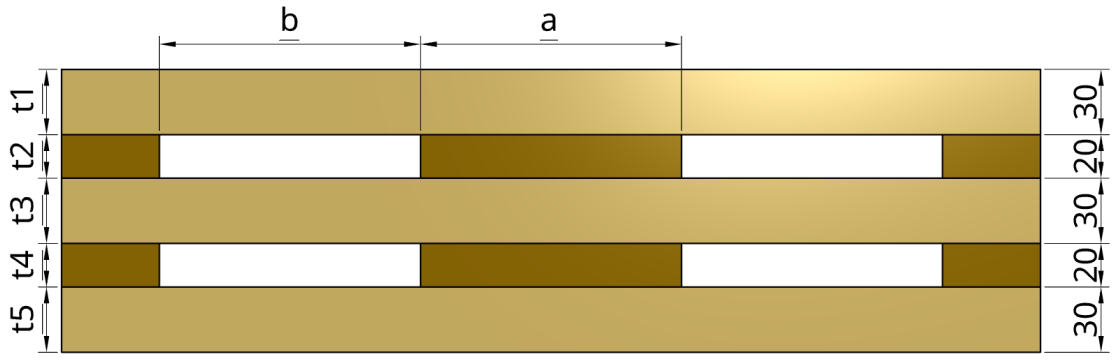

Figure 3.10: Air gap implementation example in configuration ID22

Table 3.6: Catalouge of CLT configurations

configuration id	h_{clt}	t_1	t_2	t_3	t_4	t_5
	mm	mm	mm	mm	mm	mm
1	60	20	20	20		
2	70	20	30	20		
3	80	20	40	20		
4	80	30	20	30		
5	90	30	30	30		
6	100	30	40	30		
7	100	40	20	40		
8	110	40	30	40		
9	120	40	40	40		
10	100	20	20	20	20	20
11	120	20	30	20	30	20
12	140	20	40	20	40	20
13	110	20	20	30	20	20
14	130	20	30	30	30	20
15	150	20	40	30	40	20
16	120	20	20	40	20	20
17	140	20	30	40	30	20
18	160	20	40	40	40	20
19	120	30	20	20	20	30
20	140	30	30	20	30	30
21	160	30	40	20	40	30
22	130	30	20	30	20	30
23	150	30	30	30	30	30
24	170	30	40	30	40	30
25	140	30	20	40	20	30
26	160	30	30	40	30	30
27	180	30	40	40	40	30
28	140	40	20	20	20	40
29	160	40	30	20	30	40
30	180	40	40	20	40	40
31	150	40	20	30	20	40
32	170	40	30	30	30	40
33	190	40	40	30	40	40
34	160	40	20	40	20	40
35	180	40	30	40	30	40
36	200	40	40	40	40	40

3.4 Comparison of different stiffness models.

A small study is conducted to compare the different methods of evaluating the stiffness of the cross sections which is compared with a product sheet from *Stora Enso* [Stora Enso, 2024] for floor spans of CLT. The small case study checks span from 3 to 5.5 metres with a width of 1 metre, and the loads are taken as $Q_k = 3$ kPa and $G_k = 1$ kPa and the limited deflection as $w_{inst} = L/300$ and $w_{fin} = L/250$. Worth mentioning is that the suggestions from *Stora Enso* are designed with fire resistance and also incorporates 10% C16 timber, so the dimensions are somewhat larger for shorter spans.

Table 3.7: Comparison of stiffness model.

Length [m]	3	3.5	4	4.5	5	5.5
Stora Enso recomended design						
	120 L3s	120 L3s	140 L5s	160 L5s	160 L5s	180 L5s
Shear Analogy Method						
ID	5	7	19	20	31	32
h_{clt} **[mm]**	90	100	120	140	150	170
$(EI)_{SAM}$ **[Nmm^2]**	5.81E+11	8.40E+11	1.29E+12	1.90E+12	2.62E+12	3.58E+12
γ-Method						
ID	5	6	19	20	31	32
h_{clt} **[mm]**	90	100	120	140	150	170
$(EI)_{\gamma}$ **[Nmm^2]**	6.03E+11	8.04E+11	1.32E+12	1.92E+12	2.68E+12	3.64E+12

In Table 3.7 it can be seen that the SAM produces more conservative estimations of the stiffness of the sections and ranges on average 2.15% lower than the γ-method. Based on these results, it was decided to perform the investigation based on the SAM to obtain a more conservative result.

Table 3.8: Stiffnesess for SA-method and γ-method

ID	**5**	**19**	**20**	**31**	**32**
Solid CLT					
$(EI)_{SAM}$ **[Nmm^2]**	5.81E+11	1.29E+12	1.90E+12	2.62E+12	3.58E+12
$(EI)_{\gamma}$ **[Nmm^2]**	6.03E+11	1.32E+12	1.92E+12	2.68E+12	3.64E+12
Hollow CLT: a=120, b=150 mm					
$(EI)_{SAM}$ **[Nmm^2]**	5.22E+11	1.19E+12	1.72E+12	2.44E+12	3.28E+12
$(EI)_{\gamma}$ **[Nmm^2]**	5.66E+11	1.24E+12	1.78E+12	2.53E+12	3.40E+12

The SAM model is also more appropriate for this study, as the effect of air gaps is more pronounced in the SAM than in the γ method. Whereas if an air gap ratio

of 120 mm solid and 150 mm void would be introduced, the average stiffness difference would increase to 4.38%, presented in table 3.8. Thus, the SA-method is more appropriate in an analytical study.

The two methods of determining the stiffness were further investigated by looking at how the stiffness was affected by the addition of air gaps, presented in Figure 3.11. It is clear that the SA-method is influenced to a higher degree than the γ-method.

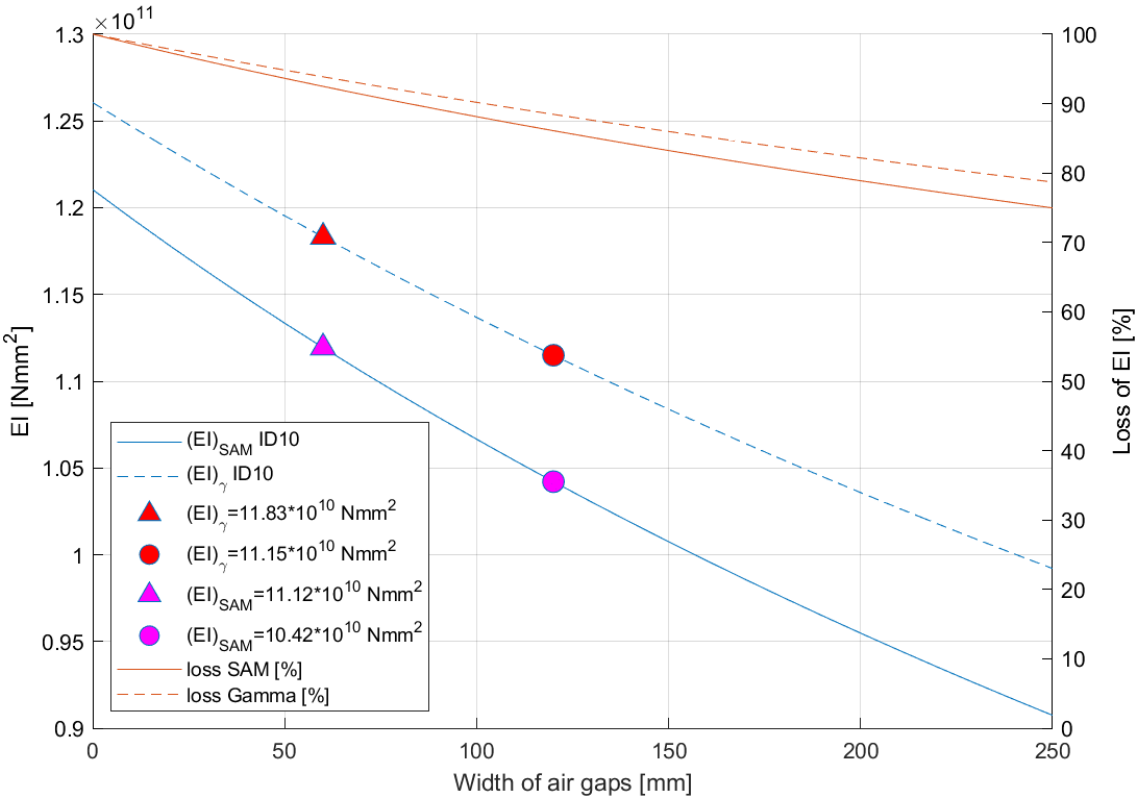

Figure 3.11: Air gaps effect on stiffness for SA-model and γ-model, ID10

3.5 Analytical computation / Logic of Operation

The computation of designing the reference building is structured in two main steps; the first is the design of the flooring and the second is the design of the walls. The reasoning of starting with the flooring was that the self-weight of the flooring was to be taken as an input to the design of the walls. This computation is made with the logical rule to reduce compact volume without increasing the thickness of the CLT elements.

3.5.1 Floor evaluation

The operation to evaluate optimal flooring in the sense of volume reduction without expanding the thickness of the element was set up in three steps; the independent evaluation of the thinnest configuration for the spans was evaluated, followed by identifying the governing floor span by maximum floor thickness. The new requirement when evaluating the floor independently is that the thickness of the resulting configurations must match the governing span. This is due to the ease of production, such that all spans will align at the top and bottom.

3.5.1.1 Determination of required stiffness

The operation of evaluating suitable CLT configurations for the floor begins with inputting all of the relevant parameters such as load case (LC), loads, span length and width. These inputs make it possible to determine what the required stiffness is in relation to the deflection and moment capacity by equations 3.18 and 3.21.

$$(EI)_{i,ed} = \frac{k_b \cdot q_{SLS,i} \cdot L_i^4}{w_{lim}} \quad ; \quad \begin{bmatrix} k_b = \frac{5}{384} & ;\text{LC 1} \\ \\ k_b = \frac{1}{185} & ;\text{LC 2} \end{bmatrix} \tag{3.18}$$

$$q_{SLS,i} = q_{SLS} + g \cdot h_{i,c} \cdot b_0 \tag{3.19}$$

Equation 3.18 is derived from section 3.3.2.1 and denotes the minimum stiffness required of the element in relation to the maximum allowed deflection. The k_b is determined if the span is simply supported (LC1) or continuous (LC2). Where w_{lim} is the the smallest allowed deflection for the floor out of the initial and final deflection limit. The limitations were decided to be L/400 for instant deflection and L/250 for final deflection. Here, it is apparent that the final deflection is the governing out of the two by extending it with the creep factor.

$$w_{fin,lim} = \frac{L_i}{250 \cdot (1 + k_{def})} \tag{3.20}$$

The required section modulus noted in Equation 3.21 where derived from Equation 3.8 and denotes the required moment capacity. Here, it denotes the maximum moment found in the span, only field moment for simply supported spans and moment

over mid support for the continuous spans. It can be noted here that then moment is determined from the ultimate limit state.

$$W_{i,Ed} = \frac{M_{i,Ed}}{k_{sys} \cdot f_{md}} \tag{3.21}$$

3.5.1.2 Determination of acting floor capacity

With the required stiffness determined, it is possible to evaluate a suitable configuration with sufficient capacity. The operation to find a suitable configuration is structured by first creating a catalogue consisting of all 36 possible configurations based on the load case, span length, and width. The catalogue consists of stiffness $(EI)_{SAM}$, section modulus (W_{SAM}), and cross section height (h_{clt}) for all configurations. The complete catalogue is then rearranged for a logical operation; where it is sorted in first order from lowest to highest stiffness, and in second order it is sorted from thinnest to thickest cross section.

With the complete and rearranged catalogue, it is possible to evaluate a suitable configuration with the least element height by returning the first configuration that satisfy both the deflection requirement and the bending capacity demand.

$$(EI)_{SAM,i,n,Rd} = \frac{(EI)_{i,n,eff}}{\left(1 + \frac{K_s (EI)_{i,n,eff}}{(GA)_{i,n,eff} L_i^2}\right)} \geq (EI)_{i,Ed} \tag{3.22}$$

$$W_{SAM,i,n,Rd} = \frac{2 \cdot (EI)_{SAM,i,n,Rd}}{E_0 \cdot h_{clt}} \geq W_{i,Ed} \tag{3.23}$$

After evaluating all of the floor span individually it is possible to determining the governing floor span by identifying the span that requires the thickest CLT element. This leads to the second iteration of the the floor evaluation where a new requirement is introduced that all configurations has to have a thickness equal to that of the governing span $(h_{gov,clt})$. Meaning that resulting configuration in all spans has to fulfil Equation 3.22 , 3.23 and 3.24.

$$h_{i,clt} = h_{gov,clt} \quad OR \quad ID_i = ID_{gov} \tag{3.24}$$

In this iteration, the incorporation of air gaps is introduced and evaluation of suitable air gap configuration. The operation is extended here with a new *for loop* where which check incorporation of air gaps from 0 to 150 mm, with increments of 10 mm and a solid counterpart of 120 mm. The logic of operation is to return the configuration with the highest possible void ratio while satisfying all three requirements.

3.5.2 Wall evaluation

After evaluating all the floor spans, it is possible to design all the walls because the load taken by the walls is dependent on the self-weight of the floor spans. The operation of designing the walls has a similar structure to that of the flooring. This operation covers and evaluates all walls on all levels.

3.5.2.1 Determination of required wall capacity

The same way as for flooring, the first operation is to determine the required capacity depending on the application and geometry of the wall. Here, the requirements are derived from Equation 3.14 to side-by-side evaluate the compression and bending capacity. For the exterior walls with wind load take both equation 3.25 and 3.27 into account while just equaiton 3.25 are inplementaed in regards to internal walls. For the wall elements where wind is acting, it is assumed to be a simply supported span, thus it is the maximum field moment that is checked.

$$P_{i,j,Ed} = N_{i,j,Ed} \cdot f_{b,i} \tag{3.25}$$

The required capacity is rearranged to primarily consist of parameters concerning the overall geometry of the wall. However, a portion of the compressive force (N_{Ed}) is dependent on the dimensions of the wall since it takes into account the self-weight of the wall, so the force is updated for each wall configuration.

$$N_{i,j,Ed} = N_{i,(j-1),Ed} + 1.35 \cdot A_{wall,i,j} \cdot h_{i,j,c} \cdot g \cdot \rho + q_{i,ULS} \cdot L_i \tag{3.26}$$

$$W_{Ed} = \frac{M_{Ed}}{f_{md}} \tag{3.27}$$

3.5.2.2 Determination of acting wall capacity

The compressive capacity of a wall is derived from Equation 3.14 where only the part containing the configuration dimension and material properties. The compressive capacity is always determined while the bending capacity is determined only if a lateral load is present. The compressive capacity of the wall (3.28) is represented by the maximum force it can maintain.

$$P_{i,n,Rd} = k_{crti,i,j} \cdot A_{net,i,j} \cdot f_{c,0,d} \tag{3.28}$$

For the cases were wind load is present the determination of bending capacity is executed the same way as for the flooring.

Where the sufficient configuration is determined by checking the combined load case. The applied logic to consider an appropriate configuration for each wall is performed by looking up the first configuration in the catalogue that can satisfy Equation 3.29.

$$\frac{P_{i,j,Ed}}{P_{i,j,n,Rd}} + \frac{W_{Ed}}{W_{Rd}} \leq 1 \tag{3.29}$$

The second evaluation were air gaps are taken n to account and evaluated are expanded with a new requirement were either the element thickness or configuration is fixed to what the solid wall was concluded to be.

$$h_{i,j,clt} = h_{i,j,initial} \quad OR \quad ID_{i,j} = ID_{i,j,initial} \tag{3.30}$$

4

Structural Results

This chapter in containing the results from appliyng the analytical model to evaluate the the floor and wall elements, with different constrains and operations.

4.1 Floor investigation results

There is a number of ways to design the floor configuration depending on the applied restriction. That is, what relations are fixed between the first iteration with solid CLT elements and the second iteration where the air gaps are introduced, this means that different relations will give a varying affect on the results such as volume reduction or degree of utilisation.

4.1.1 Air gaps effect on independent design

By investigating the floor spans independently it is possible to see how air gaps affect the performance, while the design is already fitted to be close to the limiting requirements. The two different relations that are evaluated that the hollowed section must have the same configuration as the solid evaluation presented in Table 4.3, and the relation that the hollowed section shares the same thickness as the solid evaluation presented in Table 4.5. The indicators of the flooring's performance are based on its utilisation rate in relation to moment capacity and deflection.

Table 4.1: Solid floor configuration of individual investigation

Floor ID	**L [m]**		**ID**	**CONFIG**	h_{clt}	G_k	U_M [%]		U_w
	L_1	L_2			**[mm]**	**[kPa]**	**Supp**	**Field**	[%]
F1	5.9	5.15	20	3030203030	140	1.8	94.05	30.03	98.39
F2	4.4	4.15	6	304030	100	1.6	92.97	27.67	94.39
F3	4.4	2.65	6	304030	100	1.6	67.05	27.67	94.39
F4	4.9		26	3030403030	160	1.9	0.00	30.74	99.31
F5	2.9		5	303030	90	1.55	0.00	26.01	87.97

The resulting floor configurations in Table 4.1 shows that **F4** is the governing floor span with an element thickness of 160 mm, which is expected since it is a relatively

long free span. Presented in Table 4.2 is the area of all floor spans accompanied by the volume of each span from the independent investigation of solid elements.

Table 4.2: Area and volume of each floor element independent investigation.

Flooring ID	A_i [m^2]	Nr of elements	$A_{i,tot}$ [m^2]	$V_{i,tot}$ [m^3]
F1	87.30	4	349.18	48.89
F2	32.49	4	129.96	13
F3	21.15	4	84.60	8.46
F4	18.24	2	36.48	5.84
F5	17.36	1	17.36	1.56

4.1.1.1 Hollow flooring with logic rule: ID_i=$ID_{i,initial}$

Table 4.3 presents the largest air gap possible allowed when the configurations are fixed to be the same as for the solid case, where the width of the air gaps ranged from 40 mm to 210 mm. It can be studied in Table 4.3 that floor spans 2, 3 and 5 allowed a larger width of air gaps, which is in relation to the fact that the solid use was lower than floor spans 1 and 4.

The degree of volume reductions can be seen to be influenced by the thickness of the cross-layers and the utilisation ratio of the solid composition.

Table 4.3: Hollow floor configuration, $ID_i = ID_{i,initial}$

Floor ID	ID	CONFIG	b [mm]	RED [%]	h_{clt} [mm]	G_k [kPa]	U_M [%] Supp	U_M [%] Field	U_w [%]
F1	20	3030203030	90	18.37	140	1.67	95.56	30.51	99.78
F2	6	304030	140	21.54	100	1.49	98.40	29.29	99.72
F3	6	304030	140	21.54	100	1.49	70.96	29.29	99.72
F4	26	3030403030	40	9.38	160	1.83	0.00	30.92	99.79
F5	5	303030	210	21.21	90	1.45	0.00	29.61	99.96

The resulting floor configuration in this section presents a volume reduction ranging from 9.38% up to 21.54%, where **F4** possesses the least reduction due to the fact that this span had a fairly high utilisation compared to the other spans in the solid evaluation.

Table 4.4: Resulting stiffness, $\mathrm{ID}_{i,hollow}$=$\mathrm{ID}_{i,solid}$

Floor ID	$(EI)_{solid}$ **[Nmm²]**	**b [mm]**	λ_{void} **[%]**	$(EI)_{hollow}$ **[Nmm²]**	**Differance [%]**
F1	1.93E+12	90	57	1.84E+12	4.73
F2	7.90E+11	140	46	7.26E+11	8.18
F3	7.90E+11	140	46	7.26E+11	8.18
F4	2.71E+12	40	75	2.64E+12	2.40
F5	5.77E+11	210	36	4.94E+11	14.36

In Table 4.4 it can be seen how stiffness decreases with introduction of air gaps. It looks like the stiffness decreases more rapidly for continuous spans. This could be seen more clearly in Figure 4.1 where the stiffness was investigated for two almost identical spans, the only difference being the condition of type of span. Both are of configuration **303030(ID5)** and have the span length 4.4 m. Here, it can be clearly seen that the initial stiffness is lower for the continuous spans as well as they are decreasing at a higher rate with increasing width of the air gaps.

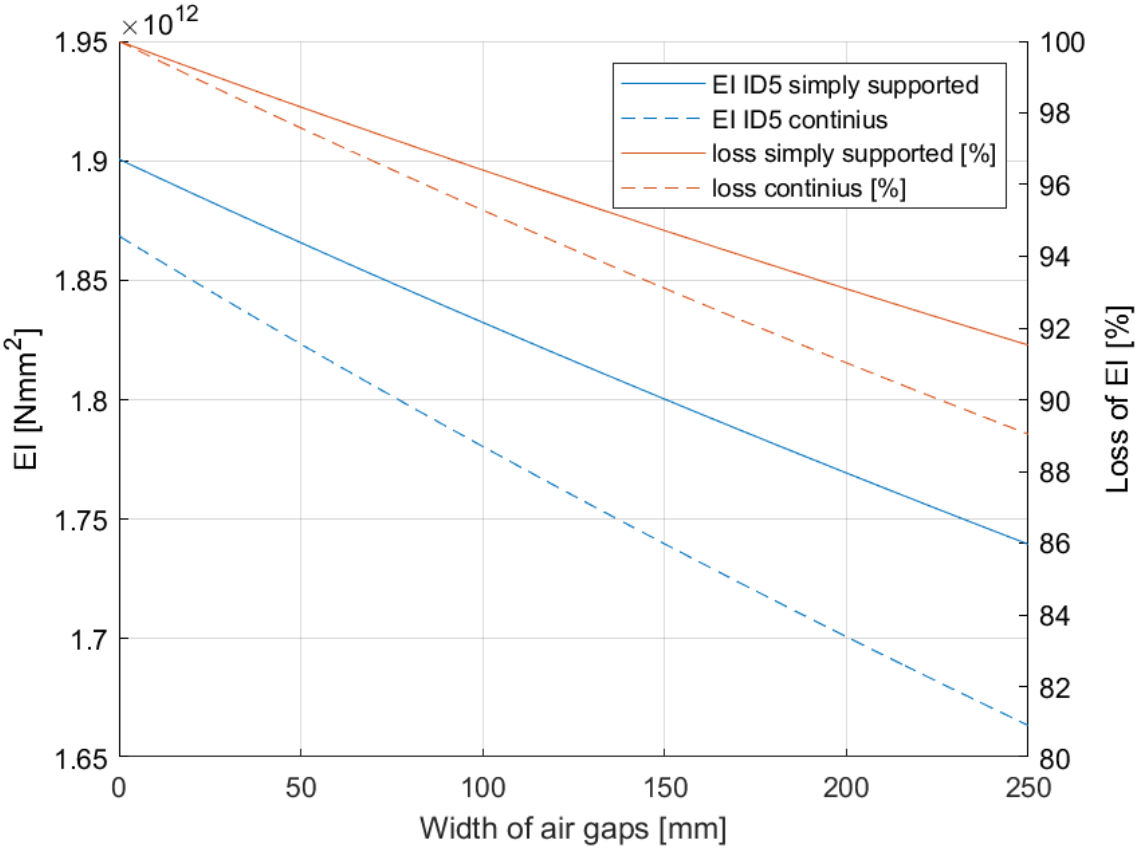

Figure 4.1: Configuration 303030 ID5, simply supported vs continuous.

4.1.1.2 Hollow flooring with logic rule: $h_i = h_{i,initial}$

The difference in the results in this section is that only the height of the flooring is fixed while the configuration is free to change to stiffer ones. Table 4.5 presents stiffer configurations to allow wider air gaps, which range from 210 mm to 410 mm.

Table 4.5: Hollow floor configuration, $h_{i,clt} = h_{i,initial}$

Floor ID	ID	CONFIG	b [mm]	RED [%]	h_{clt} [mm]	G_k [kPa]	U_M [%] Supp	U_M [%] Field	U_w [%]
F1	28	4020202040	410	22.10	140	1.65	95.73	30.56	99.91
F2	7	402040	350	14.89	100	1.53	98.47	29.31	99.85
F3	7	402040	350	14.89	100	1.53	71.01	29.31	99.85
F4	34	4020402040	400	19.23	160	1.75	0.00	30.95	99.76
F5	5	303030	210	21.21	90	1.45	0.00	29.61	99.96

Table 4.6 shows the change in stiffness in relation to its solid counter part, it can be seen that the reduction in stiffness is noted for all but floor **F5**. It also noted that for floor **F2** and **F3** the stiffness decreases but so dose also the volume reduction in Table 4.5, which show that even though the gap width is more then twice as wide as for fixed ID the resulting loss of stiffness is more rapid in relation to volume reduction for configuration **ID7** compared to configuration **ID6**.

Table 4.6: Resulting stiffness, $h_{i,hollow} = h_{i,solid}$

Floor ID	$(EI)_{solid}$ [Nmm^2]	b [mm]	λ_{void} [%]	$(EI)_{hollow}$ [Nmm^2]	Differance [%]
F1	2.18E+12	410	23	1.82E+12	16.36
F2	8.49E+11	350	26	7.32E+11	13.87
F3	8.49E+11	350	26	7.32E+11	13.87
F4	3.12E+12	400	23	2.59E+12	16.91
F5	5.77E+11	210	36	4.94E+11	14.36

4.1.2 Floor design dependent on F4; $h_{i,clt} = 160mm$

This section will evaluate a second time, the difference being that all floor elements are dictated to have the same element thickness as the governing span to ease installation of the spans. Presented in Table 4.7 is the evaluated configurations with all 160 mm element height. It can be studied that for most spans the utilisation has decreased quite significantly in comparison to the individual design as expected.

Table 4.7: Solid floor configuration, $h_{i,clt} = h_{gov,clt}$

Floor ID	ID	CONFIG	h_{clt} [mm]	G_k [kPa]	U_M [%]		U_w [%]
					Field	Supp	
F1	18	2040404020	160	1.90	99.26	31.69	90.98
F2	18	2040404020	160	1.90	62.09	18.48	39.58
F3	18	2040404020	160	1.90	44.78	18.48	39.58
F4	26	3030403030	160	1.90	0.00	30.74	99.31
F5	18	2040404020	160	1.90	0.00	15.32	29.29

4.1.2.1 Hollow flooring with logical rule: ID_i=ID_{gov}

In this section, where the floor spans are restricted to have the same ID as the governing span, there is a lower reduction over all in the governing span. The resulting dead weight of the governing span here is taken as input for the investigation of the walls. The air gaps in this section are limited to 150 mm to produce a safe estimate of the effects applied by the air gaps.

Table 4.8: Hollow floor configuration, ID_i=ID_{gov}

Floor ID	ID	CONFIG	b [mm]	RED [%]	h_{clt} [mm]	G_k [kPa]	U_M [%]		U_w [%]
							Supp	Field	
F1	26	3030403030	150	20.83	160	1.73	81.24	25.94	74.29
F2	26	3030403030	150	20.83	160	1.73	53.76	16.00	34.18
F3	26	3030403030	150	20.83	160	1.73	38.77	16.00	34.18
F4	26	3030403030	40	9.38	160	1.83	0.00	30.92	99.79
F5	26	3030403030	150	20.83	160	1.73	0.00	14.28	27.24

4.1.2.2 Hollow flooring with free gap range and logical rule: $h_{i,clt} = h_{gov,clt}$

By fixing the height of all elements to 160mm forced all the floor spans to consist of much stiffer sections than what is demanded, and by letting the width of the air gaps range freely resulted in significantly larger gaps then in the individual investigation. In Table 4.9 it is suggested that larger gaps are possible where the demanded utilisation is quite low. But, gaps in this proportion would most likely result in more issue in the local parts of the element, since the elements basically are unconnected in the span going at **F1** where the gaps suggest it possible to be wider the span itself.

Table 4.9: Hollow floor with free width range, $h_{i,clt} = h_{gov,vlt}$

Floor ID	ID	CONFIG	b [mm]	RED [%]	h_{clt} [mm]	G_k [kPa]	U_M [%] Supp	U_M [%] Field	U_w [%]
F1	34	4020402040	1130	22.60	160	1.72	99.70	31.83	91.15
F2	34	4020402040	1800	23.44	160	1.71	99.81	29.71	63.45
F3	34	4020402040	2990	24.04	160	1.71	99.95	41.26	88.10
F4	34	4020402040	400	19.23	160	1.75	0.00	30.95	99.76
F5	34	4020402040	3310	24.13	160	1.71	0.00	52.40	99.92

In table 4.10, which presents the stiffness of the hollow section in relation to the solid stiffness. The reduction of stiffness here are of a higher order to approximate as close as possible to the demanded stiffness.

Table 4.10: Resulting stiffness with free gap, $h_{i,clt} = h_{gov,clt}$

Floor ID	$(EI)_{solid}$ [Nmm^2]	b [mm]	λ_{solid} [%]	$(EI)_{hollow}$ [Nmm^2]	Differance [%]
F1	1.08E+13	1130	9.60	7.03E+12	34.88
F2	1.02E+13	1800	6.25	4.18E+12	59.17
F3	8.91E+12	2990	3.86	2.62E+12	70.63
F4	1.07E+13	400	23.08	8.93E+12	16.91
F5	9.48E+12	3310	3.50	1.83E+12	80.70

4.1.2.3 Hollow flooring with logical rule:$b_{i,max} = 150mm$, $h_{i,clt} = h_{gov,clt}$

The resulting configurations in this section is constrained to a maximum of 150 mm gap width to avoid any local problems. Due to the naturally low utilisation when applying the governing height as a requirement result with the gap being implemented with ease for all spans.

Table 4.11: Hollow floor configuration, $h_{i,clt} = h_{gov,clt}$

Floor ID	ID	CONFIG	b [mm]	RED [%]	h_{clt} [mm]	G_k [kPa]	U_M [%] Supp	U_M [%] Field	U_w [%]
F1	21	3040204030	150	27.78	160	1.68	84.64	27.02	77.34
F2	18	2040404020	150	27.78	160	1.68	66.56	19.81	42.29
F3	18	2040404020	150	27.78	160	1.68	48.00	19.81	42.29
F4	29	4030203040	150	20.83	160	1.73	0.00	29.63	95.52
F5	18	2040404020	150	27.78	160	1.68	0.00	17.44	33.24

By studying Table 4.11, it can be stated that even with a constrained air gap width, a proportionally higher reduction in volume will occur. But the utilisation stated in the same table shows that most of the floor spans are relatively under-utilised. With this it can be stated that if the constraint of the gap width is wished to be removed a more inept investigation is required for the sections that are hollow.

Table 4.12: Resulting stiffness, $h_{i,clt} = h_{i,gov}$

Floor ID	$(EI)_{solid}$ $[Nmm^2]$	**b** **[mm]**	λ_{solid} [%]	$(EI)_{hollow}$ $[Nmm^2]$	**Differance** [%]
F1	9.07E+12	150	44.4	8.2E+12	9.63
F2	7.04E+12	150	44.4	6.22E+12	11.74
F3	6.13E+12	150	44.4	5.41E+12	11.74
F4	1.03E+13	150	44.4	9.3E+12	9.97
F5	6.56E+12	150	44.4	5.46E+12	16.89

4.1.3 Local requirements of flooring; $h_{i,j,hollow} = h_{i,j,solid}$

This section aims to expand on the the flooring investigation by implementing the optimised logical operation, as well as introducing checks of the local effect for wider air gaps.

$$ID_{i,j,new} \quad if \; V_{r,i,j,new} \geq V_{r,i,j,old} \tag{4.1}$$

The added controls in this section check the capacity of the outer layers of the CLT element so that no local failure are prone to occur, where the executed checks are:

- $M_{loc,Rd}$: Bending capacity over the solid cross layer (1)

$$M_{loc,support,Ed} = \frac{q_{i,ULS} \cdot b_i^2}{8} \leq M_{loc,Rd} = \frac{W_{loc}}{f_{md}} \tag{4.2}$$

- COM_{loc}: Bending and compressive capacity for the top layer (2)

$$\frac{M_{loc,field,Ed}}{M_{loc,Rd}} + \frac{N_{loc,c,Ed}}{A_{loc} \cdot f_{c,0,d} \cdot k_{loc,crit}} \leq 1 \tag{4.3}$$

- $w_{loc,ed}$: Deflection of the the top layer (2)

$$w_{loc,Ed} = \frac{0.007 \cdot q_{i,SLS} \cdot b_i^4}{E_{\parallel} \cdot I_{loc}} \leq w_{loc,lim} = \frac{b_i}{250 \cdot (1 + k_{def})} \tag{4.4}$$

- $N_{loc,t,Rd}$: Tensile capacity for the bottom layer (3)

$$N_{loc,t,Ed} \leq A_{loc} \cdot f_{t,d} \tag{4.5}$$

Where the geometry are dependant on the outer layers:

$$I_{loc} = \frac{B_0 \cdot t_1^3}{12}; \quad W_{loc} = \frac{B_0 \cdot t_1^2}{6}; \quad A_{loc} = B_0 \cdot t_1 \tag{4.6}$$

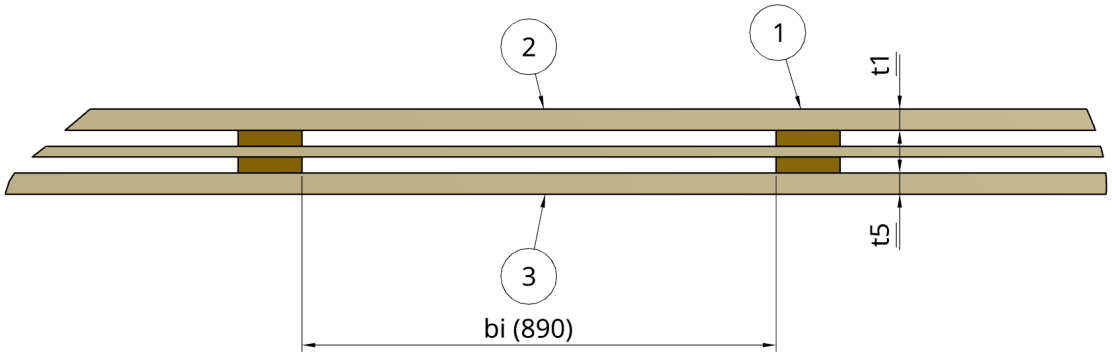

Figure 4.2: Location of local checks

The resulting layout from the implementation of the local evaluation and the optimised operation presents a significant reduction in floor volume, which can be seen

in Table 4.13. It can be stated that most of the floor spans are utilising most of the global capacity for the floor elements except for floor span **F3** and **F5** which are constrained by the local evaluation.

Table 4.13: Floor configuration with local requirements

Floor ID	**ID**	**CONFIG**	**b** [**mm**]	**RED** [%]	h_{clt} [**mm**]	G_k [**kPa**]	U_M [%]		U_w [%]
F1	21	3040204030	490	40.16	160	1.58	99.76	31.85	91.00
F2	21	3040204030	980	44.55	160	1.54	99.78	29.70	63.26
F3	21	3040204030	1300	45.77	160	1.53	84.07	34.70	73.89
F4	29	4030203040	230	24.64	160	1.70	0.00	30.95	99.71
F5	21	3040204030	1300	45.77	160	1.53	0.00	39.01	74.19

Here, it can also be studied that the over all reduction of the stiffness is relatively great but this is due to the initially low utilisation of the capacity for the solid case.

Table 4.14: Resulting stiffness local investigation

Floor ID	$(EI)_{solid}$ [Nmm^2]	**b** [**mm**]	λ [%]	$(EI)_{hollow}$ [Nmm^2]	**Differance** [%]
F1	9.07E+12	490	19.67	6.78E+12	25.27
F2	8.49E+12	980	10.91	4.00E+12	52.82
F3	7.38E+12	1300	8.45	2.97E+12	59.72
F4	1.03E+13	230	34.29	8.83E+12	14.46
F5	7.71E+12	1300	8.45	2.35E+12	69.53

4.2 Results from wall investigation

The investigation of the walls is carried out assuming that all flooring has the same configuration, which was taken as configuration ID 26 with 40 mm air gaps, giving a dead load (G_k) of 1.83 kPa. Further on, all of the walls are 3.1 metres tall and only wall 1 is subjected to wind load. The findings will be presented for different applied logics and limits of the air gap widths.

4.2.1 Wall evaluation without air gaps

From the investigation it can be seen in Table 4.15 that the walls on floor 7 and 8 as well as most of walls 9 and 10 is dominated by configuration ID 1 which is the 3-layered CLT element consisting of 20 mm lamellae. This is because it is the least stiff configuration outside the catapult, and in these locations the utilisation is quite low, in general. It is also noted that only three wall segments consist of five-layered elements, which are located in the first and second floors.

Table 4.15: Wall configuration without air gaps: ID_{solid}

Floor	W1	W2	W3	W5	W6	W9	W10
8	1	1	1	1	1	1	1
7	1	1	1	1	1	1	1
6	2	2	2	2	2	1	1
5	2	3	3	3	3	1	1
4	3	5	4	4	3	1	1
3	3	5	5	5	5	1	2
2	4	10	5	10	5	1	2
1	5	6	10	6	10	1	2

ID	CONFIG
1	202020
2	203020
3	204020
4	302030
5	303030
6	304030
10	2020202020

In Figure 4.3 all utilisation ratios based on equation 3.29 where it can be seen that any decrease in utilisation compared to the storey above is due to a change in configuration to a stiffer one. What can be seen is that the utilisation of wall 1 to 6 is approximately 75% as the lowest for floors 7 to 1, which indicates that a portion of the walls is not being utilised to its fullest extent.

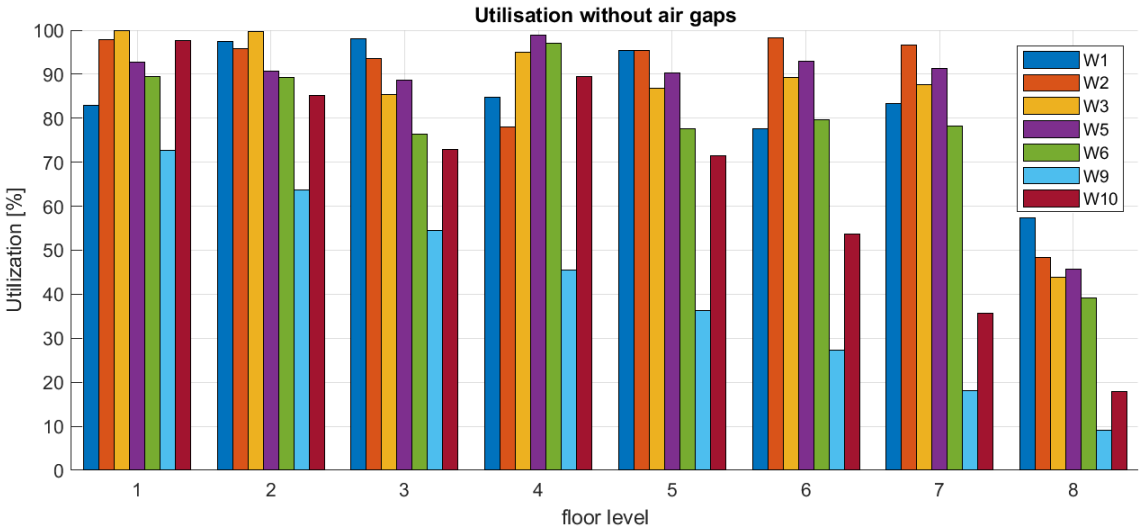

Figure 4.3: Utilisation ratio off all walls

Presented in Table 4.16 the total volume of each wall selection and the area of a single wall in the selection extended with the number of each wall per floor. Here, it can be seen that the main part of the total volume will come from wall 1 and is followed by wall 6. The volume of raw materials demanded for all these walls is **262.47 m^3**.

Table 4.16: Total volume of each wall selection, $[m^3]$

Floor	W1 $[m^3]$	W2 $[m^3]$	W3 $[m^3]$	W5 $[m^3]$	W6 $[m^3]$	W9 $[m^3]$	W10 $[m^3]$
8	7.80	5.59	2.36	4.24	2.25	2.16	1.68
7	7.80	5.59	2.36	4.24	2.25	2.16	1.68
6	9.10	6.52	2.76	4.94	2.63	2.16	1.68
5	9.10	7.46	3.15	5.65	3.00	2.16	1.68
4	10.40	8.39	3.15	5.65	3.00	2.16	1.68
3	10.40	8.39	3.55	6.35	3.38	2.16	1.96
2	10.40	9.32	3.55	7.06	3.38	2.16	1.96
1	11.70	9.32	3.94	7.06	3.75	2.16	1.96

	A $[m^2]$	nr of walls
W1	65.10	2
W2	23.31	4
W3	19.69	2
W5	17.66	4
W6	9.38	4
W9	17.98	2
W10	**13.98**	2

4.2.2 Hollow walls with logical rule: $ID_{hollow,i,j}$=$ID_{initial,i,j}$

This section will treat the investigation where the selection of configuration ID is fixed to be the same as for when the walls are evaluated as solid. The results are compared with the solid evaluation.

4.2.2.1 Limiting the air gaps to 150 mm, $ID_{i,j}$=$ID_{initial,i,j}$

When limiting the width to 150 mm, it could be seen that it was possible to implement the full range in most of the walls. In Figure 4.4 it can be seen that the utilisation ratio of the lowest approximation for walls 1 to 6 for floors 7 to 1 increases from 75% to 80%, and the utilisation of many walls is close to 100%.

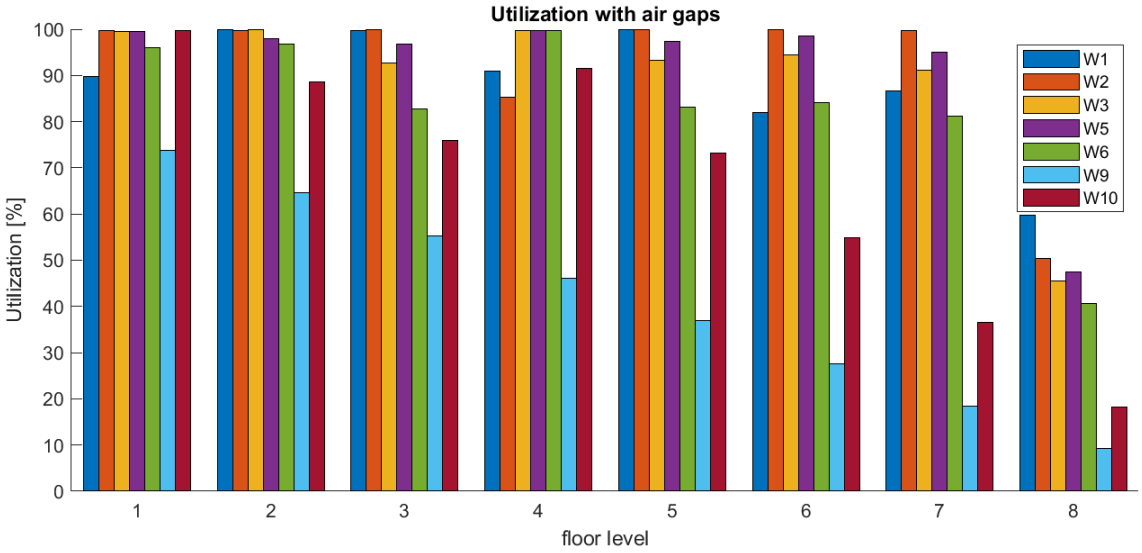

Figure 4.4: Utilisation ratio with air gap widths limited to 150 mm

In Table 4.17 the applied widths of the air gaps are presented for each individual wall. Here, it is clear that the analytical model would allow wider gaps than 150 mm for most of the walls. And for walls where the width is less than 150 mm is due to the utilisation resulting as close to 100% as possible.

Table 4.17: Air gap widths,b [mm]

Floor	W1	W2	W3	W5	W6	W9	W10
8	150	150	150	150	150	150	150
7	150	120	150	150	150	150	150
6	150	50	150	150	150	150	150
5	130	90	150	150	150	150	150
4	150	150	130	40	70	150	150
3	60	110	150	150	150	150	150
2	90	80	20	150	150	150	150
1	150	30	10	100	150	150	110

Figure 4.5 presents the magnitude of change of the utilisation in relation to the solid investigation. It can be studied here that the walls with a thicker cross layer lose more of its stiffness then the ones with 20 mm cross section thickness. This can be seen by looking at the change in wall 3 to 6 from floor 7 to 6, where the cross layer goes from 20 mm to 30 mm. Another interesting point is the small change in utilisation for wall 3 on floor 1 and 2, where the change is minimal due to only 20 mm width is allowed, and on floor one the utilisation is in fact lower where air gaps are introduced this is most likely due to the overall load being lower thanks to the volume reduction. Thus the impact on the utilisation is a combination of the width of the gaps and the height of the cross layers.

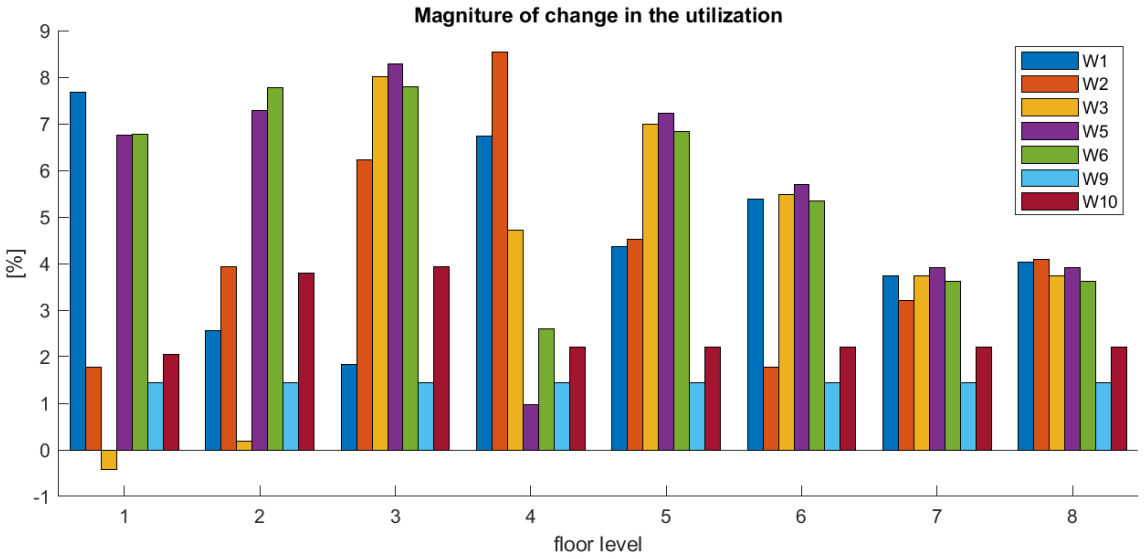

Figure 4.5: Magnitude of change in relation to solid investigation.

The overall volume reduction presented in Table 4.18 show that a meaningful saving of raw materials is plausible. Leaving a total volume reduction of 18.28% or 47.98 m^3 of the total 262.47 m^3 timber needed for the walls in the building.

Table 4.18: Volume reduction per square metre,V_r [%]

Floor	W1	W2	W3	W5	W6	W9	W10
8	18.52	18.52	18.52	18.52	18.52	18.52	18.52
7	18.52	16.67	18.52	18.52	18.52	18.52	18.52
6	23.81	12.61	23.81	23.81	23.81	18.52	18.52
5	22.29	21.43	27.78	27.78	27.78	18.52	18.52
4	27.78	18.52	13.00	6.25	18.42	18.52	18.52
3	16.67	15.94	18.52	18.52	18.52	18.52	23.81
2	10.71	16.00	4.76	22.22	18.52	18.52	23.81
1	18.52	8.00	3.08	18.18	22.22	18.52	20.50

4.2.2.2 Air gaps limited to 700 mm, $ID_{i,j}$=$ID_{initial,i,j}$

In this section the limit of the air gap width is increased to 700 mm to acquire a greater utilisation for the more part of the walls, which can be studied in Figure 4.6. The limit of 700 mm was chosen so that walls 1 to 6 on floor 7 to 1 could present the largest allowed gaps based on this structural model, which can be seen as only wall 6 on the 7th floor would allow even bigger air gaps.

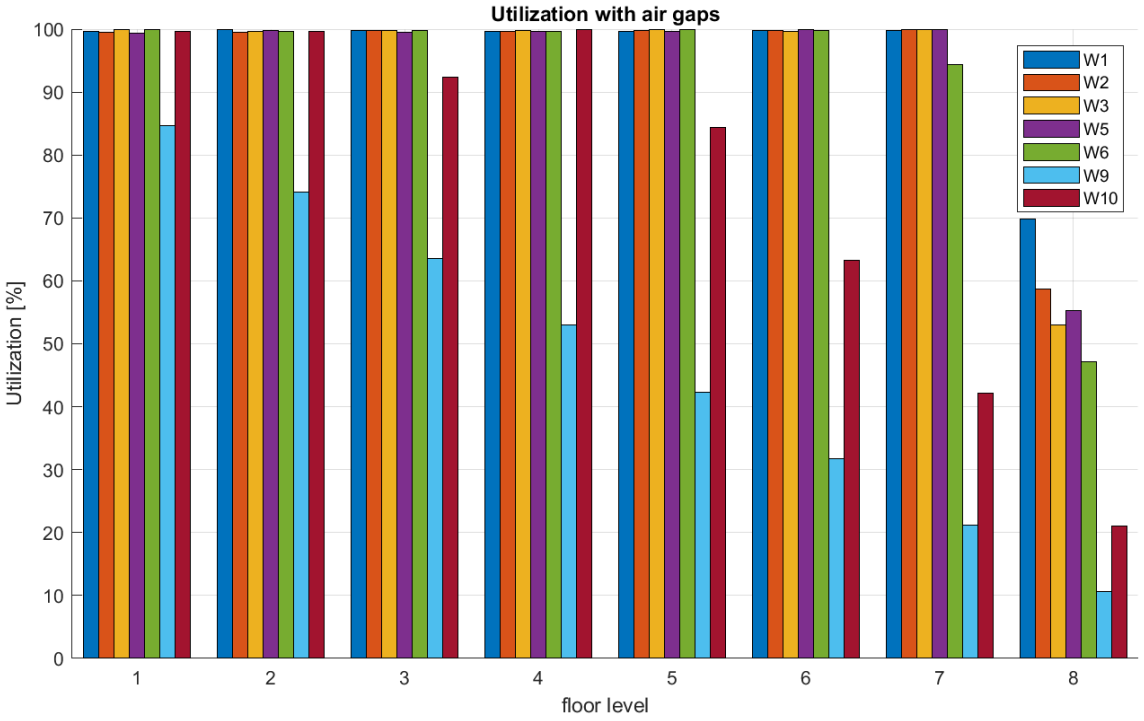

Figure 4.6: Utilisation with b_{max} = 700 mm, $ID_{hollow,i,j}$=$ID_{initial,i,j}$

By comparing Table 4.19 with Table 4.17 one can see that for some of the fully utilised walls the widths actually increase, which are highlighted in Table 4.19. The increased widths within these walls are due to a decrease in load caused by the mass reduction. Where in Table 4.19 the second values in the cells are taken from Table 4.17.

Table 4.19: Widths of air gaps, b_{max} = 700 mm, $ID_{hollow,i,j}$=$ID_{solid,i,j}$

Floor	W1 [mm]	W2 [mm]	W3 [mm]	W5 [mm]	W6 [mm]	W9 [mm]	W10 [mm]
8	700	700	700	700	700	700	700
7	660	130 (120)	480	330	700	700	700
6	670	50	290	190	600	700	700
5	140 (130)	90	290	200	540	700	700
4	340	430	140 (130)	40	80 (70)	700	500
3	70 (60)	110	280	200	500	700	700
2	100 (90)	80	20	190	210	700	480
1	340	30	20 (10)	100	240	700	140 (110)

The change in utilisation shown in Figure 4.7 shows an overall increase in utilisation for the walls that were previously constrained by the 150 mm air gaps.

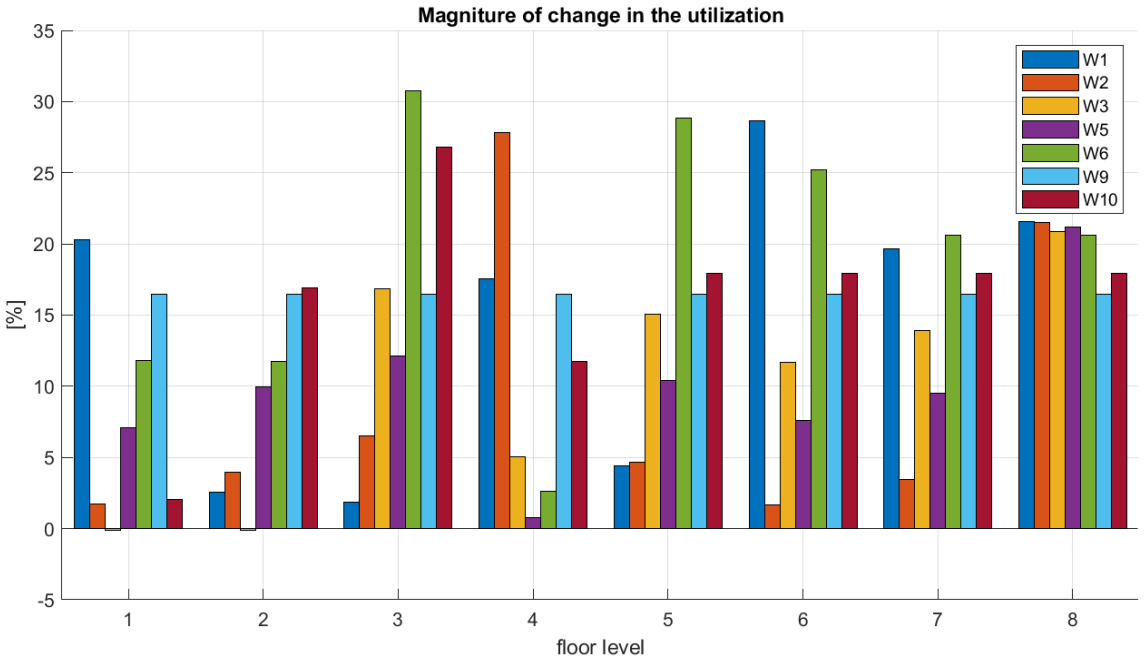

Figure 4.7: Magnitude of change in relation to solid utilisation, $b_{max} = 700\ mm$

The volume reduction was observed to be **23.27%**. This significant decrease in volume highlights the effectiveness of the method employed. The volume reduction was **61.08** m^3 when most of the walls reached the highest possible width of the air gaps. After the process, the volume was reduced to **201.39** m^3 out of the initial **262.47** m^3. This shows a substantial reduction in volume, validating the impact of air gap implementation.

Table 4.20: Volume reduction, V_r [%]

Floor	W1	W2	W3	W5	W6	W9	W10
8	28.46	28.46	28.46	28.46	28.46	28.46	28.46
7	28.21	17.33	26.67	24.44	28.46	28.46	28.46
6	36.35	12.61	30.31	26.27	35.71	28.46	28.46
5	23.08	21.43	35.37	31.25	40.91	28.46	28.46
4	36.96	26.06	13.46	6.25	20.00	28.46	26.88
3	18.42	15.94	23.33	20.83	26.88	28.46	36.59
2	11.36	16.00	4.76	24.52	21.21	28.46	34.29
1	24.64	8.00	5.71	18.18	26.67	28.46	23.08

4.2.3 Hollow walls with logical rule: $\mathbf{h}_{i,j}$=$\mathbf{h}_{initial,i,j}$

This section will investigate the the resulting impact of air gaps when the logic to only keep the thickness (h_{clt}) of the element fixed while it is free to chose a stiffer configuration then for the solid investigation.

4.2.3.1 Air gaps limited to 150 mm, $h_{i,j} = h_{initial,i,j}$

When limiting the air gap width to 150 mm will result in a current ID in 7 positions on walls 1 to 6, pressented in Table 4.21. These up-dates can be seen as having a higher characteristic stiffness, where a large part of the thickness is dedicated to the outer longitudinal layers.

Table 4.21: ID change, $b_{max} = 150\ mm$

Floor	W1	W2	W3	W5	W6	W9	W10
8	1	1	1	1	1	1	1
7	1	1	1	1	1	1	1
6	2	2	2	2	2	1	1
5	2	4 (3)	3	3	3	1	1
4	3	5	4	4	4 (3)	1	1
3	4 (3)	5	5	5	5	1	2
2	4	6 (10)	5	10	5	1	2
1	5	7 (6)	6 (10)	7 (6)	10	1	2

ID	CONFIG
1	202020
2	203020
3	204020
4	302030
5	303030
6	304030
7	402040
10	2020202020

The utilisation presented in Figure 4.8 shows that most of the wall elements can allow even wider air gaps, based on the fact that the utilisation of walls 1 to 6 on floors 7 to 1 shows utilisation ranging between approximately 80% and almost 100%.

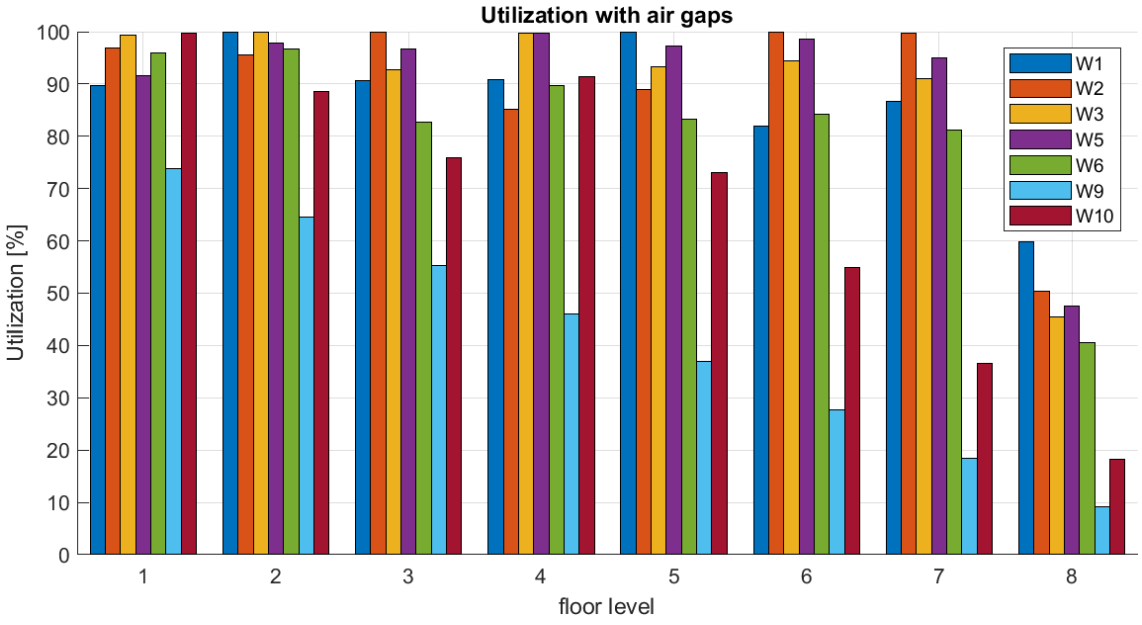

Figure 4.8: Wall utilisation with air gaps capping at 150 mm, $h_{i,j} = h_{initial,i,j}$

The air gap widths applied presented in Table 4.22 highlights the positions where the ID was updated to show the continuity of this logic, where the widths from the fixed ID are also presented. It can be noted that this logic tends to reach the width limit in these positions since the updated configuration have a stiffer character.

Table 4.22: Air gap widths, $b_{max} = 150\ mm$, $h_{hollow,i,j} = h_{solid,i,j}$

Floor	W1	W2	W3	W5	W6	W9	W10
8	150	150	150	150	150	150	150
7	150	120	150	150	150	150	150
6	150	50	150	150	150	150	150
5	130	150 (90)	150	150	150	150	150
4	150	150	130	40	150 (70)	150	150
3	150 (60)	110	150	150	150	150	150
2	90	150 (80)	20	150	150	150	150
1	150	150 (30)	150 (10)	150 (100)	150	150	110

The impact of the updated configurations becomes more apparent in Figure 4.9, where it shows a decrease in utilisation compared to the solid composition, presented by the negative bars.

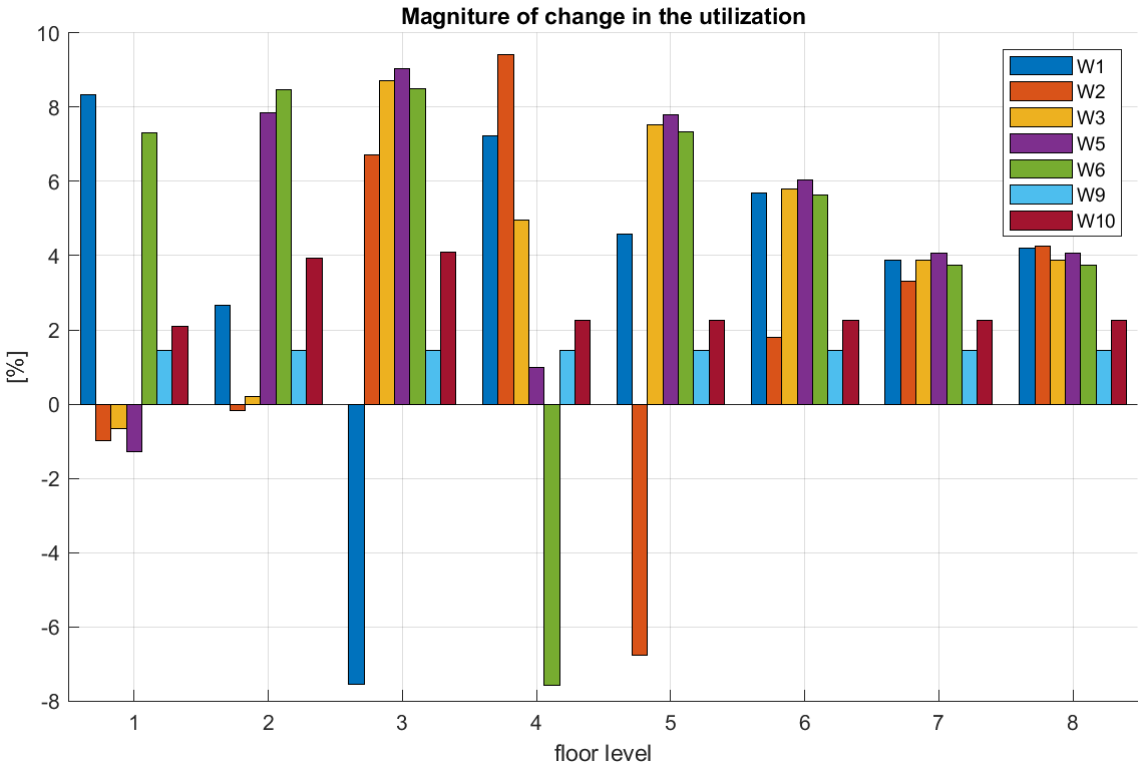

Figure 4.9: Magnitude of change, $b_{max} = 150\ mm$, $h_{i,j} = h_{soliid,i,j}$

The resulting volume reduction from this logic gives a volume reduction of 18.33% which is about 0.05% higher than for a fixed ID with the same limit. The reductions for with fixed ID are presented in Table 4.23 in the highlighted sections, where it can

be seen that the reduction increases only for three of these positions. The reason for the decrease in the reduction is the change in cross-layer height to a smaller thickness, whereas the increase in the air-gap width is proportionally small. Hence, the change of configuration is more favourable if the proportional increase of width is greater than the proportional reduction of cross-layer thickness.

Table 4.23: Volume reduction per square metre [%]

Floor	W1	W2	W3	W5	W6	W9	W10
8	18.52	18.52	18.52	18.52	18.52	18.52	18.52
7	18.52	16.67	18.52	18.52	18.52	18.52	18.52
6	23.81	12.61	23.81	23.81	23.81	18.52	18.52
5	22.29	**13.89 (21)**	27.78	27.78	27.78	18.52	18.52
4	27.78	18.52	13.00	6.25	13.89 (6)	18.52	18.52
3	**13.89 (17)**	15.94	18.52	18.52	18.52	18.52	23.81
2	10.71	22.22 (16)	4.76	22.22	18.52	18.52	23.81
1	18.52	11.11 (8)	22.22 (3)	**11.11 (18)**	22.22	18.52	20.50

4.2.3.2 Air gaps limited to 700 mm, $h_{i,j} = h_{initial,i,j}$

In this section the limit of the gap width is increased to 700 mm to provide more data on the limits of the walls on floor 7 to 1. With an increased limit of gap widths results in a larger selection of walls updating their configurations, which are highlighted in Table 4.24 and presented with the previous ID.

Table 4.24: Updated ID, $b_{max} = 700\ mm$

Floor	W1	W2	W3	W5	W6	W9	W10
8	1	1	1	1	1	1	1
7	1	1	1	1	1	1	1
6	2	2	2	2	2	1	1
5	2	4(3)	4(3)	4(3)	4(3)	1	1
4	4(3)	5	4	4	4(3)	1	1
3	4(3)	5	5	5	5	1	2
2	4	7(10)	5	7(10)	5	1	2
1	5	7(6)	7(10)	7(6)	7(10)	1	2

ID	CONFIG
1	202020
2	203020
3	204020
4	302030
5	303030
6	304030
7	402040
10	202020

With the increased limit of the gap width it is clear that walls 1 to 5 on floor 7 to 1 are utilised to its fullest extend while wall 6 is fully utilised on most floor, which is presented in Figure 4.10.

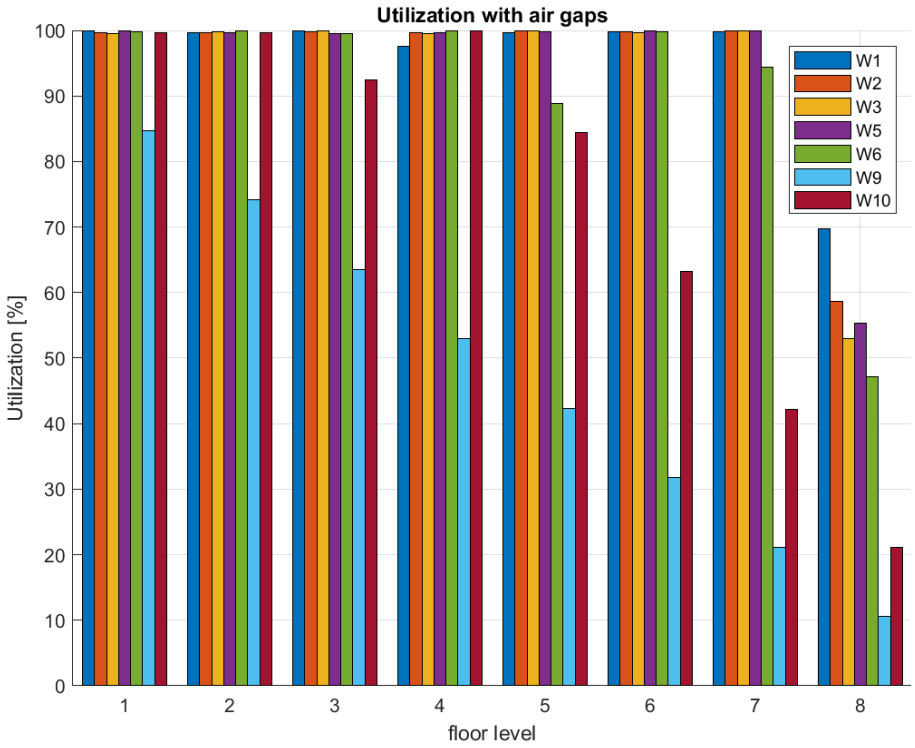

Figure 4.10: Utilisation ratio, $b_{max} = 700\ mm$, $h_{solid,i,j} = h_{hollow,i,j}$

The resulting widths of the gaps are highlighted for the walls that update the ID and also present all of the changes in the gap width in comparison with the resulting widths from having the ID fixed. It can be seen that the widths for three of the walls decrease where the ID is not updated, which indicates that the total volume reduction in these series of walls is less than for that of having the ID fixed.

Table 4.25: Width of air gaps, $b_{max} = 700\ mm$, $h_{hollow,i,j} = h_{solid,i,j}$

Floor	W1	W2	W3	W5	W6	W9	W10
8	700	700	700	700	700	700	700
7	660	130	480	330	700	700	700
6	670	50	290	190	600	700	700
5	140	430 (90)	700 (290)	580 (200)	700 (540)	700	700
4	700 (340)	430	**130 (140)**	40	410 (80)	700	500
3	390 (70)	110	280	200	**490 (500)**	700	700
2	**90 (100)**	460 (80)	20	580 (190)	210	700	480
1	340	200 (30)	380 (20)	310 (100)	630 (240)	700	140

The total volume reduction from implementation of the maximum gap widths of 700 mm comes out as **21.81%** which is in fact lower than the implementation for fixed ID that resulted in **23.27%** total volume reduction. This is the same situation

as for when the gap is limited to a maximum of 150 mm but in this case it results in a smaller reduction in mass over all.

Table 4.26: Volume reduction, V_r [%]

Floor	W1	W2	W3	W5	W6	W9	W10
8	28.5	28.5	28.5	28.5	28.5	28.5	28.5
7	28.2	17.3	26.7	24.4	28.5	28.5	28.5
6	36.4	12.6	30.3	26.3	35.7	28.5	28.5
5	23.1	19.6 (21.4)	21.3 (35.4)	20.7 (31.3)	21.3 (40.9)	28.5	28.5
4	21.3 (37)	26.1	**13 (13.5)**	6.3	19.3 (20)	28.5	26.9
3	19.1 (18.4)	15.9	23.3	20.8	**26.8 (26.9)**	28.5	36.6
2	**10.7 (11.4)**	15.9 (16)	4.8	16.6 (24.5)	21.2	28.5	34.3
1	24.6	12.5 (8)	15.2 (5.7)	14.4 (18.2)	16.8 (26.7)	28.5	23.1

4.3 Combined logic with gaps limited to 700 mm

This section will present the resulting evaluation from updating the logic for only fixing the element thickness by adding a argument where updating the ID only is allowed if the volume reduction is greater then that of previous ID. This will constrain the script from changing to stiffer configurations when it would not increase the total volume reduction.

$$ID_{new} \; if \; V_{r,new} \geq V_{r,old} \tag{4.7}$$

With the added condition, it can be seen in Table 4.27 that only 6 walls proves a increase in the V_r by updating the ID, compared to before where 13 walls were updated.

Table 4.27: Updated ID, 700 mm

Floor	W1	W2	W3	W5	W6	W9	W10
8	1	1	1	1	1	1	1
7	1	1	1	1	1	1	1
6	2	2	2	2	2	1	1
5	2	3	3	3	3	1	1
4	3	5	4	4	3	1	1
3	4 (3)	5	5	5	5	1	2
2	4	6 (10)	5	6 (10)	5	1	2
1	5	7 (6)	6 (10)	6	6 (10)	1	2

ID	CONFIG
1	202020
2	203020
3	204020
4	302030
5	303030
6	304030
7	402040
10	2020202020

It can be studied in Table 4.28 that the updated ID is only updated where the increase in width is proportionally greater than the decrease in the height of the cross layer. This is apparent by looking at the updated id in wall 2 on floor 1 where the decrease in cross-layer is 50% while the increase in gap width is 5.57 times greater.

Table 4.28: Applied air gaps, $b_{max} = 700\ mm$

Floor	W1	W2	W3	W5	W6	W9	W10
8	700	700	700	700	700	700	700
7	660	130	480	330	700	700	700
6	670	50	290	190	600	700	700
5	140	90	290	200	540	700	700
4	340	430	140	40	80	700	500
3	390 (70)	110	280	200	500	700	700
2	100	210 (80)	20	290 (190)	210	700	480
1	340	200 (30)	160 (20)	100	330 (240)	700	140

The resulting utilisation of these configurations and air gap widths presents the possibility of approaching the full capacity of each wall for this stiffness model, which can be seen in Figure 4.11. It can be clearly seen that this logical operation is effective by studying walls 1 to 6 on floors 1 to 7, where the utilisation is almost 100%.

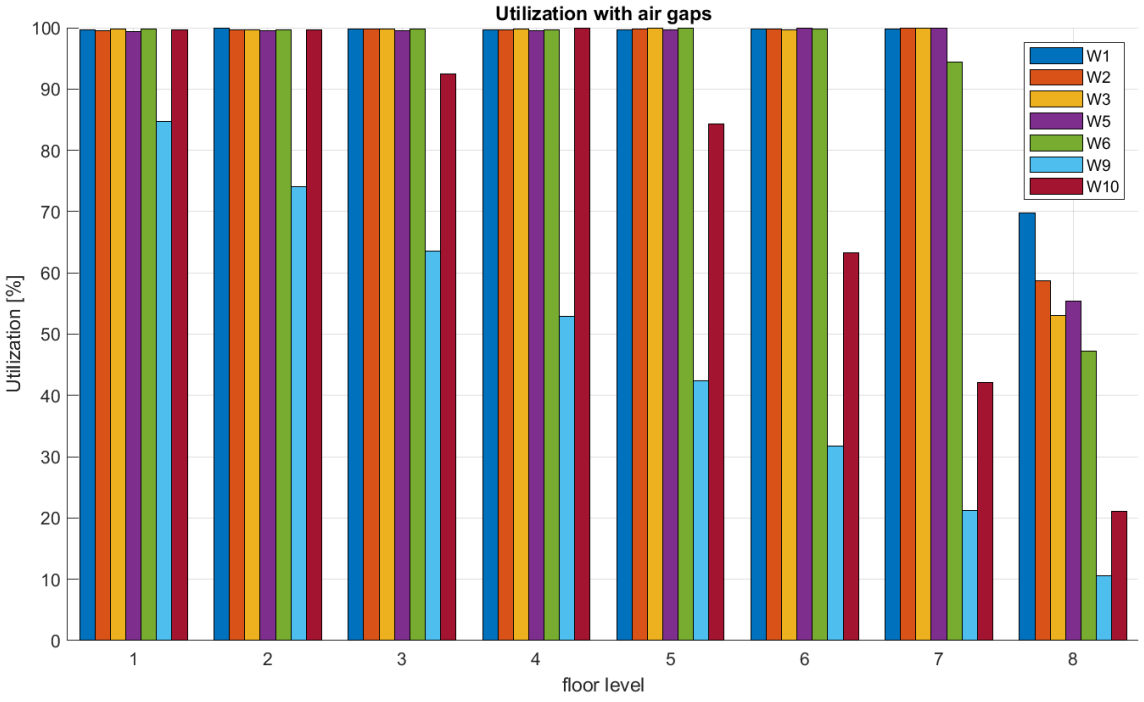

Figure 4.11: Utilisation with updated logic

The increase in utilisation can be studied in Figure 4.12 showing a steady increase for the upper floors where the gaps reach the applied limit, and as the load transcends to the lower floors the utilisation starts to vary due to the utilisation reaching its limit.

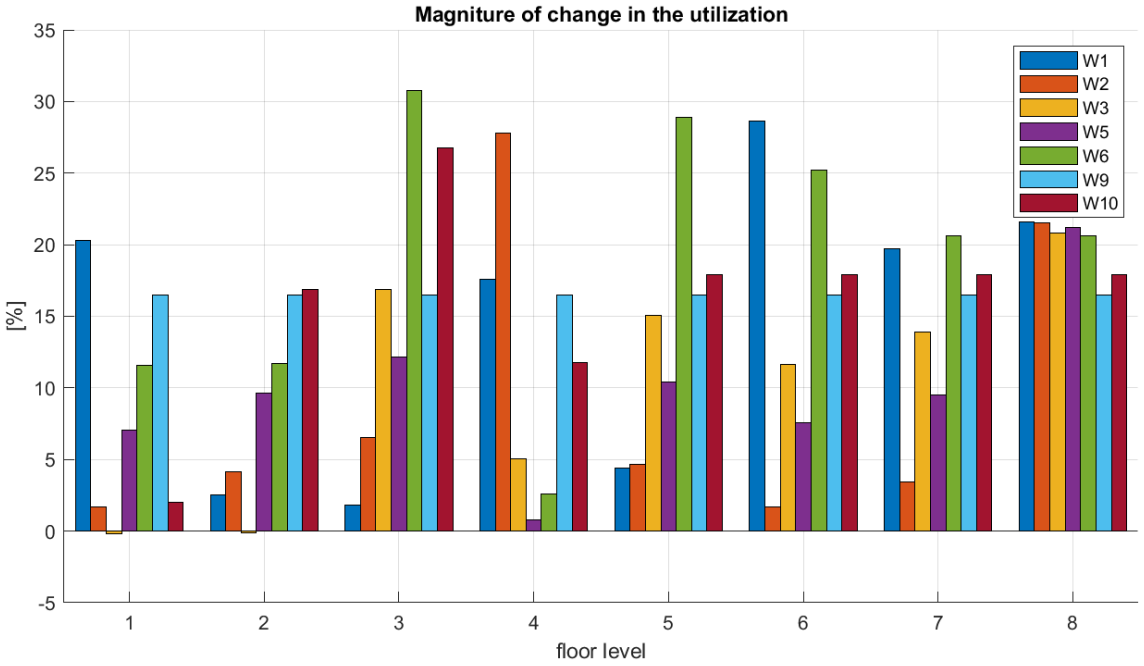

Figure 4.12: Magnitude of change, new logic, $b_{max} = 700\ mm$

All of this leads to a total volume reduction of **24.19%**, which is **2.38%** greater than that of a fixed $h_{i,j,clt}$ and **0.89%** greater than that of a fixed $\mathrm{ID}_{i,j}$. Alternatively, by investigating wall 2 on all floors, give a volume reduction of **23.55%**, where a fixed $h_{i,j,clt}$ gives a reduction of **20.84%** and fixed $\mathrm{ID}_{i,j}$ gives a reduction of **22.50%**. The total volume reduction of raw materials from the updated operation results in **63.49m**^{3} leaving **198.98 m**^{3} of timber compared to the solid composition that requires **262.47 m**^{3}.

Table 4.29: Volume reduction based on updated logic, $b_{max} = 700\ mm$

Floor	W1	W2	W3	W5	W6	W9	W10
8	28.5	28.5	28.5	28.5	28.5	28.5	28.5
7	28.2	17.3	26.7	24.4	28.5	28.5	28.5
6	36.4	12.6	30.3	26.3	35.7	28.5	28.5
5	23.1	21.4	35.4	31.3	40.9	28.5	28.5
4	37	26.1	13.5	6.3	20	28.5	26.9
3	19.1 (18.4)	15.9	23.3	20.8	26.9	28.5	36.6
2	11.4	25.5 (16)	4.8	28.3 (24.5)	21.2	28.5	34.3
1	24.6	12.5 (8)	22.9 (5.7)	18.2	29.3 (26.7)	28.5	23.1

5

Hygrothermal Investigation

In this chapter, the hygrothermal performance will be evaluated in the CLT panels. Understanding this concept is critical to ensuring the durability of hollowed CLT elements in a building. The investigation in this chapter will analyse the performance of the CLT elements when the temperature and moisture levels fluctuate over time.

5.1 Moisture transfer

Moisture conveyance in timber pertains to the movement of vapour within it. Wood is a porous material which can take in or release moisture according to its surrounding conditions. In high relative humidity settings, for example, it absorbs some amount of vapor from the air hence increasing its moisture content. On the other hand, when the ambient air is dry, it loses some amounts through desorption into space.[Sandin, 2010]

The moisture content of timber has an impact on its strength, dimensional stability and durability. Moisture control methods should therefore be observed during construction using wood so that they can last longer.[Zarr et al., 1995]

Some tips for regulating moisture transfer in timber include proper airing out systems installation like fans or vents; using moisture barriers such as paints or sealants and keeping indoor humidity levels balanced all year round among others. These measures help prevent potential problems associated with damage caused by damp conditions thus enhancing aesthetic appeal over time while still ensuring that these structures remain strong enough for many years.[Zarr et al., 1995]

The diffusion of moisture in wood is an essential factor that significantly impacts the behaviour and performance of wood-based materials. Moisture transfers from regions of high vapour pressure to those of low vapour pressure as a result of differences in vapour pressure between regions, which cause water vapour to travel through porous materials such as timber.[Jakes et al., 2019] Unregulated moisture levels can result in structural harm to building components.

Understanding wood moisture dispersion is essential for regulating building moisture and minimising material deterioration and structural damage. Effective moisture regulation and building material integrity may be achieved by addressing diffusion and timber's hygroscopicity.

5.2 Critical moisture status (Microbes/Fungi)

Different materials will be affected differently by the moisture status, where different risk may act. Risks can be defined by a negative effect on structural capacity, hygrothermal performance, or health impact on the residents. The most common consequence in timber is that fungi may manifest if the moisture content exceeds a certain level. The two types of fungi that can ocarer are rot fungi and mould fungi, which come with different risks. Table 5.1 presents the moisture thresholds for when mould and rot are more or less likely to manifest.

5.2.1 Rot fungi

Brown rot degrades the structural capacity of the timber by breaking down the cellulose, hemicellulose, and cell walls, to obtain nutrition. Infested wood becomes brittle as a result of rot, worsening structural capacity [Ringman et al., 2019]. For brown rot to manifest there are some conditions that need to be present; the rot needs nutrition (the wood), oxygen needs to be present, a habitable temperature and moisture content over a certain thresh hold. The threshold for when there is a high risk of rot is a moisture content greater than 25% with a temperature of 22 $°C$ [Ringman et al., 2019].

5.2.2 Mould fungi

Mould fungi mainly grow on surfaces and not in the solid timber, thereby being partly dependent on the surface moisture but mainly dependent on the fibre saturation. If the mould manifests, it can be identified by a discolouration on the infested surface and a characteristic smell [Wiedenhoeft, 2009]. The main risk of mould is the impact on the aesthetics and health of residents. The spores produced by mould can cause asthma and the ordure can be unpleasant to be exposed to over time [Crook and Burton, 2010]. The environmental requirements for mould to prosper are dependant on; a certain relative humidity, a habitable temperature and duration of the first conditions. Mould demands a temperature range of 0 to 50^oC and a relative humidity range dependant on the temperature described by following function [Hukka and Viitanen, 1999]:

$$RH_{crit} = \begin{cases} -0.00267 \cdot T^3 + 0.16 \cdot T^2 - 3.13 \cdot T + 100 & when\, T \leq 20°C \\ \\ 80\% & when\, T > 20°C \end{cases} \tag{5.1}$$

Table 5.1: Critical moisture of mould and rot.

	No risk	Low risk	High risk
Rott			
u (%)	<16	16-25	>25
RH (%)	<75	75-95	>95
Mold			
u (%)	<15	15-20	>20
RH (%)	<70	70-85	>85

5.3 Hygrothermal properties

This section covers the analytical model that is applied to acquire the hygrothermal properties of the CLT wall with air gaps introduced. The model in constructed in two steps being; first to evaluate the thermal performance of the hollow CLT lements, and based on the thermal properties evaluate the hygrothermal properties.

5.3.1 Thermal Conductivity of different layers

Thermal conductivity determines the thermal performance of CLT building materials. The thermal conductivity of a substance characterises its system of heat transfer. The capacity of a material governs the degree of heat transfer achievable. One has to know the thermal conductivity of the constituent materials of CLT panels in order to assess their thermal behaviour. This calls for in-depth knowledge of the heat conductivity of the several woods and adhesives used to create laminated timber. The numerous wood species used to make CLT panels have unique thermal properties. Wood species, density, and cellular structure all influence cross-laminated timber panel heat conductivity. Changes might be rather significant.

According to [Sandin, 2010] the CLT panels have a thermal conductivity of 0.13 $\frac{W}{mK}$. The timber's density, moisture content, and cellular structure affect its heat conductivity. As insulators, the air spaces in wood fibers slow down heat transmission.

5.3.1.1 Thermal conductivity of un-ventilated air gaps

The equivalent thermal conductivity for air gaps in the CLT panels can be defined as the entire thermal performance of an air gap inside the element composition. There is a need to find comparable thermal conductivity for air gaps since their sizes might vary. Each air gap's equivalent thermal conductivity λ_{eq} is determined using the particular technique or equation detailed [ISO 6946:2017,]. To calculate the equivalent thermal conductivity by using equation 5.2 where d is the total thickness for each air gap within the CLT panel m and R_{eq} is the equivalent thermal resistance $\frac{m^2K}{W}$.

$$\lambda_{air,eq} = \frac{D}{R_{air,eq}} \quad ; \quad \left[\frac{W}{m^2K}\right] \tag{5.2}$$

to calculate the equivalent thermal resistance the following equations can be used.

$$R_{air,eq} = \frac{1}{h_a + h_r} \quad ; \quad \left[\frac{m^2K}{W}\right] \tag{5.3}$$

where the h_r the radiative coefficient in and h_a is the convection/conduction coefficient.

$$h_a = \frac{0.025}{d} \quad ; \quad \left[\frac{W}{m^2K}\right] \tag{5.4}$$

$$h_r = \frac{h_{r0}}{\frac{1}{\epsilon_1} + \frac{1}{\epsilon_2} + \frac{2}{\sqrt{1 + \frac{d^2}{b^2}} - \frac{d}{b}}} \quad ; \quad \left[\frac{W}{m^2K}\right] \tag{5.5}$$

ϵ_1, ϵ_2 are the hemispherical emissivities of the surfaces on the warm and cold faces of the airspace. b is the width of the airspace in m

$$h_{r0} = 4 * \sigma * T_{mn}^3 \quad ; \quad \left[\frac{W}{m^2K}\right] \tag{5.6}$$

where h_{r0} is the radiative coefficient for a black-body surface in , σ is the Stefan-Boltzmann constant 5,67 * 10^{-8} $\frac{W}{m^2K}$ and T_{mn} is the mean thermodynamic temperature of the surface and of its surroundings.
For equation 5.7 represents the service temperature of the air gaps in kelvin, where T_1 and T_2 are shown in figure 5.1 which presents the service temperature of the air gaps

$$T_m = \frac{T_1 + T_2}{2} \quad [K] \tag{5.7}$$

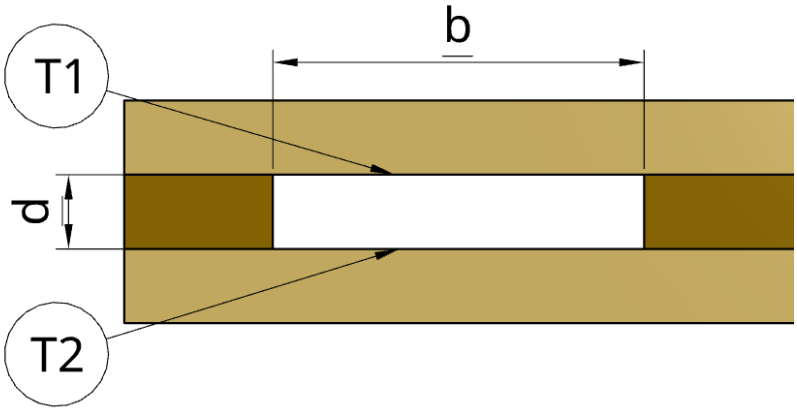

Figure 5.1: Hollow CLT cross-section with surface temperatures.

5.3.2 Equivalent thermal conductivity

Thermal resistance is the property of constraining heat flux for a composite system. Thermal resistance and determining its value is important when evaluating the insulating properties of the CLT elements. If the R value is high, it means that the walls will keep the heat from transferring and this leads to not consuming a large amount of energy for cooling or heating.

To determine the equivalent thermal resistance according to Rebecka N and Tove N [Nilsson and Nilsson, 2022], to begin with, calculate the λ_{eq} by using equation 5.8 where D is the thickness of panels for different configurations and for the R_{eq} can be calculated by using equation 5.9 where B_i is the width of each panel configuration, B_{tot} is the total width of the panels and R_i is the total thermal resistance for each panel. Equation 5.10 can be used to calculate the total thermal resistance, where λ_n is for each layer in the panel and d_i is the thickness for each layer.

$$\lambda_{eq} = \frac{d_{tot}}{R_{eq}} \tag{5.8}$$

$$\frac{1}{R_{eq}} = \sum \frac{1}{R_i} \cdot \frac{B_i}{B_{tot}} \tag{5.9}$$

$$R_i = \sum \frac{d_{i,j}}{\lambda_{i,j}} \tag{5.10}$$

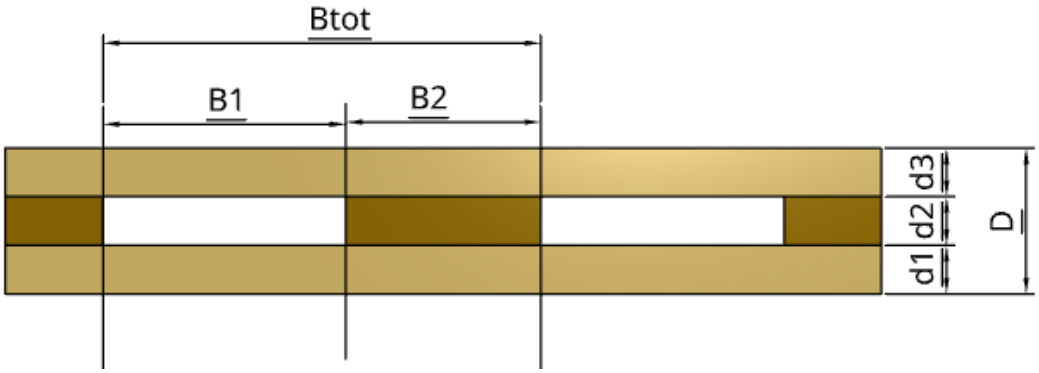

Figure 5.2: Shows the CLT panel with air gaps and all notations

By considering the properties of the materials and thicknesses of panels and layers these equations can calculate R of all configurations.to determine the service temperature for the airgaps equation 5.11 can be used,where the T_i is the interior temperature and T_e is the exterior temperature while R_i is the thermal resistance an R_{tot} is the total thermal resistance.

$$T(x) = T_i - \frac{R(x)}{R_{tot}} (T_i - T_e) \tag{5.11}$$

5.3.3 Vapour permeability of different layers

To evaluate the hygrothermal performance of a CLT section with introduced air gaps demands to define the equivalent vapour permeability (δ_{eq}), which is a uniform value designed for each unique section. This characteristic is important to know since it influences the interior air quality and structural durability by the fact that the moisture level is the main factor for microbe infestations, so it is necessary to assess the moisture management capacities of building materials.

The insulation that is applied in the outer layer of the building is XPS with a permeability of $0.197{\cdot}10^{-6}$ m^2/s to decrease the heat fluxuation and maintain the thermal resistance bellow 0.18 W/m^2K for wall section.

With the help of the closed cell structure of the XPS, moisture destruction could be avoided and similar damages. That's because the XPS closed cell structure is moisture and water resistant. Due to the high resistance to mould and moisture, XPS is considered a good solution to avoid the high cost of maintenance and replacement in the long run.[XPSA,]

The vapour permeability of wood are varying dpendent on the specis where in this project it is taken as spruce. The permeability of spruce is dependent on the humidity, which are shown in Figure 5.3, and vary in a approximet range of 0,3-$2{\cdot}10^{-6}$ m^2/s.

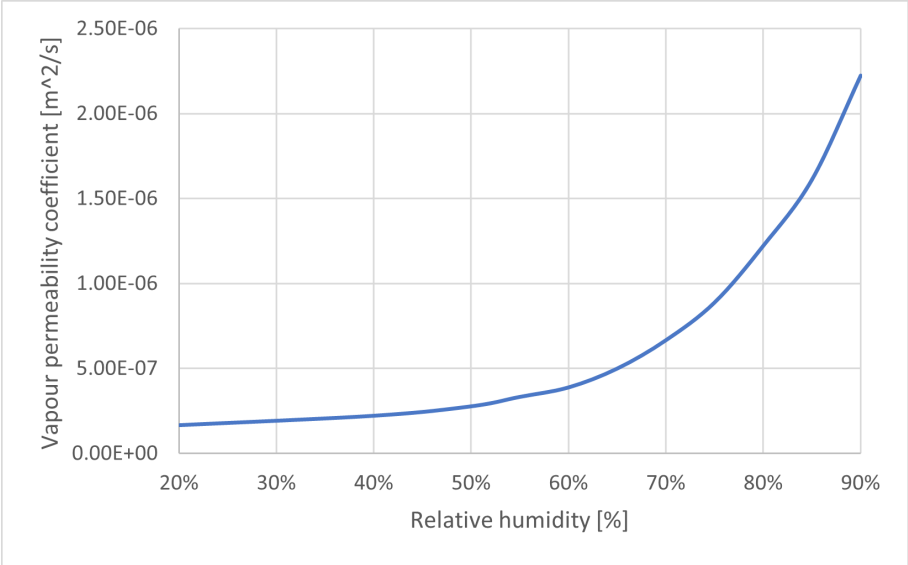

Figure 5.3: Vapour permeability of spruce dependent on RH [Sandin, 2010]

One especially susceptible to temperature changes is the vapour permeability of air δ_{air}. An increased vapour permeability may result from the air's ability to retain water vapour rising with temperature. It follows that air spaces in building components may be more capable of transferring moisture in warmer weather.

Equation 5.12 explain how quickly water vapour moves through that material. Assessing the moisture transport properties of building materials requires knowledge of this coefficient, whose value depends on the material's composition, porosity, and temperature. Importantly, models of moisture transport in building structures need to include the temperature dependence of δ_{air}.[Marko Pinterić, 2017]

$$\delta_{air} = 2.31 \cdot 10^{-5} \left(\frac{p_{atm}}{p}\right) \left(\frac{T_m}{273.15}\right)^{1.81} \tag{5.12}$$

The values in the previous equation 5.12 are represented the $\left(\frac{P_{atm}}{P}\right)$ the difference between atmosphere pressure and pressure over the building is very small it is assumed to be equal 1 and for the T_m was calculated by using the equation 5.11.

5.3.4 Equivalent vapour permeability

To calculate the equivalent vapour permeability coefficient by using equation 5.13 where D is the thickness of each configuration and Z_{eq} is the vapour transmission resistance. The calculations of the vapour transmission resistance based on Rebecka N and Tove N in their thesis, equation 5.14 represents the equivalent vapour transmission resistance for each configuration where Z_i is the total vapour transmission resistance for each panel subdivision, B_i is the width of each configuration subdivision and for B_{tot} the total width of the panel, figure 5.2 shows all notations of the configuration. [Nilsson and Nilsson, 2022]

$$\delta_{eq} = \frac{d_{tot}}{Z_{eq}} \tag{5.13}$$

$$\frac{1}{Z_{eq}} = \sum \left(\frac{1}{Z_i} \frac{B_i}{B_{tot}}\right) \tag{5.14}$$

To determine the Z_i value can be calculated by using equation 5.15 where d_i is the thickness of each layer in configuration, δ_i is the vapour permeability coefficient of the material for each layer.

$$Z_i = \sum \frac{d_{i,j}}{\delta_{i,j}} \tag{5.15}$$

Conversely, in equation 5.16, the water vapour diffusion resistance of a substance is measured compared to that of stagnant air by the water vapour resistance factor, μ. Diffusion coefficients of materials may be compared to those of stagnant air δ_{air} to evaluate how well a material prevents the diffusion of water vapour. By using the Schirmer equation, which estimates the water vapour diffusion coefficient in stagnant air depending on temperature and atmospheric pressure, temperature dependence in moisture transport studies may be reduced. [Marko Pinterić, 2017] In equation 5.16 the δ_{air} can be calculated from equation 5.12 and for δ_{eq} by using equation 5.13 so the difference between those values must be larger than 1.

$$\mu = \frac{\delta_{air}}{\delta_{eq}} \geq 1 \tag{5.16}$$

5.4 Result of Hygrothermal investigation

This section will cover the hygrothermal properties applied for the exterior wall **W1** from section 4.2.2.1 which is presented in Table 5.2. The resulting properties in this studie is apllied for the exteriour based on climate data for Gothenburg, while the indore climate is determined based on guidelines from Boverket , which is presented in section 5.4.1.

In Table 5.2 an exhaustive summary of the many wall 1 configurations on different levels is given in this table. It comprises necessary information such as the thickness of insulation, CLT height, the width of air gaps (B1) and solid portions (B2). The knowledge of the structural differences inside the CLT panels and their effect on thermal performance depends on these configurations, which are obtained from section 4.2.2.1. The insulation thickness where set to 180 mm in order to maintain a heat transfer coeficient (U-value) below $0,18$ $[W/m^2K]$ recomended by Boverket. [Boverket, 2011]

Table 5.2: Shows the different configurations for the wall 1 on different floors.

Floors	CONFIG	B1[mm]	B2[mm]	h_{clt} [mm]	Height [mm]	$d_{insulation}$ [mm]
8	202020	150	120	60	3100	180
7	202020	150	120	60	3100	180
6	203020	150	120	70	3100	180
5	203020	130	120	70	3100	180
4	204020	150	120	80	3100	180
3	204020	60	120	80	3100	180
2	302030	90	120	80	3100	180
1	303030	150	120	90	3100	180

5.4.1 Applied Climate data

Table 5.3 shows the indoor and outdoor temperature and RH in summer and winter in Gothenburg. According to Sandin [Sandin, 2010] the outdoor temperature and RH are $22°C$ and 40% respectively.

Table 5.3: The temperature and relative humidity in summer and winter in Gothenburg

	Gothenburg			
	Outdoor		Indoor	
	Winter	**Summer**	**Winter**	**Summer**
T [$°C$]	-1.9	17.3	22	22
RH	82%	73%	40%	40%

Table 5.4 shows the average of the service temperature of air gaps in summer and winter where for example floors 8 and 7 are the same temperature because they have the same dimensions so the temperature is dependant of the dimension of the CLT where approximation this calculation is for the solid CLT by using equation 5.7 average temperature will be calculated.

Table 5.4: Air gap temperature for summer and Winter in Gothenburg

	Gothenburg	
	Temperature [K]	
Floors	**Summer**	**Winter**
8	294.84	293.58
7	294.84	293.58
6	294.81	293.44
5	294.81	293.44
4	294.79	293.30
3	294.79	293.30
2	294.79	293.30
1	294.76	293.16

Outdoor Climate

Timber structures are greatly affected by the external weather conditions. Two main points that affect how wood behaves in open-air settings are heat and humidity. It is important to know how these two values relate because it helps estimate the dampness of timber, which then affects its robustness and proneness to rot.[Sandin, 2010]

Indoor Climate

Indoor climate, which includes air flow and heat range, is very important for occupant pleasure and health in buildings. Because of its unique characteristics that affect ventilation, heat control and general quality of air, among other things; timber

constructions are highly instrumental in shaping the internal environment.[Sandin, 2010]

The temperature of the indoor climate is designed in relation to thermal comfort of residents, guidelines in the Swedish BBR 2011:6 suggest the temperature to be in a range of 18 to 20 $°C$ to obtain a habitable indoor climate [Boverket, 2011]. Another parameter to provide a comfortable indoor climate is to keep the relative humidity above 20% to avoid any displeasure from the dry air such as irritation in eyes, throat and nose, according to the Swedish health department [Sverige. Socialstyrelsen., 2005].

5.4.2 Determined properties of air gaps

The table 5.5 presents significant information related to $\lambda_{air,eq}$ for the gaps of air in CLT panels, which is fundamental for understanding how these gaps affect the thermal behavior of the panels. to calculate $\lambda_{air,eq}$ by using the equation 5.2. Each of the columns from this table provides values of $\lambda_{air,eq}$ at different times of the year thereby showing how their conductivity changes under various environmental conditions. These $\lambda_{air,eq}$ specific values show the rate at which heat moves through air spaces thereby differentiating their performance in different seasons. Air gaps control much of the heat transmission in CLT panels. These gaps affect the panels' whole thermal behaviour and hence affect the $\lambda_{air,eq}$values. Air gaps increase the thermal resistance of the panels as insulators and slow down heat transfer.

Table 5.5: The equivalent air conductivity for winter and summer, [W/mK]

Equivilant	**Gothenburg**	
lambda air gap	**Summer**	**Winter**
8	0.1152	0.1141
7	0.1152	0.1141
6	0.1695	0.1676
5	0.1680	0.1662
4	0.2217	0.2191
3	0.2024	0.2001
2	0.1122	0.1109
1	0.1694	0.1673

Table 5.6 shows the $\delta_{air,eq}$ for wall 1 on 8 floors where the equivalent vapour permeability in summer is higher than in winter this is due to the height temperature in summer and in winter the permeability indicates less in colder weather.to calculate the delta air eq by using equation 5.12.

Table 5.6: the $\delta_{air,eq}$ in summer and winter in Gothenburg

	Gothenburg $\delta_{air,eq}$ $[m^2/s]$	
Floors	**Summer**	**Winter**
8	2.65E-05	2.63E-05
7	2.65E-05	2.63E-05
6	2.65E-05	2.63E-05
5	2.65E-05	2.63E-05
4	2.65E-05	2.63E-05
3	2.65E-05	2.63E-05
2	2.65E-05	2.63E-05
1	2.65E-05	2.63E-05

5.4.3 Equivelant properties of hollow CLT element

The table 5.7 presents the equivalent thermal conductivity and equivalent vapour permeability in two seasons in the year in Gothenburg for wall 1 on 8 stories. The values of λ_{eq} and δ_{eq} changes in the floors changing due to the relative humidity and dimensions. If the RH is high the δ_{eq} will increase and for the λ_{eq} is dependent on the temperature so that's why the λ_{eq} is higher in summer than winter.

Table 5.7: The λ_{eq} and δ_{eq} on winter and summer in Gothenburg

	Summer		**Winter**	
Panel	δ_{eq} $[\mathbf{m^2/s}]$	λ_{eq} **[W/(mK)]**	δ_{eq} $[\mathbf{m^2/s}]$	λ_{eq} **[W/(mK)]**
8	7.988E-07	0.1270	9.119E-07	0.1268
7	7.988E-07	0.1270	9.119E-07	0.1268
6	8.818E-07	0.1380	1.006E-06	0.1377
5	8.657E-07	0.1373	9.876E-07	0.1370
4	9.638E-07	0.1488	1.099E-06	0.1484
3	8.303E-07	0.1394	9.472E-07	0.1392
2	7.172E-07	0.1279	8.191E-07	0.1277
1	7.988E-07	0.1361	1.072E-06	0.1358

By studying the data in Table 5.7 in relation to the geometry presented in Table 5.8, it can be seen that the permeability of each wall panel correlates with the volume reduction caused by the air gaps. This can be seen in the fact that the wall on the second floor has the lowest permeability and volume reduction, while the wall on

the fourth floor possesses the greatest permeability and air portion.

The same correlation can not be found in the conductivity as the wall on the secound floor dose not possese the lowes conductivity. instead it can be seen that a increase in the width of the air gaps increases the conductivity by comparing the wall on the fourth floor with the wall on the third floor which only have a differance in the air gap width. While by comparing the wall on the eigth floor with the wall on the first floor which are both composses of the same portportion of air but different total thicknesses, suggests the inpact of the air gaps is more dependant on the relation between the width and height of the air gaps.

Table 5.8: Volumetric properties of each storey

STOREY	$\mathbf{t_1}$ **[mm]**	$\mathbf{t_2}$ **[mm]**	$\mathbf{t_3}$ **[mm]**	λ_{solid,t_2} [%]	**RED** [%]
8	20	20	20	44	18.52
7	20	20	20	44	18.52
6	20	30	20	44	23.81
5	20	30	20	48	22.29
4	20	40	20	44	27.78
3	20	40	20	67	16.67
2	30	20	30	57	10.71
1	30	30	30	44	18.52

6

Hygrothermal Simulation

6.1 WUFI simulation

WUFI is an application for modeling hygrothermal behaviour in real life. where it is dynamic calculations include the changes in the external conditions over time. WUFI 2D 4.4 is the software version that is used in this study with different climates and materials. The theoretical background of WUFI is based on fusing the heat transfer and moisture movement equations, and the input parameters include material properties, climate data, and boundary conditions such as humidity, temperature moisture, and heat resistance. [WUFI, 2025]

6.1.1 Geometry

The wall that was being investigated is wall 1 in all stories, the wall was built as a homogenised body from floors 1 to 8 with different thicknesses and the same height of 3.1 m. The insulation was applied at the same height as CLT walls but with different thicknesses.

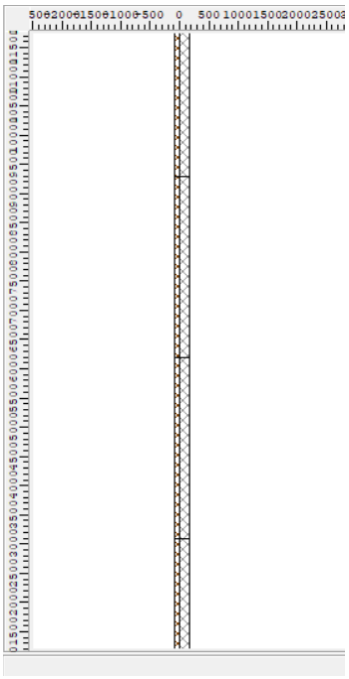

Figure 6.1: The model geometry for the wall 1 in all stories

Figure 6.1 shows the model geometry for wall 1 from floor 1 to 8 On the other hand, the mesh that was investigated is medium mesh, as shown in figure 6.2

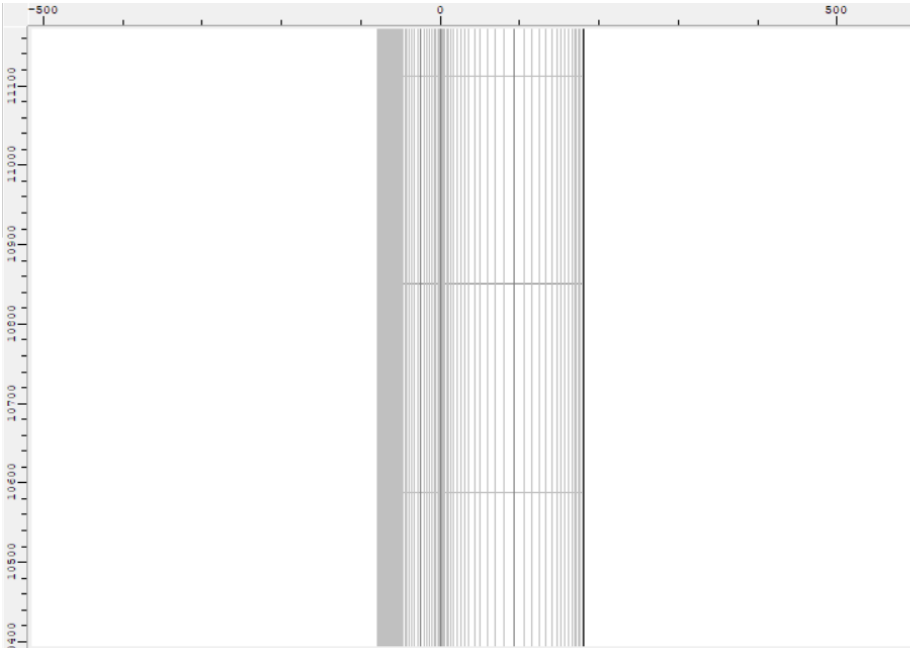

Figure 6.2: The numerical grid for the model

6.1.2 Material proprieties

For the first simulation, the material used in the CLT walls was from the Stora Enso CLT data based on the material catalogue for the solid building without air gaps. for the insulation material data the material that is chosen Armaflex Schlauch AF5+AF6. The table 6.1 represent the thermal conductivity and the density of the CLT and XPS that are used in the simulation for solid CLT walls as mentioned in section 5.3.3. Correct values of the thermal conductivity of CLT and insulation provide accurate thermal performance evaluation.

Table 6.1: Applied material data from WUFI

Material	ρ [kg/m^3]	λ [w/mK]
XPS	50	0.037
CLT	410	0.098

Material data for the CLT walls with air gaps is dependent on the dimensions of the wall; therefore, in this simulation, all values used are the average between summer and winter, and the location is Gothenburg. Table 6.2 presents the values of μ and λ in equations 5.16 and 5.8 which can be used to determine these values. For the λ, that is dependent on the temperature where the temperature is 20 $°C$ for the μ values are dependent on the relative humidity that presents in the table 6.2.

Table 6.2: Input data WUFI

Storey	$\mu_{57\%}$ [-]	$\mu_{61\%}$ [-]	$\lambda_{20°C}$ [W/(mK)]	k_λ [-]
8	33	29	0.1269	1.99E-04
7	33	29	0.1269	1.99E-04
6	30	26	0.1378	2.33E-04
5	31	27	0.1371	2.18E-04
4	28	24	0.1486	2.66E-04
3	32	28	0.1393	1.58E-04
2	37	32	0.1278	1.18E-04
1	33	24	0.1359	1.73E-04

Table 6.2 showed the values of thermal conductivity dependent on the temperature k_λ used in WUFI program. The equation 6.1 explains the calculation of k_λ where $\Delta\lambda_{eq}$ is the difference between equivalent thermal conductivity at two different temperatures.

$$k_\lambda = \frac{\Delta\lambda_{eq}}{\Delta T} \tag{6.1}$$

6.1.3 Initial conditions and surface climate

Table 6.3 show the temperature in the two different materials the CLT walls and the XPS insulation, for the water content these two values are the standard for CLT and XPS with 80% of relative humidity. The applied climate data used in the simulation by the database from Gothenburg data. Representing the actual maximum and average temperatures, indoor and outdoor temperatures allows the simulation of the thermal behaviour of the building under various circumstances.

Table 6.3: The initial conditions of two different material

Identifier	Temp	WC [kg/m^3]	RH %
All floors	20	63	80%
XPS	20	1.8	80%

6.1.4 Computational parameters and processing

The studied period of the simulation was determined by a time span in which all walls reached a steady state for one entire cycle. In this study, it was determined that the solid 90 mm wall took 5 years to stabilise, from April 2019 to April 2024. The time steps for this study is 43800 hours and the heat resistance of $0,125$ $[m^2K/W]$ on the inside and $0,0588$ $[m^2K/W]$ at the exterior.

For the output, a file providing the simulation's findings contains: Water Content: Essential for determining the likelihood of moisture-related problems such as mould development or material deterioration, this gauges the quantity of moisture inside the materials. The RH, of air, is the amount of moisture it can contain at a particular temperature the RH must be under 80% as mentioned in section 5.2.2. Testing the comfort and quality of the indoor air requires RH. Temperature: To fully grasp heat transmission and thermal comfort, one must monitor the temperature both inside and outside of the structure. The S_d value in the software where taken as non specific.

6.2 The result of Simulation

This section represents the result of the simulation of WUFI program for the solid CLT without air gaps and the Hollow with air gaps.

6.2.1 Comparison of solid and hollow performance

This section will cover the resulting moisture status of the walls over time in a Swedish condition, and compare the changes between solid composition of the walls and the hollowed CLT elements.

6.2.1.1 Hygrothermal performance of W1 on the 8th and 7th floor

Figure 6.3 presents the results of wall 1 on floors 8 and 7 from WUFI simulation for two configurations the first one is for solid CLT without air gaps and the other is hollow ID1 with air gaps to the similar walls. The monitoring position is between the first layer of CLT and insulation that gets the highest moisture content.

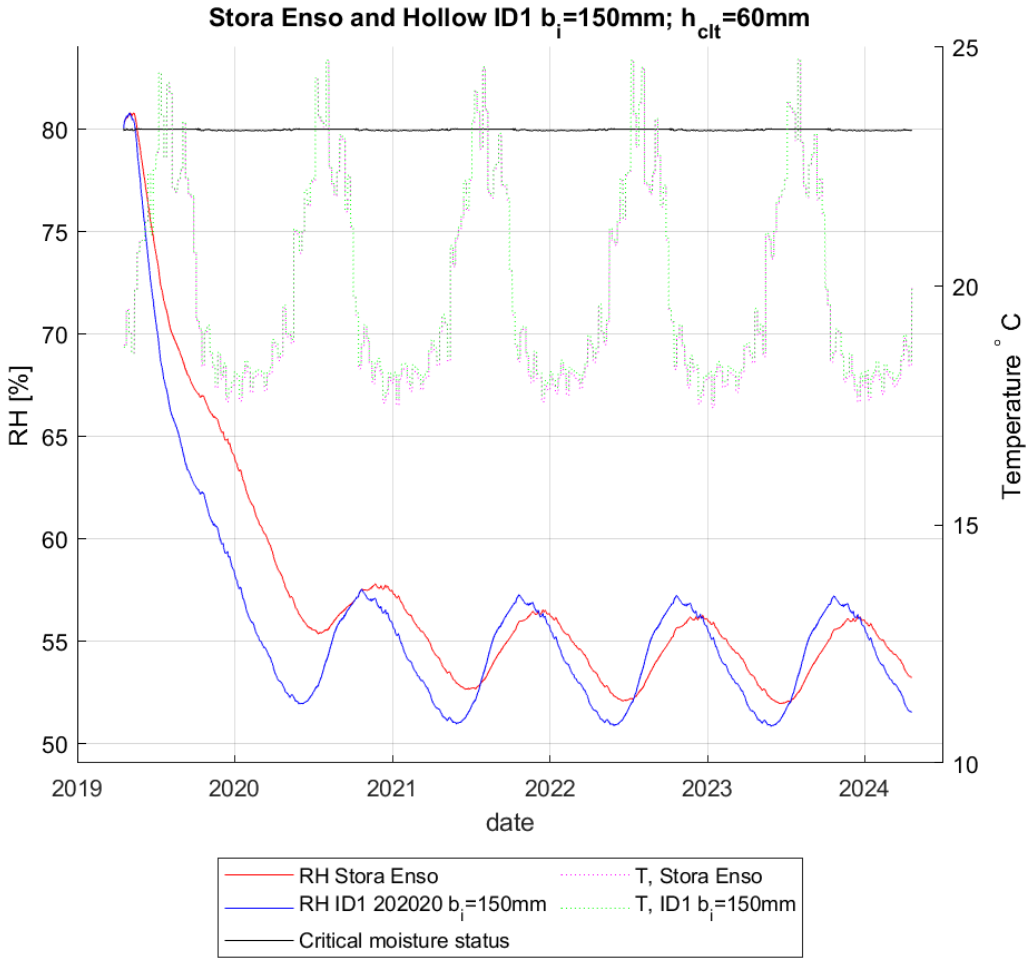

The

Figure 6.3: Moisture status in wall 1 on floors 8 and 7

The RH starts at 80% for both configurations at the beginning of the first year. at the end of 2020, the RH for the solid CLT decreases to 65% and It has an annual fluctuating cyclic pattern that stays between 58% and 53% after the first decline.

For the walls with air gaps decrease faster than solid CLT at the end of 2020 the RH is around 52% It has an annual fluctuating cyclic pattern that stays between 57% and 50% after the first decline. Both solid and Hollow approximately have the same change of temperature between 25 and 18 with midyear peaks and beginning and end of each year troughs. Over the annual cycles, Hollow also maintains slightly lower relative humidity, indicating better moisture management. Even though the temperature trends suggest that the presence of air gaps does not compromise the thermal behaviour of the wall, the result still shows that the RH for the CLT with air gaps is lower than the Stora Enso configuration.

6.2.1.2 Hygrothermal performance of W1 on the 6th floor

Figure 6.4 shows the result of WUFI simulation for wall 1 on floor 6. The hollow wall on floor 6 has the same width of air gaps as on floors 8 and 7 but with different thicknesses of the panel, the width of air gaps, and the thicknesses of the wall are 150 mm and 70 mm respectively.

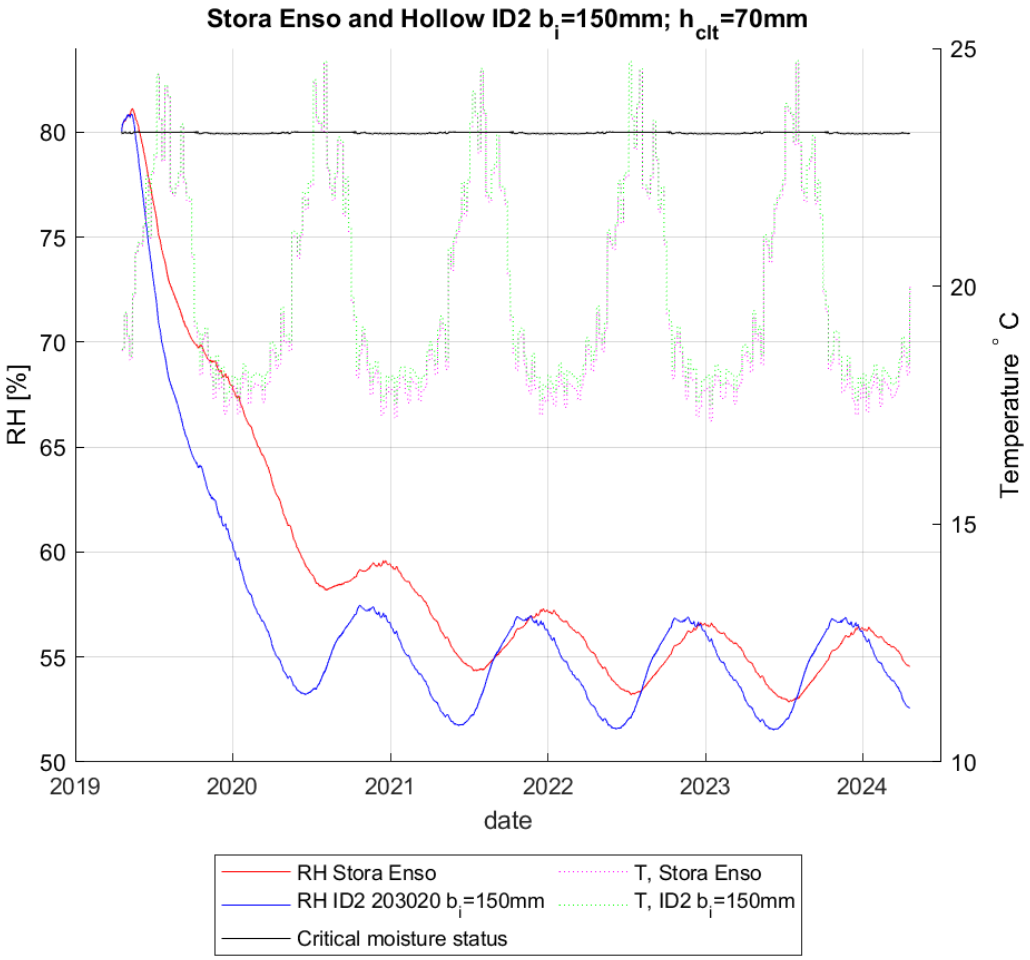

Figure 6.4: Moisture status for wall 1 on floor 6

The result shows that the solid CLT and ID2 start at the beginning of the simulation with 80% of relative humidity and then these two configurations decrease but with different decreases the ID2 decreases faster than solid CLT in 2020 the solid has around 68% RH while the ID2 has 60% but between 2020 and 2021 the two curves change up and down in solid CLT the variation is not so big for the other years but for the ID2 the variation is big.

On the other hand, the temperature variation is likely the same for the two configurations but it is more in the solid CLT. The temperature is between 17 and 25 $°C$.

6.2.1.3 Hygrothermal performance of W1 on the 5th floor

Figure 6.5 shows the variation of temperature and the relative humidity for two configurations of CLT on floor 5. The air gaps widths are 130 *mm* with the same thickness as wall 1 on floor 6.

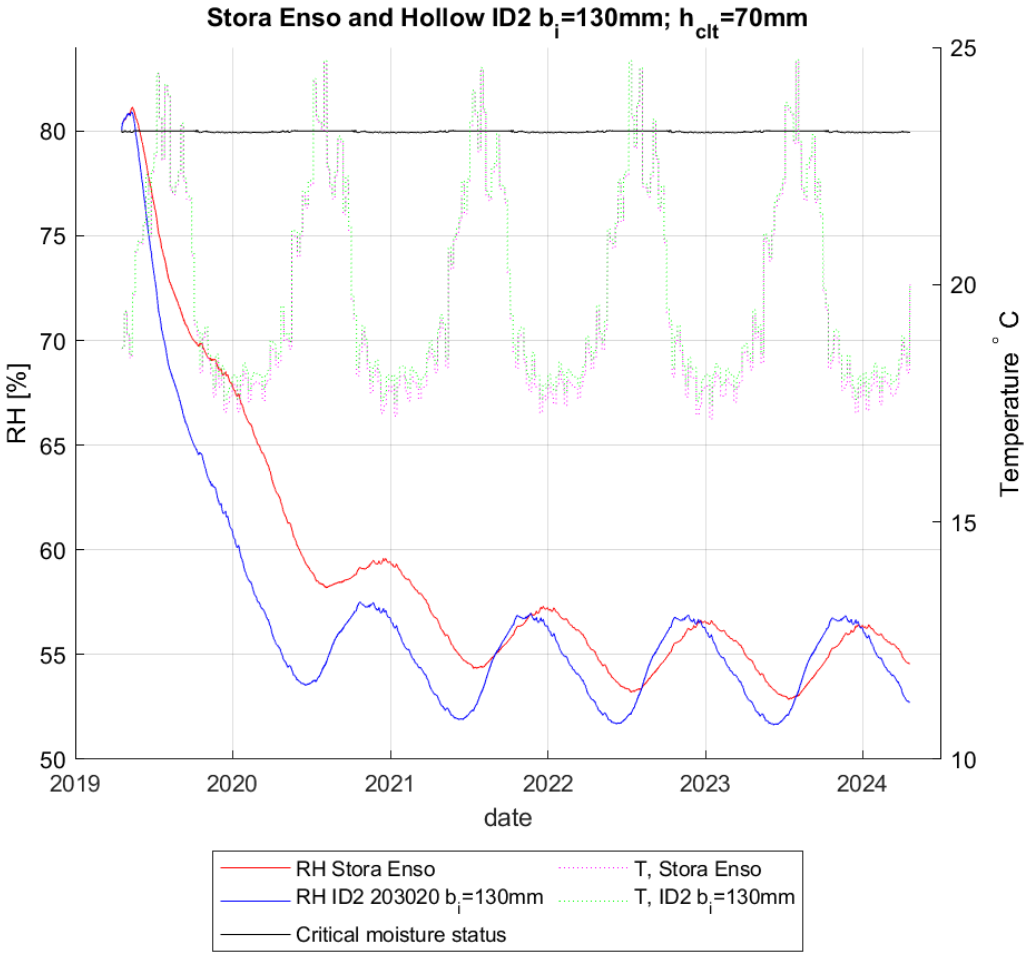

Figure 6.5: Moisture status of wall 1 on floor 5

The simulation on floor 5 indicates that the two configurations have likely had the same temperature variation in the last five years, but for the relative humidity, the solid CLT and hollow CLT start with the same RH at 80%, but the curve of RH for the hollow CLT decreases faster than the solid CLT in the first two years. After that, the two configuration variations are not so different while the change in RH in the last three years is clearly in the hollow CLT, where the curve goes up and down more than the curve for the solid CLT.

6.2.1.4 Hygrothermal performance of W1 on the 4th floor

Figure 6.6 shows the result for the simulation of wall 1 on floor 4 with a thickness of 80 mm for both configurations and an air gap with 150 mm.

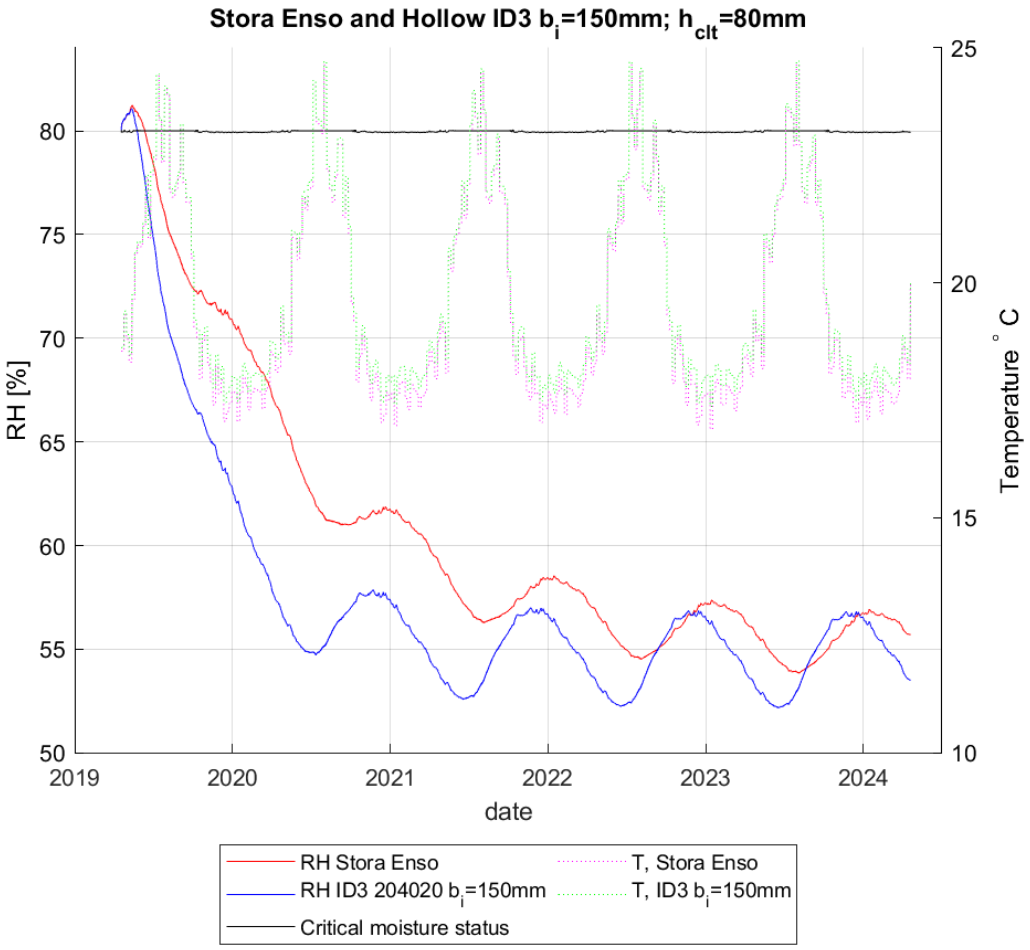

Figure 6.6: Moisture status of wall 1 on floor 4

The temperature curves do not change for both hollow and solid CLT so it is between 25 $C°$ 17 $C°$ for the RH curves, which decreases for the middle of the first years. the variations between the two curves are great from the beginning of 2020 to the middle of 2021 after that, the two curves' variations are likely the same.

6.2.1.5 Hygrothermal performance of W1 on the 3rd floor

Figure 6.7 shows the result of the simulation for wall 1 on floor 3 with a thickness of 80 mm for both solid and hollow CLT, and the air gap width is 60 mm.

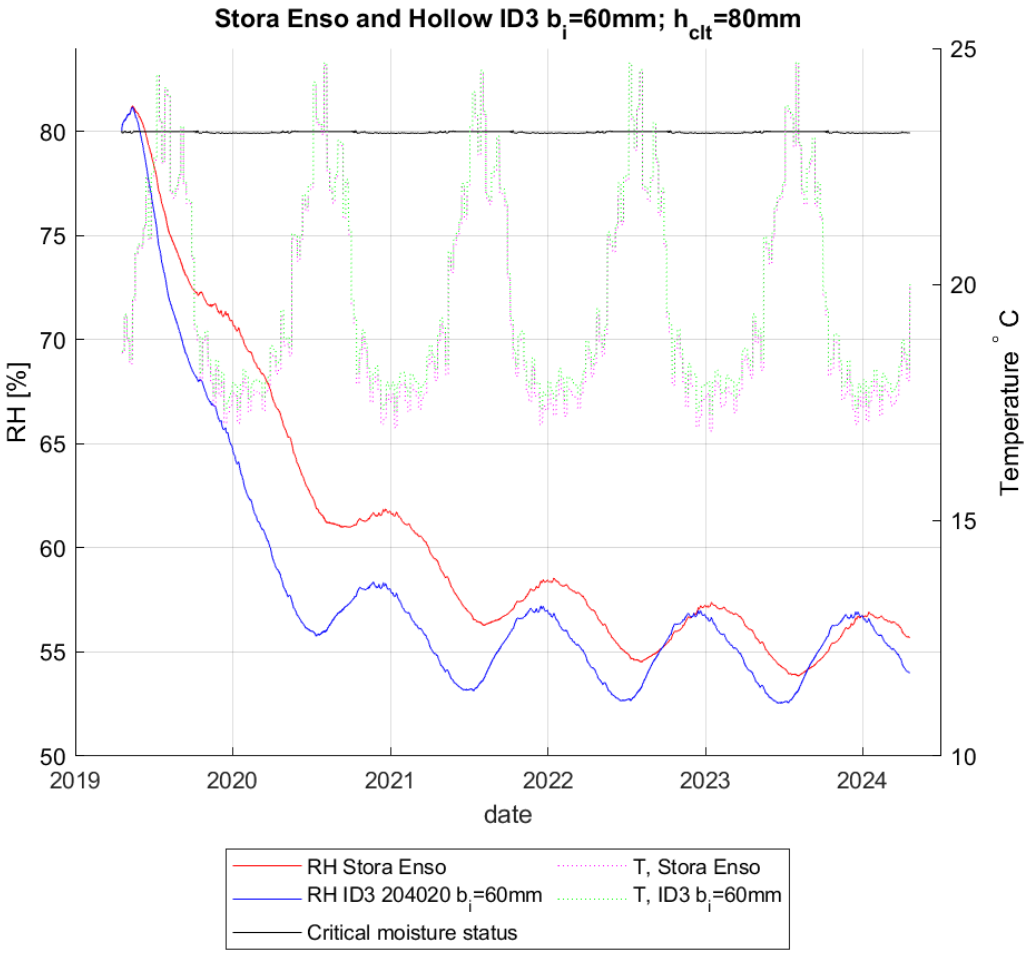

Figure 6.7: Moisture status of wall 1 on floor 3

The RH for hollow and solid CLT decreases over time, while the variation of RH in hollow CLT is greater than in solid CLT in the last three years, and for both configurations, wintertime temperatures are lower than summertime temperatures. Patterns in temperature for hollow and solid CLT are similar.

6.2.1.6 Hygrothermal performance of W1 on the 2nd floor

Figure 6.8 shows the simulations for the solid and hollow CLT on floor 2 with a thickness of 80 mm and an air gap width of 90 mm. The wall has the same thickness as the wall on floors 3 and 4, but with different widths of air gaps.

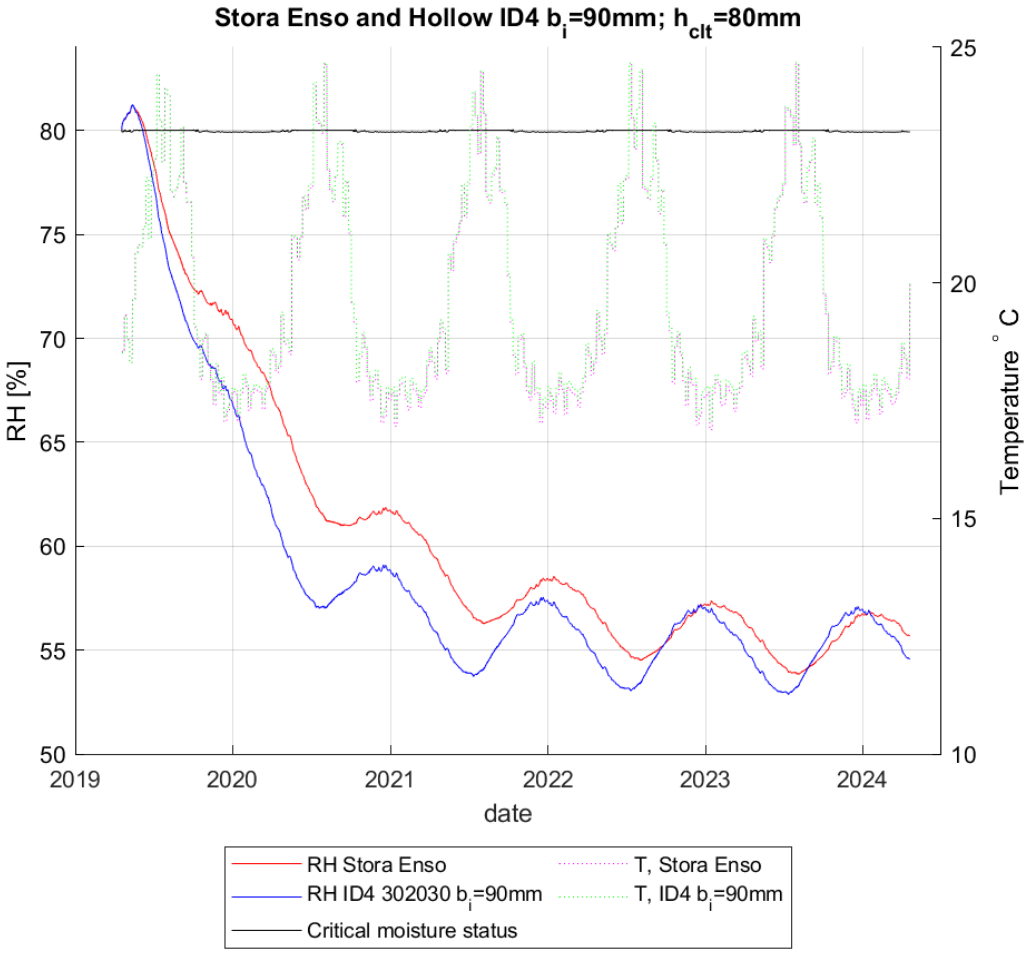

Figure 6.8: Moisture status wall 1 on floor 2

By looking into the result that shows the temperature curves are likely the same for the two configurations between 25 $C°$ and 18 $C°$ and the RH curves still decrease but are not the same for example, floors 4 and 3, the variations are not so great the last two years are likely the same result.

6.2.1.7 Hygrothermal performance of W1 on the 1st floor

For the solid CLT walls without air gaps and hollow CLT on floor 1 in figure 6.9 the RH over the first two years exhibits a declining tendency; it stabilises around the third year and subsequently varies with the season. There are obvious seasonal swings that match changes in the outside weather. Reactivity of the building to outside humidity levels is seen by higher RH readings in winter and lower in summer.

Figure 6.9: Moisture status of wall 1 on floor 1

There are clear seasonal oscillations in the temperature within the building. The summertime highs and wintertime lows in temperature are a reflection of the Gothenburg environs. The inside temperature keeps a quite constant range in spite of changes in the outside temperature. The seasonal variations in relative humidity are correlated with little variations in water content. This implies that the structure's lifetime and robustness depend on the CLT panels' efficient moisture management.

Annual variations in the RH are seen, with summertime readings being lower and wintertime readings being greater. This pattern suggests that the walls react to outside weather by collecting moisture in the humid months and releasing it in the dry ones. The walls had apparently achieved a moisture balance in the third year, which is essential to preserve structural integrity and avoid moisture-related problems such as mould development.

7
Conclusion

The aims of this thesis where to investigate the theoretical impact of introducing air gaps in the cross layers of the CLT elements, and with this basis implement the air gaps in the most volume effective way. Further research is needed to provide a better basis on the implementation of airgaps in the structural and hygrothermal performance.

7.1 Air gap impact on structural performance

In conclusion it could be studied that even with constrained widths of air gaps would result in a impactfull reduction of the raw material volume while still maintaining sufficient capacity. Another preservation from the air gaps is the fact that with a lower volume leads to a reduced load for the following elments resulting in the possibility of reducing the volume more effectively.

7.1.1 Logical operation of choice

From the results it could be seen that based on what logical operation is applied it would lead to different characteristics of the resulting configurations. Where fixing the ID would result in the least stiff solid configuration possible, where as only fixing the thickness resulted in the stiffest solid configuration possible. But in the end, the most optimal logic to apply was the combined logic, since it always suggested the most volume efficient configuration. However, with this logic could lead to a somewhat large selection of different configurations instead of generalising the configurations.

7.2 Hygrothermal findings

It was concluded that air gaps in the elements would not degrade the hygrothermal performance in relation to solid configurations to a degree that would lead to a significant increase in moisture-related risks. Where as the lines for a safe moisture status are to maintain a relative humidity below 80% over time in order to avoid mold and below approximately 95% over a long period to prevent rot from manifesting within the CLT elements. The regulation of the moisture level is important since the temperature with in the walls was concluded to be in the range which is prospered for the fungi.

Bibliography

[Anders Gustafsson, 2019] Anders Gustafsson (2019). *The CLT Handbook*.

[Boverket, 2011] Boverket (2011). Konsoliderad version av Boverkets byggregler (2011:6) – föreskrifter och allmänna råd. Technical report.

[Boverket, 2024] Boverket (2024). Utsläpp av växthusgaser från bygg- och fastighetssektorn.

[Brandner et al., 2016] Brandner, R., Flatscher, G., Ringhofer, A., Schickhofer, G., and Thiel, A. (2016). Cross laminated timber (CLT): overview and development. *European Journal of Wood and Wood Products*, 74(3):331–351.

[Crook and Burton, 2010] Crook, B. and Burton, N. C. (2010). Indoor moulds, Sick Building Syndrome and building related illness.

[Hukka and Viitanen, 1999] Hukka, A. and Viitanen, H. A. (1999). A mathematical model of mould growth on wooden material. Technical report.

[ISO 6946:2017,] ISO 6946:2017. Building components and building elements - Thermal resistance and thermal transmittance - Calculation methods. Technical report.

[Jakes et al., 2019] Jakes, J. E., Hunt, C. G., Zelinka, S. L., Ciesielski, P. N., and Plaza, N. Z. (2019). Effects of moisture on diffusion in unmodified wood cell walls: A phenomenological polymer science approach. *Forests*, 10(12).

[Kurzawinska and Tahmasebi, 2023] Kurzawinska, H. and Tahmasebi, M. (2023). Performance optimization of CLT (NextGenCLT). Matster thesis, Chalmers.

[Marko Pinterić, 2017] Marko Pinterić (2017). Building Physics From physical principles to international standards. Technical report.

[Nilsson and Nilsson, 2022] Nilsson, R. and Nilsson, T. (2022). Fuktanalys av KL-trä Där luftspalter integrerats i tvärskikten Examensarbete inom högskoleingenjörsprogrammet Samhällsbyggnadsteknik. Technical report.

[pro Holz, 2018] pro Holz (2018). Cross-Laminated Timber Structural Design Volume 2.

[Rahman et al., 2020] Rahman, M. T., Ashraf, M., Ghabraie, K., and Subhani, M. (2020). Evaluating timoshenko method for analyzing clt under out-of-plane loading. *Buildings*, 10(10):1–21.

[Ringman et al., 2019] Ringman, R., Beck, G., and Pilgård, A. (2019). The importance of moisture for Brown Rot degradation of Modified Wood: A critical discussion.

[Sandin, 2010] Sandin, K. (2010). *Praktisk Byggnadsfysik*. 9 edition.

[SSI 16351:2015,] SSI 16351:2015. Träkonstruktioner-Massivträ för byggsystem-Krav Timber structures-Cross laminated timber-Requirements. Technical report.

[Stora Enso, 2024] Stora Enso (2024). CLT by Stora Enso Technical brochure. Date accsesed: 29/05/2024, https://www.storaenso.com/-/media/documents/download-center/documents/product-brochures/wood-products/clt-by-stora-enso-technical-brochure-en.pdf.

[Sverige. Socialstyrelsen., 2005] Sverige. Socialstyrelsen. (2005). *Temperatur inomhus.* Socialstyrelsen.

[Wiedenhoeft, 2009] Wiedenhoeft, A. C. (2009). Moisture-Related Properties of Wood and the Effects of Moisture on Wood and Wood Products. Technical report.

[WoodSolutions, 2019] WoodSolutions (2019). *Mid-rise Timber Building Structural Engineering Appendix 2: Worked Example for a CLT Mass Timber Panel Apartment Building A2.*

[WUFI, 2025] WUFI (2025). What is WUFI? https://wufi.de/en/software/what-is-wufi.

[XPSA,] XPSA. Physical Properties https://xpsa.com/technical-information/physical-properties/.

[Zarr et al., 1995] Zarr, R. R., Burch, D. M., Fanney, A. H., Brown, R. H., Good, M. L., and Prabhakar, A. (1995). NIST BUILDING SCIENCE SERIES 173 Heat and Moisture Transfer in Wood-Based Wall Construction: Measured Versus Predicted Technology Administration NationalInstitute of Standardsand Technology. Technical report.

A

Appendix 1

A.1 Structural investigation script

```
clear
clc
close all
addpath('C:\Users\Elliot\Desktop\Chalmers\EXjobb\Code')
load("dimensions.mat");
load("CAD1.mat");
load("CAD2.mat");
load("Af.mat");
load("Aw.mat");

%Material data
kmod = 0.8;
y_M = 1.25;

fck = 21;
fmk = 24;
ftk = 14.5;
ksys = 1.15;

E0 = 11000;
E90 = 370; %370
G0 = 690; % 690
G90 = G0/10;
E005 = 7400;
fcd = kmod*fck/y_M;
fmd = kmod*ksys*fmk/y_M;
ftd = kmod*ftk/y_M;
rho = 500;

MOE = [E0, E90, G0, G90, E005, fcd, fmd, rho, ftd];

% catalog dimensions
n = zeros(36,1);
n(:) = 5;
```

```
n(1:9) =3;
d = configdim;

%% Load kombinations
Qk = 2;
Gk = 1.1; % floor addon
fork1 = 1;
fork2 = 1;
Z = 1;
CIMP = 1;

%% outputs
EI_floor =zeros(5,5);
FLOOR1 = zeros(5, 17);
FLOOR2 = FLOOR1;
GkF = zeros(3, 5);
hgov=0;

EI_floor2 =zeros(5,6);
bid = zeros(5,1);
wout = zeros(5,2);
%% Indpendant Evaluation
Cid = [2 2 2 1 1; 1 1 1 1 1];%
Cid = Cid(CIMP,:);

for j = 1:5
i = j;
[Lid, L1id, L2id, Bid] = FLOOR(CAD1, i);

[qsls, quls] = Load(Qk, Gk, fork1, Bid);

[id1, EIid, h, hc, Gki] = StiffnesF(Z, qsls, quls, ...
    L1id, L2id, Bid, Cid(i), n, d, MOE);
Wid = EIid/(MOE(1)*h/2);

% freq
[f1, w_f, v, crit] = freq(EIid, Bid, Lid, ...
                          d(id1,:), n(id1), MOE, Cid(i));

[qsls, quls] = Load(Qk, Gk+Gki, fork1, Bid);

[EI_ed,~ , W_edm, W_eds, wi] = EIrdF(qsls, quls, L1id, ...
    L2id, Cid(i), MOE(7), EIid);

GkF(1, i) = Gk+Gki;
EI_floor(i,1) = id1;
```

```
EI_floor(i,2) = h;
EI_floor(i,3) = EIid;
EI_floor(i,4) = EI_ed;
EI_floor(i,5) = Gk+Gki;

FLOOR1(i,[1 2]) = [L1id, L2id]/1000;
FLOOR1(i, 3) = id1;
config = 0;
for g = 1:5
    config = config + d(id1,g)*10^(g*2)/100;
end
FLOOR1(i,4) = config;
FLOOR1(i,5) = h;
FLOOR1(i,6) = Gk+Gki;
FLOOR1(i,7) = (W_eds/Wid)*100;
FLOOR1(i,8) = W_edm/Wid*100;
FLOOR1(i,9) = EI_ed/EIid*100;

wout(i, 1) = wi;

if h>hgov
    hgov = h;
    idgov = id1;
end
end

%% Couparative Evaluation
for t = 1:2
for j = 1:5

i = j;
[Lid, L1id, L2id, Bid] = FLOOR(CAD1, i);

hi = FLOOR1(i,5);
idi = FLOOR1(i,3);

[qsls, quls] = Load(Qk, Gk, fork1, Bid);

[id1, EIid, h, hc, Gki, bi] = StiffnesF2(Z, ...
    qsls, quls, L1id, L2id, Bid, Cid(i), n, d, MOE, ...
    hgov, 0); %hgov, idgov

[f1, w_f, v, crit] = freq(EIid, Bid, Lid, ...
                          d(id1,:), n(id1), MOE, Cid(i));

Wid = EIid/(MOE(1)*h/2);
```

```
[qsls, quls] = Load(Qk, Gk+Gki, fork1, Bid);

[EI_ed, ~, W_edm , W_eds, wi] = EIrdF(qsls, quls, ...
    L1id, L2id, Cid(i), MOE(7), EIid);

GkF(t+1, i) = Gk+Gki;
EI_floor2(i,1) = id1;
EI_floor2(i,2) = h;
EI_floor2(i,3) = EIid;
EI_floor2(i,4) = EI_ed;
EI_floor2(i,5) = Gk+Gki;
EI_floor2(i,6) = SAV(Bid, Lid, d(id1,:), n(id1), ...
                     Cid(i), MOE);
bid(i) = bi;

FLOOR2(i,[1 2]) = [L1id, L2id]/1000;
FLOOR2(i, 3) = id1;
config = 0;
for g = 1:5
    config = config + d(id1,g)*10^(g*2)/100;
end
FLOOR2(i,4) = config;
FLOOR2(i,5) = 120;
FLOOR2(i,6) = bi;
FLOOR2(i,7) = (1-hc/h)*100;
FLOOR2(i,8) = h;
FLOOR2(i,9) = Gk+Gki;
FLOOR2(i,10) = W_eds/Wid*100;
FLOOR2(i,11) = W_edm/Wid*100;
FLOOR2(i,12) = EI_ed/EIid*100;

wout(i, 2) = wi;
end
end
bid

%% ---------------------------------------
% Wall
Hw = CAD2(contains(CAD2(:,1),'h'), 3);
Hw = Hw{1,1}*1000;
Levels = CAD2(contains(CAD2(:,1),'Levels'), 3);
Levels = Levels{1,1};
% Levels =31    ;
GkF = max(GkF(end,:));
Qw = zeros(10,1);
```

```
Qw(1) = 1.7;

C = [3 2 3 3 2 3 3 3 3 1;
     1 1 1 1 1 1 1 1 1 1];
C = C(CIMP,:);
Ned  = zeros(Levels,10);
Ned1 = Ned;
id1  = Ned;
Ped  = Ned;
Ped1 = Ped;
id2  = id1;
h    = id1;
bi   = h;
Ut_void    = h;
Ut_initial = h;
RED  = h;

for i = [1 2 3 5 6 9 10]
    [Did, B0id, Bidef] = WALL(CAD1, C, i);

    [~, quls] = Load(Qk, GkF, fork1, B0id);
    [~, qwind] = Load(Qw(i), 0, fork2, B0id);

    for j = 1:Levels
        if j==1
           Nedi = quls*Did;
        else
           Nedi = quls*Did + Ned(j-1,i);
        end
        [idi, EIout, hi, hc, Nid, Uti] = StiffnesW(Z, ...
            Nedi, qwind, Hw, B0id, Bidef, n, d, MOE);

        Ned(j,i) = Nid;
        Ped(j,i) = Nid/(B0id*sum(d(idi,:)));
        id1(j,i) = idi;
        h(j, i) = hi;
        Ut_initial(j,i) = Uti;
    end
end
id1;
h;
% Ut_initial
Ned;
% Ut
for i = [1 2 3 5 6 9 10]
```

```
    [Did, B0id, Bidef] = WALL(CAD1, C, i);

    [~, quls] = Load(Qk, GkF, fork1, B0id);
    [~, qwind] = Load(Qw(i), 0, fork2, B0id);

    for j = 1:Levels
        if j==1
           Nedi = quls*Did;
        else
           Nedi = quls*Did + Ned1(j-1,i);
        end
        [idi, EIout, hi, hc, Nid, Uti, bid] = ...
        StiffnesW(Z, Nedi, qwind, Hw, B0id, Bidef, ...
        n, d, MOE, h(j,i), 1); %, id1(j,i)

        Ned1(j,i) = Nid;
        Ped1(j,i) = Nid/(B0id*sum(d(idi,:)));
        id2(j,i) = idi;
        h(j, i) = hi;
        bi(j, i)= bid;
        Ut_void(j,i) = Uti;
        RED(j,i) = round((1-(hc/hi))*100,2);
    end
end
% Ned
id2;
% Ut_void
bi
RED
h
id_change=id1-id2;
Ut_change = Ut_void-Ut_initial;
Ut_c2 = zeros(8,10);
Ut_c1 = Ut_c2;
for i = 1:8
    for j = 1:10
        if Ut_initial(i,j)==0
            "hey";
        else
Ut_c2(i,j) = (Ut_void(i,j)-Ut_initial(i,j))/Ut_void(i,j);
Ut_c1(i,j) = (Ut_void(i,j)-Ut_initial(i,j))/...
              Ut_initial(i,j);
        end
    end
end
```

```
Vw = zeros(8,10);
Vhw = Vw;
for i = 1:8
    for j=[1 2 3 5 6 9 10]
        Vw(i,j) = Aw(j)*h(i,j)*10^-9;
        Vhw(i,j) = Vw(i,j)*(1-RED(i,j)/100);
    end
end
Vf = zeros(5,1);
Vhf = Vf;
for i = 1:5
    Vf(i) = Af(i)*hgov*10^-9;
    Vhf(i) = Vf(i)*(1-FLOOR2(i,7)/100);
end
figure(10+Z)
hold on
bar(Ut_c1(:,[1 2 3 5 6 9 10]), 1)
hold off

figure(30+Z)
hold on
% bar(Ped(:,[1 2 3 5 6 9 10]), 1)
plot([1 2 3 4 5 6 7 8],Ped(:,[1 2 3 5 6 9 10]), ...
     [1 2 3 4 5 6 7 8],Ped1(:,[1 2 3 5 6 9 10]))
title('Applied stress')
hold off

figure(50+Z)
hold on
x = flip([1:length(id1(:,1))]);
bar(x ,Ut_initial(:,[1 2 3 5 6 9 10])*100, 1)
title('Utilisation without air gaps')
grid on
legend({'W1', 'W2', 'W3', 'W5', 'W6', 'W9', 'W10'}, ...
    'location', 'northeastoutside', 'AutoUpdate','off')
xlabel('floor level')
ylabel('Utilization [%]')
hold off

figure(60+Z)
x = [8 7 6 5 4 3 2 1];
hold on
U=bar(x, Ut_void(:,[1 2 3 5 6 9 10])*100, 1)
hold off
legend(U,{'W1', 'W2', 'W3', 'W5', 'W6', 'W9', 'W10'}, ...
    'location', 'northeast', 'AutoUpdate','off')
```

```
hold on
U2=bar(x ,Ut_initial(:,[1 2 3 5 6 9 10])*100, 0.9, ...
    'FaceColor','flat', ...
    'EdgeColor','black', 'LineWidth',1.5)
grid on
title('Utilization with air gaps')

xlabel('floor level')
ylabel('Utilization [%]')


figure(70+Z)
hold on
x = [8 7 6 5 4 3 2 1];
bar(x, Ut_c1(:,[1 2 3 5 6 9 10])*100, 1)
grid on
title('Magniture of change in the utilization')
legend({'W1', 'W2', 'W3', 'W5', 'W6', 'W9', 'W10'}, ...
    'location', 'northeastoutside')
xlabel('floor level')
ylabel('[%]')
hold off

figure(80+Z)
hold on
bar(RED(:,[1 2 3 5 6 9 10]), 1)
% plot([1 2 3 4 5 6 7 8],Ut_c2(:,[1 2 3 5 6 9 10]))
title('reduction of volume')
hold off

id1
bi
```

A.2 Script functions of structural investigation

```
%% ------------------------------------------------------
%% freq
function [f1, w_f, v, crit] = freq(EIid, Bid, Lid, ...
                                   d, n, MOE, Cid)

h = sum(d);
m = (h*Bid*10^-6)*MOE(8);
f1 = pi()/(2*(Lid/1000)^2)*sqrt((EIid*10^-6)/m);

MOEb = MOE;
```

```
MOEb([1 3]) = MOE([2 4]);
MOEb([2 4]) = MOE([1 3]);
EIb = SAV(Lid, Bid, d, n, Cid, MOEb);
Bef = Lid/1.1*sqrt(EIb/EIid);

w_f = 1000*Lid^3/(48*EIid*Bef);

n40 = (((40/f1)^2-1)*(Bid/Lid)^4*(EIid/EIb))^(1/4);
v = 4*(0.4+0.6*n40)/(m*(Lid*10^-3)+200);

b = 100^(f1*0.025-1);
a = 1.5;
if a>w_f && b>v
    crit = 1;
else
    crit =0;
end

end

%% ------------------------------------------------------
function [Lid, L1id, L2id, Bid] = FLOOR(CAD1, i)

F = 'F';
Fid = i;
Fid = append(F,num2str(Fid));

Bid = CAD1(contains(CAD1(:,1),append(Fid, 'b')), 3);
Bid = Bid{1,1}*1000;
Bid = min(Bid, 3450);

L1id = CAD1(contains(CAD1(:,1),append(Fid, '1')), 3);
L1id = L1id{1,1}*1000;
L2id = CAD1(contains(CAD1(:,1),append(Fid, '2')), 3);
L2id = L2id{1,1}*1000;

Lid = max(L1id, L2id);

end

%% ------------------------------------------------------
function [Did, B0id, Bidef] = WALL(CAD1, C, i)
    W = 'W';
    Wid = i;
    Wid = append(W,num2str(Wid));
```

```
    B0id = CAD1(contains(CAD1(:,1),append(Wid, 'b')), 3);
    B0id = B0id{1,1}*1000;

    Bid1b = CAD1(contains(CAD1(:,1), ...
                append(Wid, '1b')), 3);
    Bid1b = Bid1b{1,1}*1000;
    Bid2b = CAD1(contains(CAD1(:,1), ...
                append(Wid, '2b')), 3);
    Bid2b = Bid2b{1,1}*1000;
    Bidef = Bid1b + Bid2b;

    Did1 = CAD1(contains(CAD1(:,1),append(Wid,'d1')), 3);
    Did1 = Did1{1,1}*1000;
    Did2 = CAD1(contains(CAD1(:,1),append(Wid,'d2')), 3);
    Did2 = Did2{1,1}*1000;
    Did = wallspan(Did1, C(i)) + wallspan(Did2, C(i));
end

%% ------------------------------------------------------
%% BUCKLING REDUCTION
function [k_crit, D_Rd, W_Rd] = ...
          Wkcrit(EI_sav, d, Hw, MOE, B0)

Isav = EI_sav/MOE(1);
W_Rd = 2*Isav/sum(d);
if sum(d>0)==3
    Anet = sum(d([1 3]))*B0;
else
    Anet = sum(d([1 3 5]))*B0;
end
iid = sqrt(Isav/Anet);
LamndY = Hw/iid;
fcok = 21; %MOE(6)
LamndRel = LamndY/pi*sqrt(fcok/MOE(5));
Betac = 0.1;
k_y = 0.5*(1+Betac*(LamndRel-0.3)+LamndRel^2);
k_crit = (k_y+sqrt(k_y^2-LamndRel^2))^-1;
D_Rd = k_crit*Anet/B0;
end

%% ------------------------------------------------------
%% EVALUATED WALL CONFIGURATION
function [id, EIout, h, hc, Nidi, Ut, bidi] = ...
          StiffnesW(Z, Nid, qwind, Hw, B0, Bef, n, d, ...
          MOE, hi, V2, idin )
```

```
if exist('V2', 'var')==1 && V2==1
    red = 0;
    "hey";
end

if exist('idin', 'var')
    d = d(idin,:);
    n = n(idin);
end
if exist('hi', 'var')==1
    aid = 700; %150
    bid =linspace(0, aid, aid/10+1);
    j=length(bid);
    aid = 120;%(bid(end));
else
    j=1;
    bid = 0;
    aid = 1;
end
for g = 1:j
    Vri = VR(aid, bid(g));
    MOEi = MOE;
    MOEi([2 4]) = MOEi([2 4])*Vri;
    if Z ==1
        [EI_sav] = SAVdataset(B0, Hw, d, n, 1, MOEi);
    else
        [EI_sav] = GammaDataset(B0, Hw, d, n, 1, MOEi);
    end
    for i = 1:length(n)
        [~, D_Rd, W_Rd] = Wkcrit(EI_sav(i,2), ...
            d(EI_sav(i,1),:), Hw, MOEi, B0);
        Nedi = Nid + 1.35*EI_sav(i,4)*MOEi(8)*B0*Hw
           *10^-8;
        [D_ed, W_ed] = EIrdW(Nedi, ...
            Bef, Hw, MOE(6), MOEi(7), qwind);
        if exist('hi', 'var')==1
            if 1>D_ed/D_Rd + W_ed/W_Rd && ...
               EI_sav(i, 3)==hi
                if V2==0 ||...
                   1-(EI_sav(i,4)/EI_sav(i,3))>red
                if exist('idin', 'var')==1
                    id = idin;
                else
                    id = EI_sav(i,1);
                end
                EIout  = EI_sav(i,2);
```

```
                h       = EI_sav(i,3);
                hc      = EI_sav(i,4);
                Nidi    = Nedi;
                bidi    = bid(g);
                Ut = D_ed/D_Rd + W_ed/W_Rd;
                red = 1-(EI_sav(i,4)/EI_sav(i,3));
                break
                end
            end
        else
            if 1>D_ed/D_Rd + W_ed/W_Rd
                if exist('idin', 'var')==1
                    id = idin;
                else
                    id = EI_sav(i,1);
                end
                EIout   = EI_sav(i,2);
                h       = EI_sav(i,3);
                hc      = EI_sav(i,4);
                Nidi    = Nedi;
                Ut = D_ed/D_Rd + W_ed/W_Rd;
                break
            end
        end
    end
end
end

%% ------------------------------------------------------
%% NEEDED STIFFNESS FONCTION FOR WALL
function [D_ed, W_ed] = ...
          EIrdW(Ned, Bef, Wh, fcod, fmd, qwind)

D_ed = Ned/(fcod*Bef);
if exist('qwind', 'var')==1
    Med = (Wh/1000)^2 *  qwind/8;
    W_ed = Med*10^6/fmd;
end
end

%% ------------------------------------------------------
%% ACCTING FLOOR SPAN ON WALL
function [Did] = wallspan(Di, C)
    if C == 1
        Did = Di*0.5;
    else
```

```
        if C == 2
            Did = Di*0.6;
        else
            Did = Di*0.4;
        end
    end
end

%% ------------------------------------------------------
%% REDUCTION FACTOR BASED ON MOHANNAD AND HANNA
function [Vr] = VR(a, b)
Vr=a/(a+b);
end

%% ------------------------------------------------------
%% ACCTING LOADS ACCORDING TO EURO CODE
function [q_SLS, q_ULS] = Load(Qk, Gk, fork, B)
q_SLS = (Qk + Gk*fork)*B/1000;
q_ULS = (1.35*Gk + 1.5*Qk*fork)*B/1000;
end

%% ------------------------------------------------------
%% DEFLECTION LIMITS OF FLOOR ACCORDING TO EU 5
function [wlim, winst, wfin, lim] = deflectionEU5(L)
    kdef = 0.8;
    winst = L/400;
    wfin = L/250;
    wlim = min(winst, wfin/(1+kdef));
    if wlim==winst
        lim = 1;
    else
        lim = 1+kdef;
    end
end

%% ------------------------------------------------------
%% EVALUATED FLOOR CONFIGURATION
function [id, EIout, h, hc, Gki, bi] = StiffnesF(Z, ...
    qsls, quls, L1, L2, B, C, n, d, MOE, hi, V2, idin)

L = max(L1,L2);
if exist('V2', 'var')==1 && V2==1
    red = 0;
    "hey";
end
if exist('idin', 'var')
```

```
    d = d(idin,:);
    n = n(idin);
end
if exist('hi', 'var')==1
    aid = 4000; %150
    bid =linspace(0, aid, aid/10+1);
    j=length(bid);
    aid = 120;%(bid(end));
else
    j=1;
    bid = 0;
    aid = 120;
end
for g = 1:j
    Vri = VR(aid, bid(g));
    MOEi = MOE;
    MOEi([2 4]) = MOEi([2 4])*Vri;
    if Z==1
        [EI_Rd] = SAVdataset(B, L, d, n, C, MOEi);
    else
        [EI_Rd] = GammaDataset(B, L, d, n, C, MOEi);
    end
    for i = 1:length(n)
        qslsi = qsls + EI_Rd(i,4)*MOEi(8)*B*10^-8;
        qulsi = quls + 1.35*EI_Rd(i,4)*MOEi(8)*B*10^-8;
        [EI_ed, ~, W_edm, W_eds] = EIrdF(qslsi, qulsi, ...
            L1, L2, C, MOEi(7));
        W_Rd = EI_Rd(i,2)/(MOEi(1)*EI_Rd(i,3)/2);
        if exist('hi', 'var')==1
            if EI_ed<EI_Rd(i,2) ...
                && EI_Rd(i, 3)==hi ...
                && W_edm<W_Rd ...
                && W_eds<W_Rd
                if V2==0 || 1-(EI_Rd(i,4)/EI_Rd(i,3))>red
                if exist('idin', 'var')==1
                    id = idin;
                else
                    id = EI_Rd(i,1);
                end
                EIout = EI_Rd(i,2);
                h     = EI_Rd(i,3);
                hc    = EI_Rd(i,4);
                Gki   = EI_Rd(i,4)*MOEi(8)*10^-5;
                bi    = bid(g);
                red = 1-(EI_Rd(i,4)/EI_Rd(i,3));
                break
```

```
                end
            end
        else
            if EI_ed<EI_Rd(i,2) ...
                && W_edm<W_Rd ...
                && W_eds<W_Rd

                if exist('idin', 'var')==1
                    id = idin;
                else
                    id = EI_Rd(i,1);
                end
                EIout = EI_Rd(i,2);
                h     = EI_Rd(i,3);
                hc    = EI_Rd(i,4);
                Gki   = EI_Rd(i,4)*MOEi(8)*10^-5;
                break
            end
        end
    end
end
end

%% ------------------------------------------------------
%% NEEDED STIFFNESS FUNCTION FOR FLOOR
function [EI_ed, W_ed, W_edm, W_eds, w, Med] = EIrdF( ...
    qsls, quls, L1, L2, C, fmd, EIinp)

if C == 1
    k_b = 5/384;
    k_s = 1/8;
    L = L1/1000;
    Med = k_s* L^2 *  quls;
    W_edm = Med*10^6/fmd;
    W_eds = 0;
else
    k_b = 1/185;
    k_s = 9/128;
    L = max(L1, L2)/1000;
    Medm = k_s*L^2*quls;
    Meds = ((L1/1000)^2*quls + (L2/1000)^2*quls)/8;
    Med = Medm;
    W_edm = Medm*10^6/fmd;
    W_eds = Meds*10^6/fmd;
end
[w, ~, ~, lim] = deflectionEU5(L);
```

```
W_ed = max(W_eds,W_edm);
EI_ed = k_b * qsls * (L*1000)^4 / (1000*w);
if exist('EIinp', 'var') == 1
    w = lim * k_b * qsls * (L*1000)^4 / EIinp;
end
end

%% ------------------------------------------------------
%% SHEAR ANalogy Method (SAV)
function [EIsav, GA_ef] = SAV(B, L, d, n, C, MOE)
d = d(:, 1:n);
y =zeros(1,n);
yc = sum (d)/2;
a = y;
for i= 1:n
    y(i) = sum(d(1,(i+1):end))+d(1,i)/2;
    a(i) = sqrt((y(i)-yc)^2);
end
I = zeros(3,n);
EIi = I(1,:);
for i = 1:n
    I(1, i) = B*d(i)^3/12;
    I(2, i) = B*d(i)*a(i)^2;
    I(3, i) = sum(I(1:2, i));
    if rem(i,2) == 0
        E = MOE(2);
    else
        E = MOE(1);
    end
    EIi(i) = I(3,i)*E;
end
EI_ef = sum(EIi);

GA = zeros(1,n);
for i = 1:n
    if rem(i,2) == 0
        G = MOE(4);
    else
        G = MOE(3);
    end
    if i==1 || i==n
        GA(i) = d(i)/(2*G*B);
    else
        GA(i) = d(i)/(G*B);
    end
```

```
end
GA_ef = (a(1)+a(n))^2 / (sum(GA));

Y = 1.2;
if C == 1
    k_s = 1/8;
    k_b = 5/384;
else
    k_s = 9/128;
    k_b = 1/185;
end
K_s = Y*(k_s/k_b);
EIsav = EI_ef/(1 + K_s*EI_ef/(GA_ef*L^2));
end
%% ------------------------------------------------------
function [EI_sav] = SAVdataset(B, L, d, n, C, MOE)
    EIsav = zeros(length(n),4);
    for i= 1:length(n)
        EIsav(i, 2) = SAV(B, L, d(i,:), n(i), C, MOE);
        EIsav(i,1) = i;
        EIsav(i,3) = sum(d(i,:));
        if n(i)==5
            EIsav(i,4) = sum(d(i,[1 3 5])) +...
            sum(d(i,[2 4]))*10*MOE(4)/MOE(3);
        else
            EIsav(i,4) = sum(d(i,[1 3])) +...
            sum(d(i,2))*10*MOE(4)/MOE(3);
        end
    end
    EIsav = sortrows(EIsav,2, "ascend");
    EIsav = sortrows(EIsav,3, "ascend");
    EI_sav = EIsav;
end

%% ------------------------------------------------------
%% GAMMA METHOD
function [EIef] = Gamma(B, L, d, n, C, MOE)
d = d(:, 1:n);
if C==2
    L=L*0.8;
end
y =zeros(1,n);
yc = sum (d)/2;
a = y;
for i= 1:n
    y(i) = sum(d(1,(i+1):end))+d(1,i)/2;
```

```
    a(i) = sqrt((y(i)-yc)^2);
end
I = zeros(3,n);
EI = I(1,:);
Y = EI;
for i = 1:n
    if i==1 || i==5
        Y(i) = (1 + pi()^2* ...
            MOE(1)*d(i)*d(2)/(L^2*MOE(4)))^-1;
    else
        Y(i)=1;
    end
    if rem(i,2) == 0
        "hey";
    else
        I(1, i) = B*d(i)^3/12;
        I(2, i) = Y(i)*B*d(i)*a(i)^2;
        I(3, i) = sum(I(1:2, i));
    end
    if rem(i,2) == 0
        "hey";
    else
        E = MOE(1);
        EI(i) = I(3,i)*E;
    end
end
EIef = sum(EI);
end
%% ------------------------------------------------------
function [EI_y] = GammaDataset(B, L, d, n, C, MOE)
    EIy = zeros(length(n),4);
    for i= 1:length(n)
        EIy(i, 2) = Gamma(B, L, d(i,:), n(i), C, MOE);
        EIy(i,1) = i;
        EIy(i,3) = sum(d(i,:));
        if n(i)==5
            EIy(i,4) = sum(d(i,[1 3 5])) +...
            sum(d(i,[2 4]))*10*MOE(4)/MOE(3);
        else
            EIy(i,4) = sum(d(i,[1 3])) +...
            sum(d(i,2))*10*MOE(4)/MOE(3);
        end
    end
    EIy = sortrows(EIy,2, "ascend");
    EIy = sortrows(EIy,3, "ascend");
```

```
    EI_y = EIy;
end

%% ------------------------------------------------------
%% CELEBRATION
function halleluja
load handel
sound(y,Fs)
end

%% ------------------------------------------------------
function [CRIT] = localCHECK(L, bi, B0,  d, n, MOE, ...
                             quls, Med, qsls)

    kv = 0.007;
    kf = 0.08;
    ks = -0.125;

if n==3
    ti = d(:,3);
else
    ti = d(:,5);
end

%%% Geometry
I = B0 * ti^3/12;
W = 2*I/ti;
A = B0*ti;

%%% Moment Check
% acting
Mf = quls * bi^2 * kf;
Ms =  quls *bi^2 * ks;
% capacity
MRd = W*MOE(7)/1.15;

%%% Tension check
% acting
Ned = Med / ((sum( d(:,:))-d(:,1)));
% capacity
NRdt = A*MOE(9);

%%% Combined
i = sqrt(I/A);
lam = bi*0.7/i;
lamrel = lam/pi() * sqrt(21/MOE(5));
```

```
    k = 0.5*(1+0.2*(lamrel-0.3)+lamrel^2);
    kc = (k + sqrt(k^2 - lamrel^2))^-1;
    NRdc = A*MOE(6)*kc;
    COM = Mf/MRd + Ned/(NRdc);

%%% deflection
wed = kv * qsls*bi^4/(MOE(1)*I);
wlim = deflectionEU5(bi);
wlim = min(wlim, d(:,2));

if wlim>wed && MRd>Mf && MRd>Ms...
    && NRdt>Ned && COM<1 && L/2>bi
    CRIT = 1;
else
    CRIT = 0;
end
end

%% ------------------------------------------------------
function [id, EIout, h, hc, Gki, bi] = StiffnesF2(Z, ...
    qsls, quls, L1, L2, B, C, n, d, MOE, hi, V2, idin)

L = max(L1,L2);
if exist('V2', 'var')==1 && V2==1
    red = 0;
    "hey";
end
if exist('idin', 'var')
    d = d(idin,:);
    n = n(idin);
end
if exist('hi', 'var')==1
    aid = 1900; %150
    bid =linspace(0, aid, aid/10+1);
    j=length(bid);
    aid = 120;%(bid(end));
else
    j=1;
    bid = 0;
    aid = 120;
end
for g = 1:j
    Vri = VR(aid, bid(g));
    MOEi = MOE;
    MOEi([2 4]) = MOEi([2 4])*Vri;
```

```
if Z==1
    [EI_Rd] = SAVdataset(B, L, d, n, C, MOEi);
else
    [EI_Rd] = GammaDataset(B, L, d, n, C, MOEi);
end
for i = 1:length(n)
    qslsi = qsls + EI_Rd(i,4)*MOEi(8)*B*10^-8;
    qulsi = quls + 1.35*EI_Rd(i,4)*MOEi(8)*B*10^-8;
    [EI_ed, ~, W_edm, W_eds, ~, Medi] = EIrdF( ...
        qslsi, qulsi, L1, L2, C, MOEi(7));
    W_Rd = EI_Rd(i,2)/(MOEi(1)*EI_Rd(i,3)/2);
    idint = EI_Rd(i,1);
    [CRIT] = localCHECK(L, bid(g), ...
                        B, d(idint,:), ...
                        n(idint), MOE, ...
                        qulsi, Medi, qslsi);
    if exist('hi', 'var')==1
        if EI_ed<EI_Rd(i,2) ...
            && EI_Rd(i, 3)==hi ...
            && W_edm<W_Rd ...
            && W_eds<W_Rd ...
            && CRIT==1
            if V2==0 || 1-(EI_Rd(i,4)/EI_Rd(i,3))>red
                if exist('idin', 'var')==1
                    id = idin;
                else
                    id = EI_Rd(i,1);
                end
                EIout = EI_Rd(i,2);
                h     = EI_Rd(i,3);
                hc    = EI_Rd(i,4);
                Gki   = EI_Rd(i,4)*MOEi(8)*10^-5;
                bi    = bid(g);
                red = 1-(EI_Rd(i,4)/EI_Rd(i,3));
                break
            end
        end
    else
        if EI_ed<EI_Rd(i,2) ...
            && W_edm<W_Rd ...
            && W_eds<W_Rd

            if exist('idin', 'var')==1
                id = idin;
            else
                id = EI_Rd(i,1);
```

```
                end
                EIout = EI_Rd(i,2);
                h     = EI_Rd(i,3);
                hc    = EI_Rd(i,4);
                Gki   = EI_Rd(i,4)*MOEi(8)*10^-5;
                break
            end
        end
    end
end
end
```

A.3 Hygrothermal simulation script

```
close all
clear

addpath('C:\Users\Elliot\Desktop\Chalmers\EXjobb\Code')

W87 = readtable('floor 8 7 data.txt');
W65 = readtable('floor 6 5 data.txt');
W432 = readtable('floor 4 3 2 data.txt');
W1 = readtable('floor1 data.txt');

W87h = readtable('floor 7,8h.txt');
W6h = readtable('floor 6h.txt');
W5h = readtable('floor 5h.txt');
W4h = readtable('floor 4h.txt');
W3h = readtable('floor3h.txt');
W2h = readtable('floor2h.txt');
W1h = readtable('floor 1h.txt');

date = W87;
date = sortrows(date, "Time_dd_MM_yyyy_");


Tav87 = avT(W87.Temperature_Av__Temperature__C__);
Tav65 = avT(W65.Temperature_Av__Temperature__C__);
Tav432 = avT(W432.Temperature_Av__Temperature__C__);
Tav1 = avT(W1.Temperature_Av__Temperature__C__);

Tav87h = avT(W87h.Temperature_Av__Temperature__C__);
Tav6h = avT(W6h.Temperature_Av__Temperature__C__);
Tav5h = avT(W5h.Temperature_Av__Temperature__C__);
Tav4h = avT(W4h.Temperature_Av__Temperature__C__);
```

```
Tav3h = avT(W3h.Temperature_Av__Temperature__C__);
Tav2h = avT(W2h.Temperature_Av__Temperature__C__);
Tav1h = avT(W1h.Temperature_Av__Temperature__C__);

RHc87h = RHmould(W87h.Temperature_Av__Temperature__C__);
RHc6h = RHmould(W6h.Temperature_Av__Temperature__C__);
RHc5h = RHmould(W5h.Temperature_Av__Temperature__C__);
RHc4h = RHmould(W4h.Temperature_Av__Temperature__C__);
RHc3h = RHmould(W3h.Temperature_Av__Temperature__C__);
RHc2h = RHmould(W2h.Temperature_Av__Temperature__C__);
RHc1h = RHmould(W1h.Temperature_Av__Temperature__C__);

figure(87)
hold on
title('Stora Enso and Hollow ID1 b_i=150mm; h_{clt}=60mm'
   )
grid on
xlabel('date')
yyaxis left
ylabel('RH [%]')
ylim([49 84])
plot(date.Time_dd_MM_yyyy_, ...
    W87.RelativeHumidity_RelativeHumidity____,'red', ...
    date.Time_dd_MM_yyyy_, ...
    W87h.RelativeHumidity_RelativeHumidity____, 'blue',
       ...
    date.Time_dd_MM_yyyy_, RHc87h, 'black', ...
    'LineStyle', '-' )
yyaxis right
ylabel('Temperature ^\circ C')
ylim([10 25])
plot(date.Time_dd_MM_yyyy_, Tav87,'magenta', ...
    date.Time_dd_MM_yyyy_, Tav87h,'green','LineStyle', ':
       ')
legend( {'RH Stora Enso', 'RH ID1 202020 b_i=150mm', ...
    'Critical moisture status', ...
    'T, Stora Enso', 'T, ID1 b_i=150mm'},'location', ...
    'southoutside', 'numcolumns', 2)
ax =gca;
ax.YAxis(1).Color = 'k';
ax.YAxis(2).Color = 'k';
hold off

figure(6)
hold on
```

```
title('Stora Enso and Hollow ID2 b_i=150mm; h_{clt}=70mm'
   )
grid on
xlabel('date')
yyaxis left
ylabel('RH [%]')
ylim([50 84])
plot(date.Time_dd_MM_yyyy_, ...
    W65.RelativeHumidity_RelativeHumidity____,'red', ...
     date.Time_dd_MM_yyyy_, ...
     W6h.RelativeHumidity_RelativeHumidity____, 'blue',
        ...
     date.Time_dd_MM_yyyy_, RHc6h, 'black', ...
     'LineStyle', '-')
yyaxis right
ylabel('Temperature ^\circ C')
ylim([10 25])
plot(date.Time_dd_MM_yyyy_, Tav65,'magenta', ...
     date.Time_dd_MM_yyyy_, Tav6h,'green', ...
     'LineStyle', ':')
legend( {'RH Stora Enso', 'RH ID2 203020 b_i=150mm', ...
    'Critical moisture status', ...
    'T, Stora Enso', 'T, ID2 b_i=150mm'},'location', ...
    'southoutside', 'numcolumns', 2)
ax =gca;
ax.YAxis(1).Color = 'k';
ax.YAxis(2).Color = 'k';
hold off

figure(5)
hold on
title('Stora Enso and Hollow ID2 b_i=130mm; h_{clt}=70mm'
   )
grid on
xlabel('date')
yyaxis left
ylabel('RH [%]')
ylim([50 84])
plot(date.Time_dd_MM_yyyy_, ...
    W65.RelativeHumidity_RelativeHumidity____,'red', ...
     date.Time_dd_MM_yyyy_, ...
     W5h.RelativeHumidity_RelativeHumidity____, 'blue',
        ...
     date.Time_dd_MM_yyyy_, RHc5h, 'black', ...
     'LineStyle', '-')
yyaxis right
```

```
ylabel('Temperature ^\circ C')
ylim([10 25])
plot(date.Time_dd_MM_yyyy_, Tav65,'magenta', ...
     date.Time_dd_MM_yyyy_, Tav5h,'green','LineStyle', ':
        ')
legend( {'RH Stora Enso', 'RH ID2 203020 b_i=130mm', ...
    'Critical moisture status','T, Stora Enso', ...
    'T, ID2 b_i=130mm'},'location', ...
    'southoutside', 'numcolumns', 2)
ax =gca;
ax.YAxis(1).Color = 'k';
ax.YAxis(2).Color = 'k';
hold off

figure(4)
hold on
title('Stora Enso and Hollow ID3 b_i=150mm; h_{clt}=80mm'
   )
grid on
xlabel('date')
yyaxis left
ylabel('RH [%]')
ylim([50 84])
plot(date.Time_dd_MM_yyyy_, ...
    W432.RelativeHumidity_RelativeHumidity____,'red', ...
     date.Time_dd_MM_yyyy_, ...
     W4h.RelativeHumidity_RelativeHumidity____, ...
     'blue',date.Time_dd_MM_yyyy_, RHc4h, 'black', ...
     'LineStyle', '-')
yyaxis right
ylabel('Temperature ^\circ C')
ylim([10 25])
plot(date.Time_dd_MM_yyyy_, Tav432,'magenta', ...
     date.Time_dd_MM_yyyy_, Tav4h,'green','LineStyle', ':
        ')
legend( {'RH Stora Enso', 'RH ID3 204020 b_i=150mm', ...
    'Critical moisture status','T, Stora Enso', ...
    'T, ID3 b_i=150mm'},'location', 'southoutside', ...
    'numcolumns', 2)
ax =gca;
ax.YAxis(1).Color = 'k';
ax.YAxis(2).Color = 'k';
hold off

figure(3)
hold on
```

```
title('Stora Enso and Hollow ID3 b_i=60mm; h_{clt}=80mm')
grid on
xlabel('date')
yyaxis left
ylabel('RH [%]')
ylim([50 84])
plot(date.Time_dd_MM_yyyy_, ...
    W432.RelativeHumidity_RelativeHumidity____,'red', ...
     date.Time_dd_MM_yyyy_, ...
     W3h.RelativeHumidity_RelativeHumidity____, 'blue',
        ...
     date.Time_dd_MM_yyyy_, RHc3h, 'black', ...
     'LineStyle', '-')
yyaxis right
ylabel('Temperature ^\circ C')
ylim([10 25])
plot(date.Time_dd_MM_yyyy_, Tav432,'magenta', ...
     date.Time_dd_MM_yyyy_, Tav3h,'green','LineStyle', ':
        ')
legend( {'RH Stora Enso', 'RH ID3 204020 b_i=60mm', ...
    'Critical moisture status','T, Stora Enso', ...
    'T, ID3 b_i=60mm' },'location', 'southoutside', ...
    'numcolumns', 2)
ax =gca;
ax.YAxis(1).Color = 'k';
ax.YAxis(2).Color = 'k';
hold off

figure(2)
hold on
title('Stora Enso and Hollow ID4 b_i=90mm; h_{clt}=80mm')
grid on
xlabel('date')
yyaxis left
ylabel('RH [%]')
ylim([50 84])
plot(date.Time_dd_MM_yyyy_, ...
    W432.RelativeHumidity_RelativeHumidity____,'red', ...
     date.Time_dd_MM_yyyy_, ...
     W2h.RelativeHumidity_RelativeHumidity____, 'blue',
        ...
     date.Time_dd_MM_yyyy_, RHc2h, 'black', ...
     'LineStyle', '-')
yyaxis right
ylabel('Temperature ^\circ C')
ylim([10 25])
```

```
plot(date.Time_dd_MM_yyyy_, Tav432,'magenta', ...
     date.Time_dd_MM_yyyy_, Tav2h,'green','LineStyle', ':
        ')
legend( {'RH Stora Enso', 'RH ID4 302030 b_i=90mm', ...
    'Critical moisture status','T, Stora Enso', ...
    'T, ID4 b_i=90mm'},'location', 'southoutside', ...
    'numcolumns', 2)
ax =gca;
ax.YAxis(1).Color = 'k';
ax.YAxis(2).Color = 'k';
hold off

figure(1)
hold on
title('Stora Enso and Hollow ID5 b_i=150mm; h_{clt}=90mm'
   )
grid on
xlabel('date')
yyaxis left
ylabel('RH [%]')
ylim([50 84])
plot(date.Time_dd_MM_yyyy_, ...
    W1.RelativeHumidity_RelativeHumidity____,'red', ...
     date.Time_dd_MM_yyyy_, ...
     W1h.RelativeHumidity_RelativeHumidity____, 'blue',
        ...
     date.Time_dd_MM_yyyy_, RHc1h, 'black', ...
     'LineStyle', '-')
yyaxis right
ylabel('Temperature ^\circ C')
ylim([10 25])
plot(date.Time_dd_MM_yyyy_, Tav1,'magenta', ...
     date.Time_dd_MM_yyyy_, Tav1h,'green','LineStyle', ':
        ')
legend( {'RH Stora Enso', 'RH ID5 303030 b_i=150mm', ...
    'Critical moisture status','T, Stora Enso', ...
    'T, ID5 b_i=150mm'},'location', 'southoutside', ...
    'numcolumns', 2)
ax =gca;
ax.YAxis(1).Color = 'k';
ax.YAxis(2).Color = 'k';
hold off

%% ------------------------------------------------------
function RH = RHmould(T)
```

```
RH = zeros(length(T),1);
for i = 1:length(T)
    if T(i)>20
        RHi = 80;
    else
        RHi = ...
        -0.00267*T(i)^3 + 0.16*T(i)^2 - 3.13*T(i) + 100;
    end
    RH(i) = RHi;
end
end

%% ---------------------------------------------------
function Tav = avT(Tseries)

e = 150;
b =43800/e;
Tav = zeros(b,1);
for i = 1:b
    Tday65 =  Tseries;
    Tday65 = mean(Tday65((i*e)-(e-1):i*e,1));
    Tav(i) = Tday65;
end
Tav = repelem(Tav, e);
Tav(43801) = 20;

end
```

DEPARTMENT OF SOME SUBJECT OR TECHNOLOGY
CHALMERS UNIVERSITY OF TECHNOLOGY
Gothenburg, Sweden
www.chalmers.se

CHALMERS
UNIVERSITY OF TECHNOLOGY